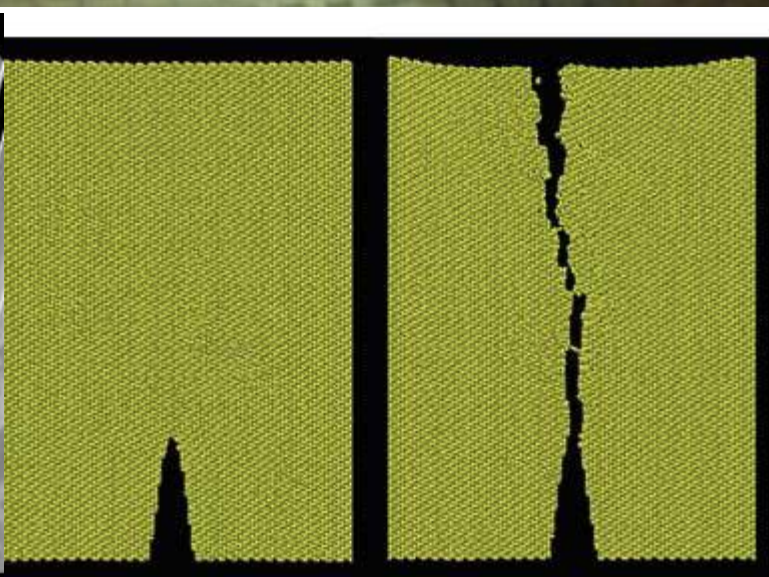
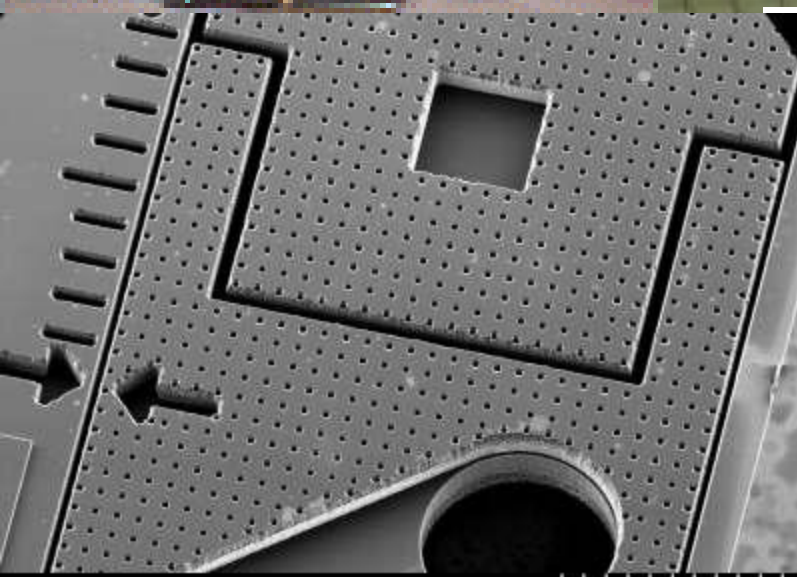


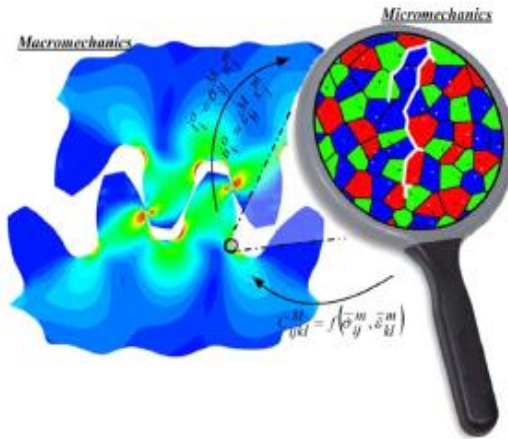
Atomistic- and Multiscale Modeling of Materials Failure

Christian Thaulow,
Dept Engineering Design and Materials, NTNU, Norway



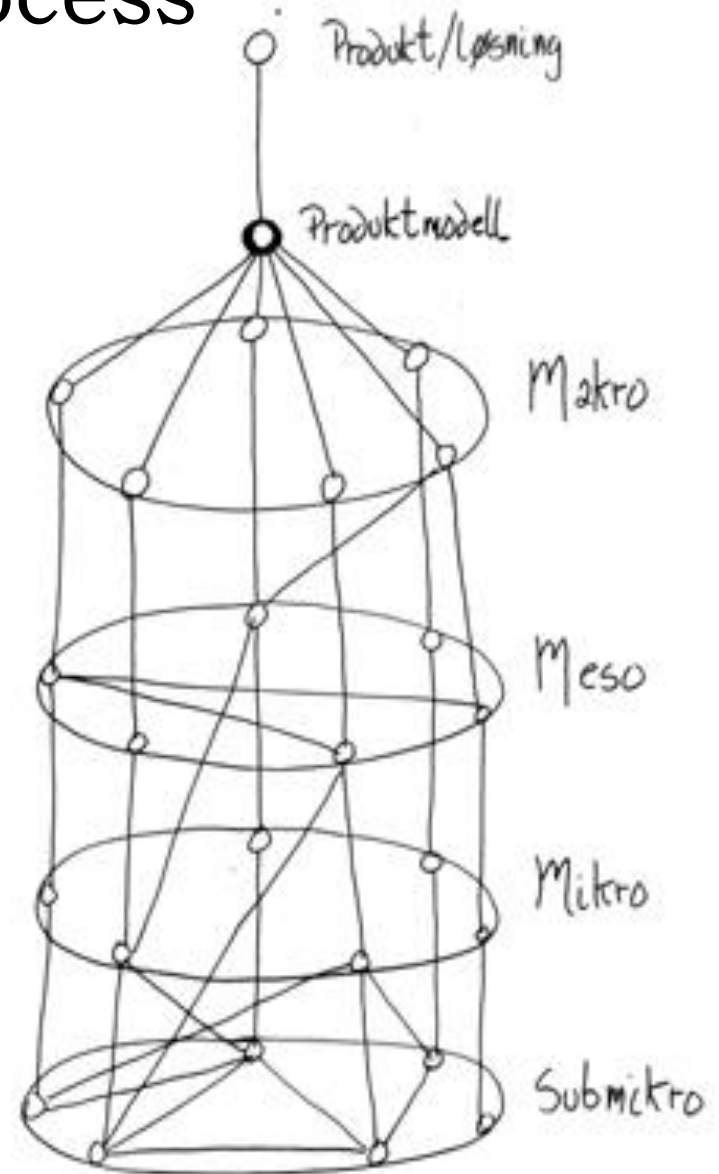
S4700 25.0kV 5.9mm x35 SE(U) 1.00mm

Material optimization process

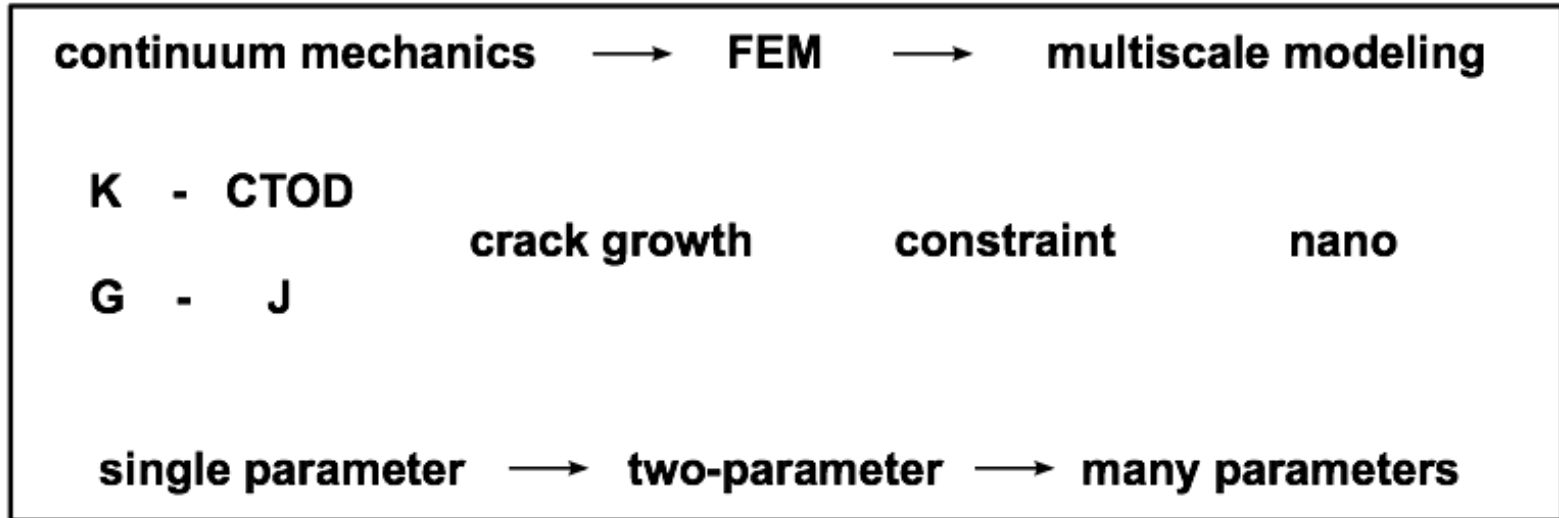


**All knowing depends on
the structure of the knower**

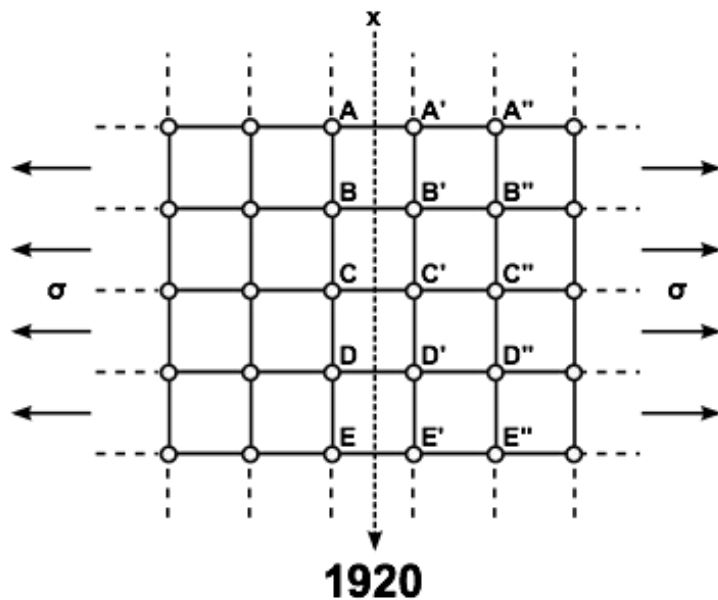
**We do not see that we
do not see**



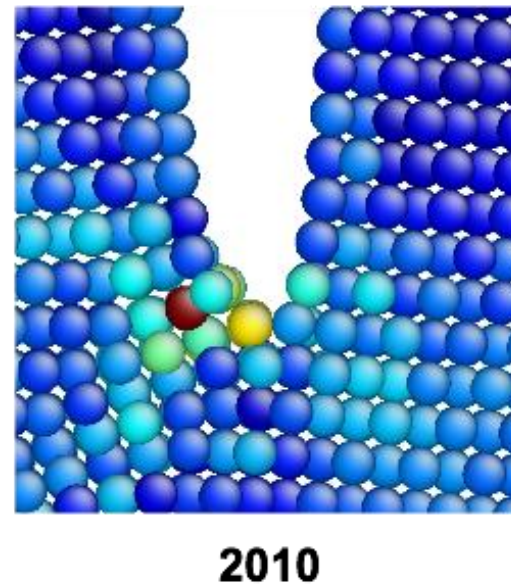
Fracture Mechanics Historical Development



from atomistic view



to atomistic modeling

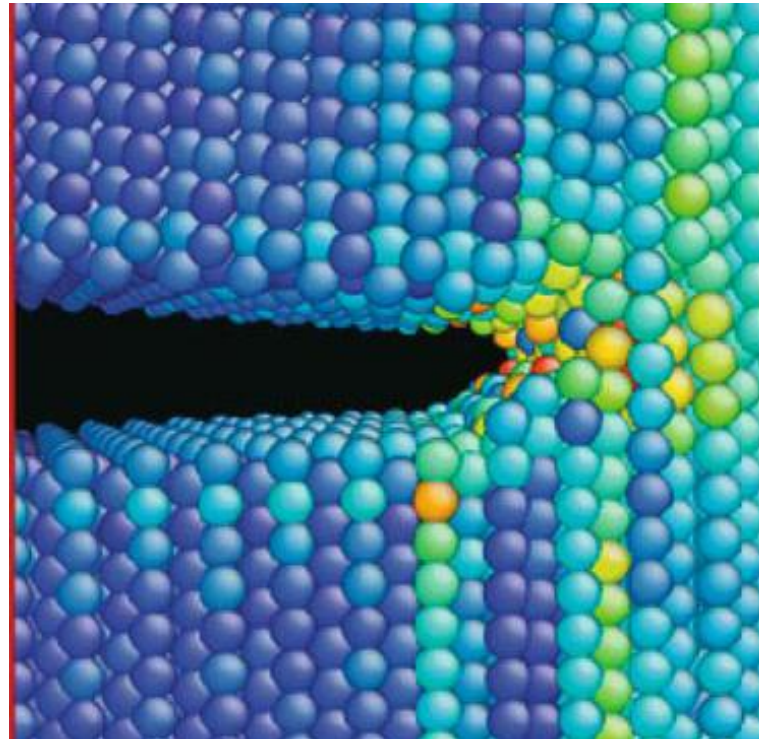


1 000 000 000 000 000 000

From LARGE Scale testing: 100MN and 10 minutes

to

Atomistic Mechanics: 10pN and 1 femtosecond



Laboratory for Atomistic and Molecular Mechanics (LAMM)

Markus J. Buehler

**PI, Laboratory for Atomistic and Molecular
Mechanics Department of Civil and
Environmental Engineering
Massachusetts Institute of Technology**

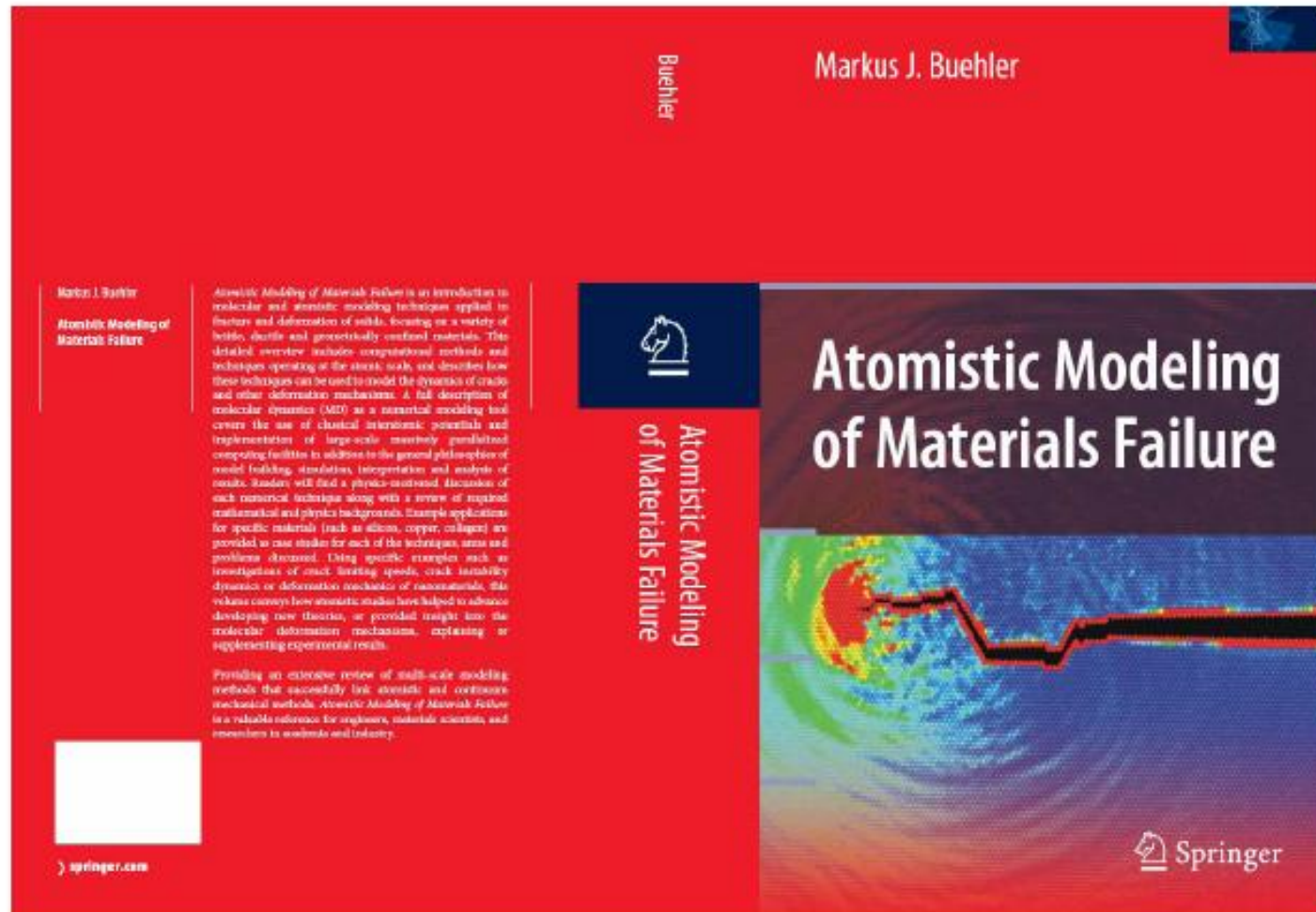
E-mail: mbuehler@MIT.EDU

URL: <http://web.mit.edu/mbuehler/www/>



Massachusetts Institute of Technology

1.545 – Atomistic Modeling and Simulation of Materials and Structures



Visions for the future...

Marcus Buehler

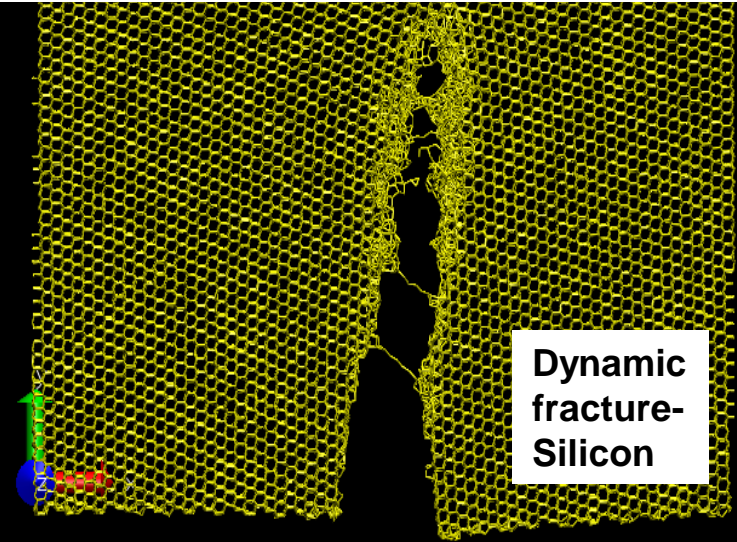
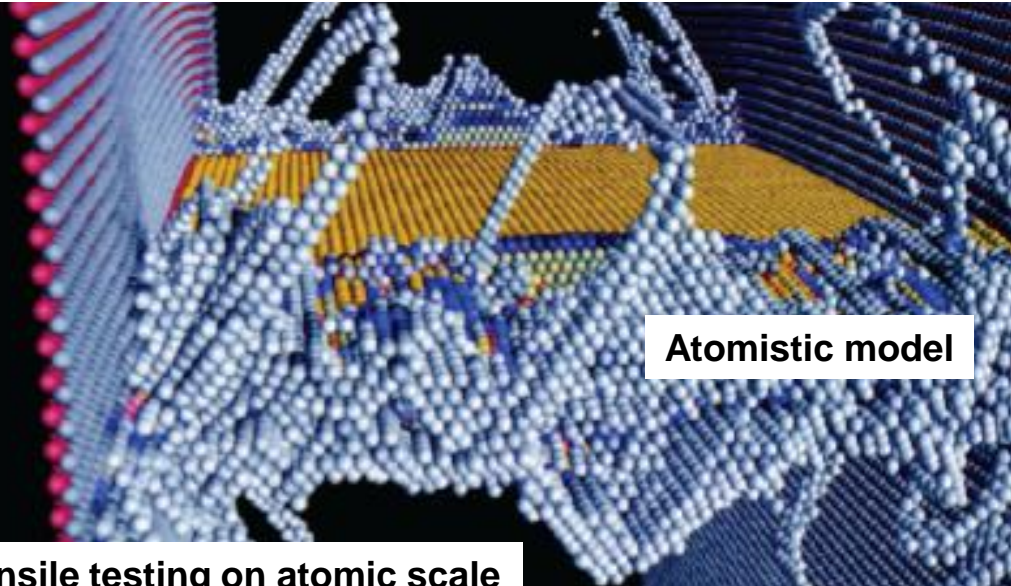
- **Atomistic simulations in material design becomes normal**
- **The next generation of CAE software will integrate nano and micro structures**
- **Concurrent multi-field variational FEM equations that couple nano and micro structures and continuum.**
- **A predictive multiscale constitutive law that bridges nano and micro structures with the continuum concurrently via statistical averaging and monitoring the microstructure/defect evolutions (i.e., manufacturing processes).**
- **Improved methods for the hierarchical and concurrent analyses**
- **Probabilistic simulation-based design techniques enabling even more realistic simulations**
- **..**

Want to learn how to design tomorrow's materials?

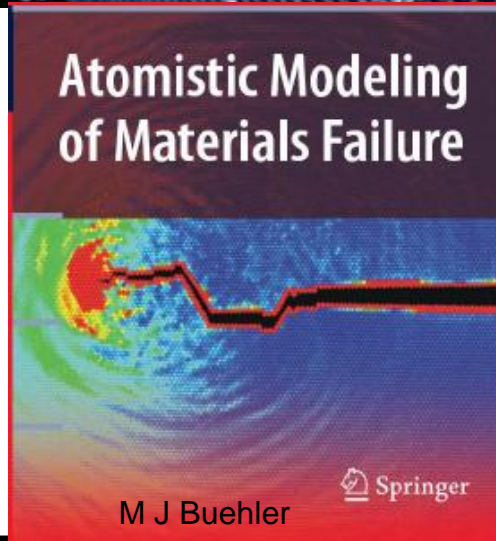
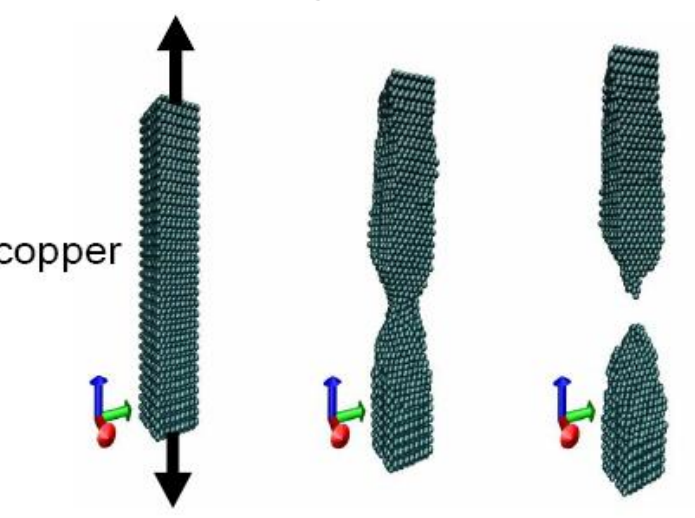
Did you know that it can be done with nanoscience and a computer?

TMM4162/MM8406 - Atomistic Modeling of Materials Failure

New from spring 2010



Tensile testing on atomic scale

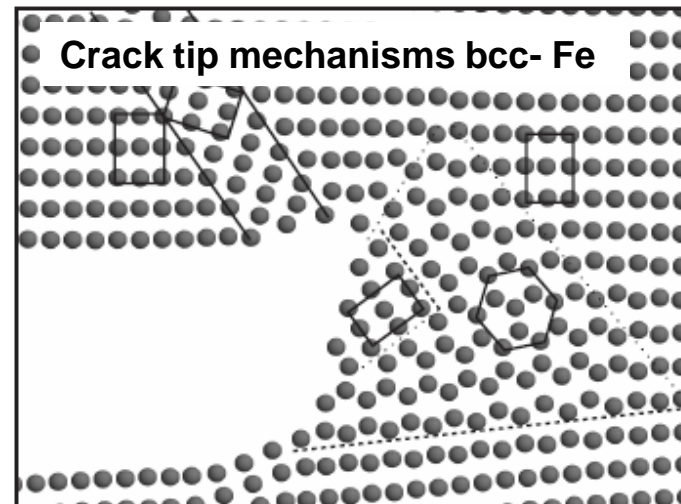


Atomistic Modeling of Materials Failure

M J Buehler

Springer

The book cover features a central image of a crack tip with a color-coded stress field. The crack tip is highlighted in red, and the surrounding material is shown in shades of blue and green. The title and author's name are prominently displayed.



MULTISCALE MATERIAL MODELING AND TESTING LESSONS FROM NATURE



MASTER AND PHD STUDENTS FALL 2010

Research group at NTNU

Atomistic and Multiscale Material Modeling and Testing

NTNU Department of Engineering Design and Materials

Christian Thaulow – Atomistic- and Multiscale Material Modeling and Testing

Christer H Ersland, PhD Arctic Materials - Atomistic modeling of bcc-Fe

Inga Ringdalen Vatne, PhD Arctic Materials - Multiscale Material Modeling
of Fracture in Iron and Steel

Adina Basa, PhD HISC Petromaks project - Nanoindentation of steels
with in situ hydrogen charging

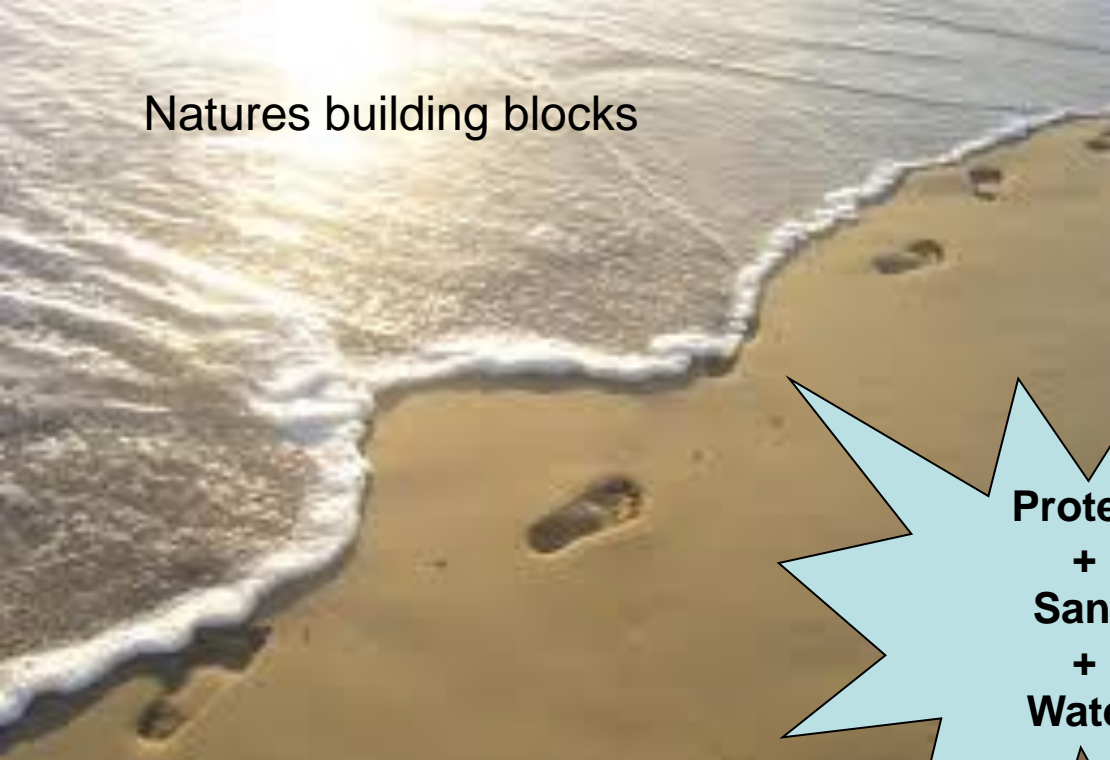
Bjørn Rogne, PhD Nanomechanical testing of steel

5 Masterstudents on nanotechnology, fall 2010

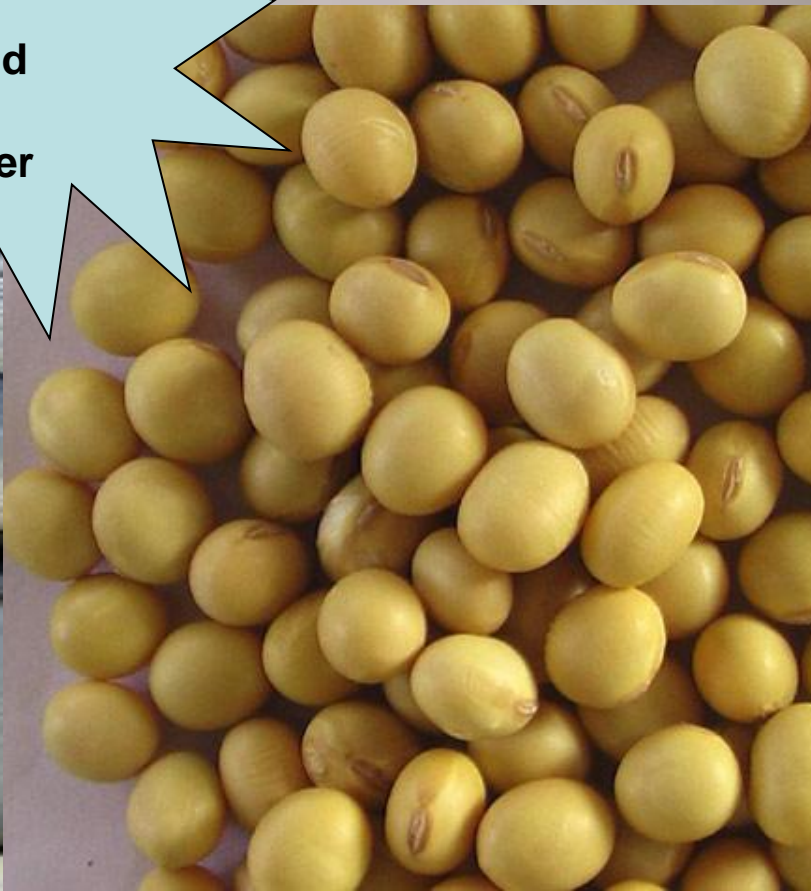
Cooperation:

NTNU NanoLab, NTNU Supercomputer; SINTEF, MIT, Fraunhofer IWM

Natures building blocks

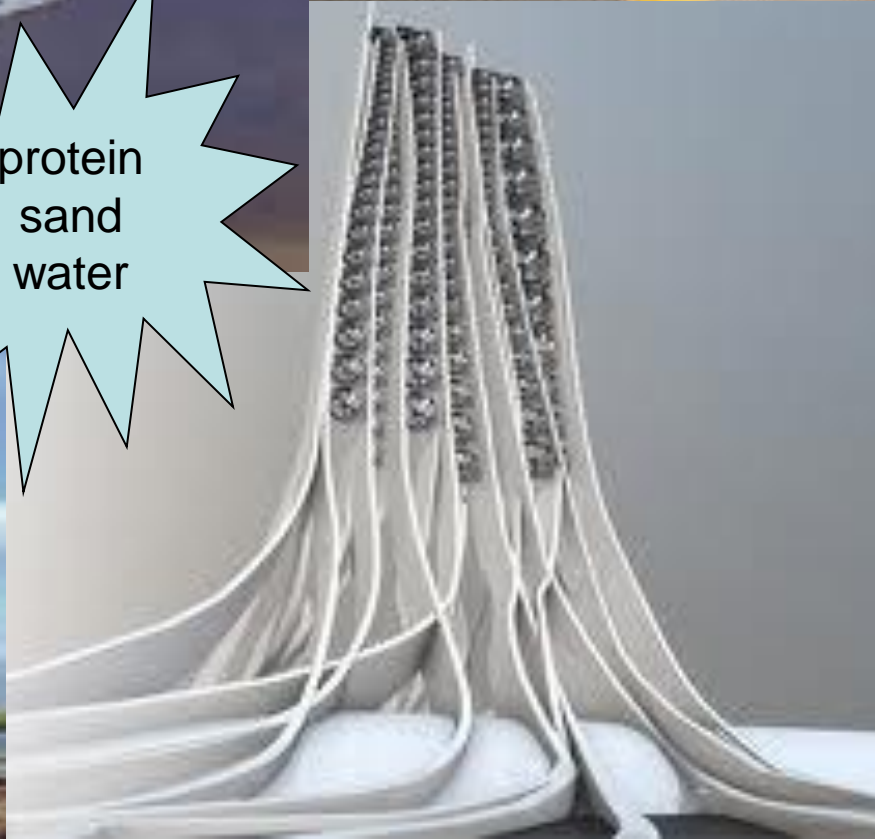


**Protein
+
Sand
+
Water**





protein
sand
water



The Space Elevator

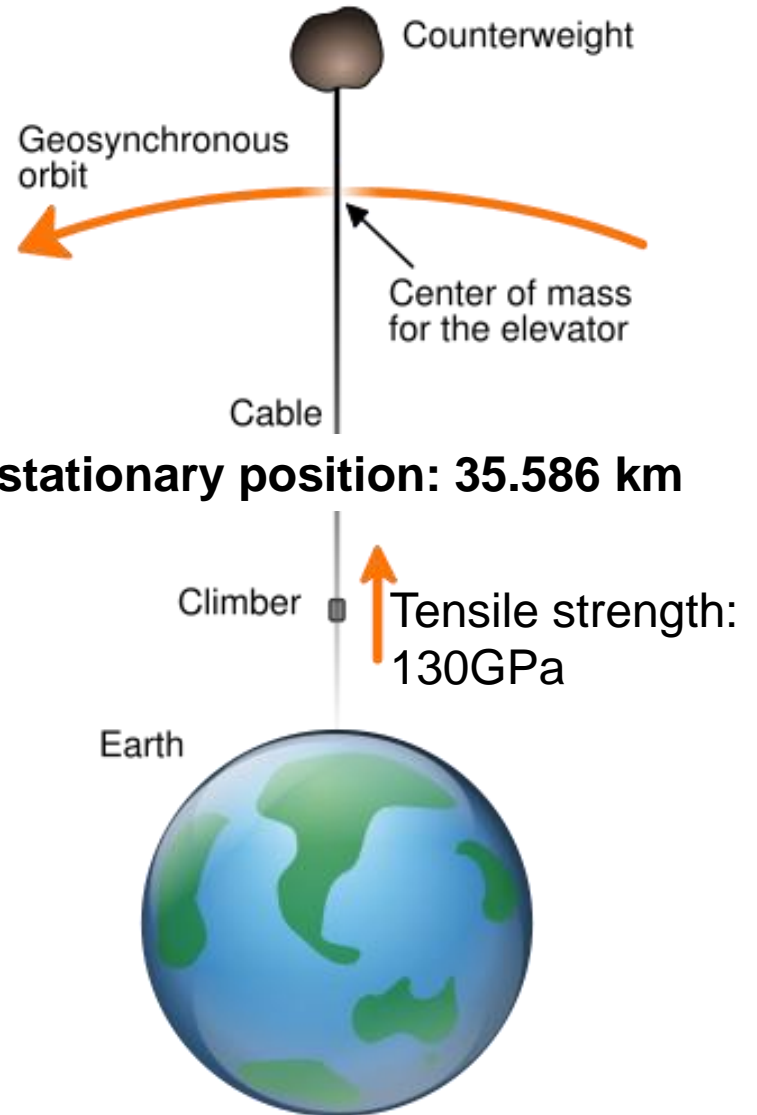


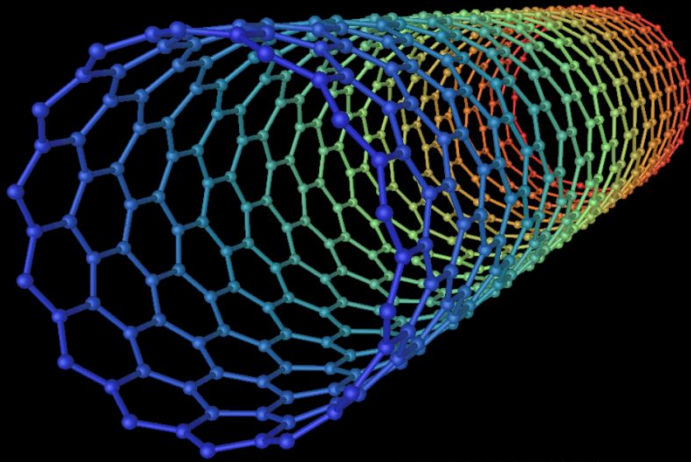
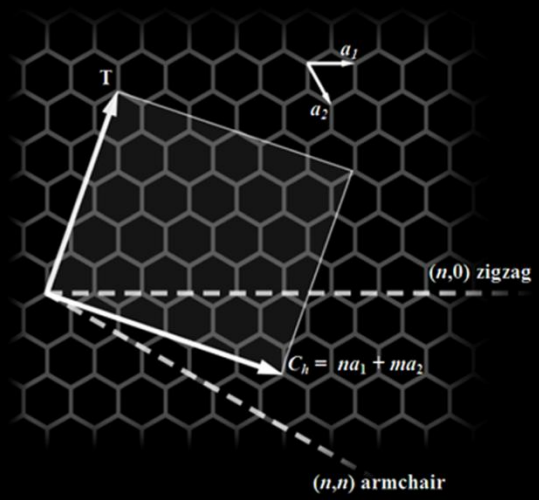
Material for the elevator-project



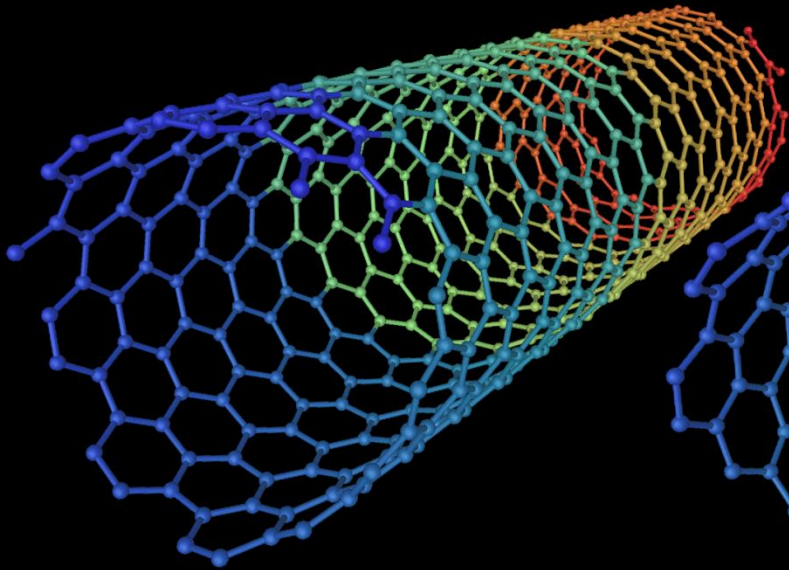
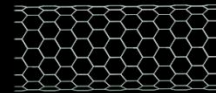
Length to geostationary position: 35.586 km

100.000 km
launching into outer space

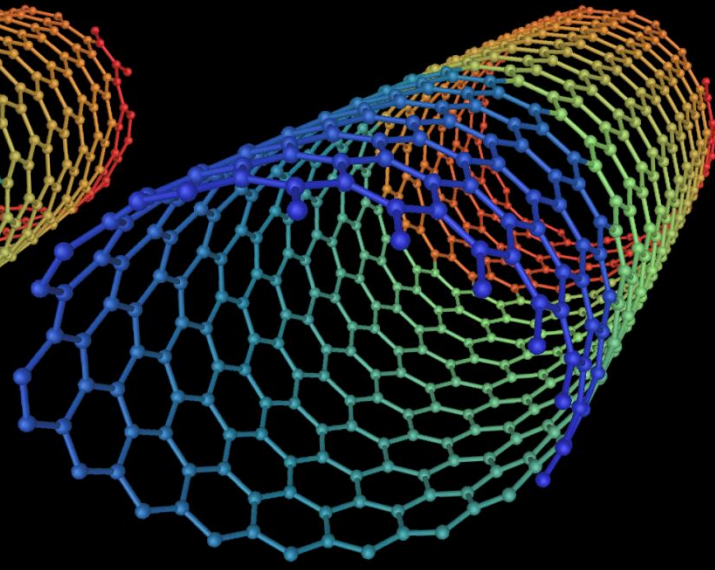
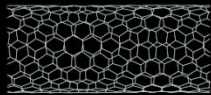




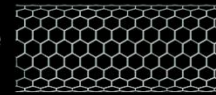
(0,10) nanotube
(zig-zag)



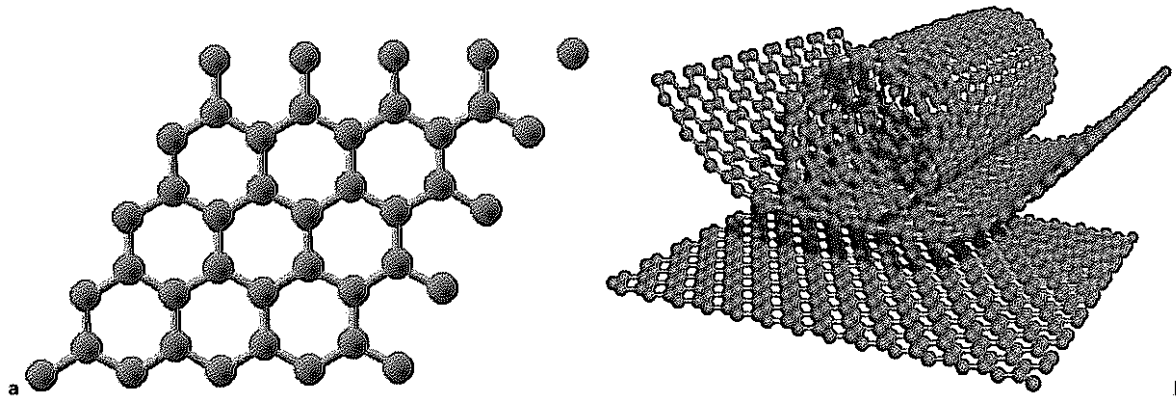
(7,10) nanotube
(chiral)



(10,10) nanotube
(armchair)



Carbon nanotubes

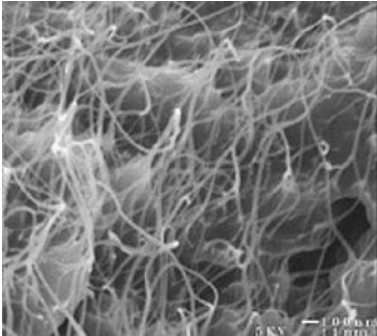
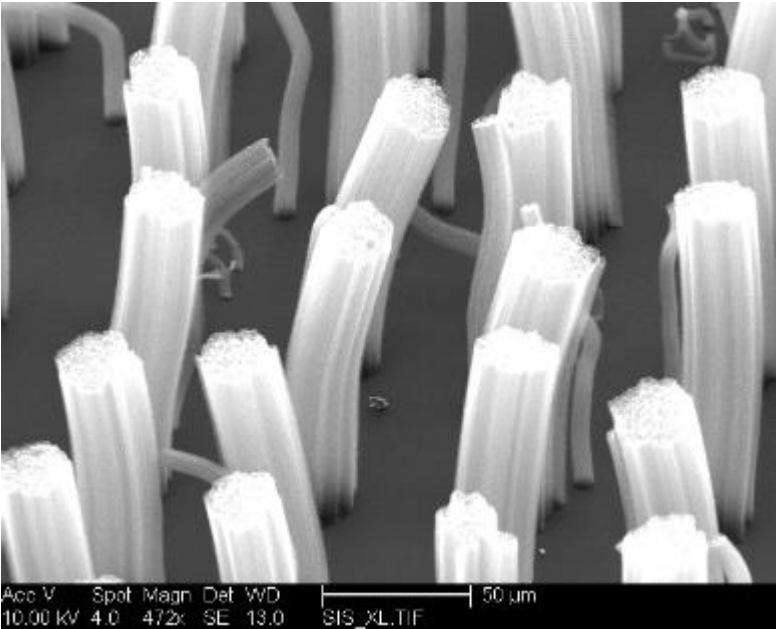
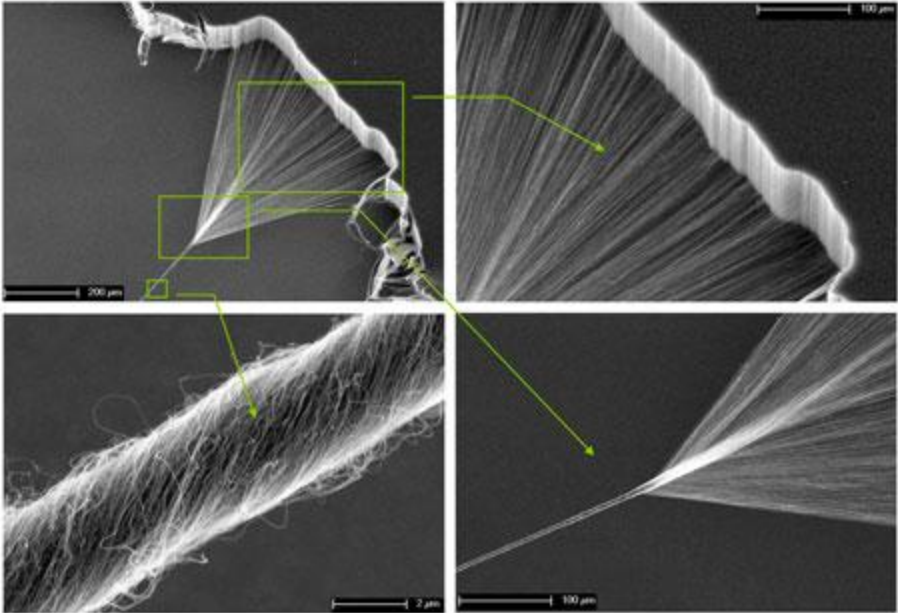
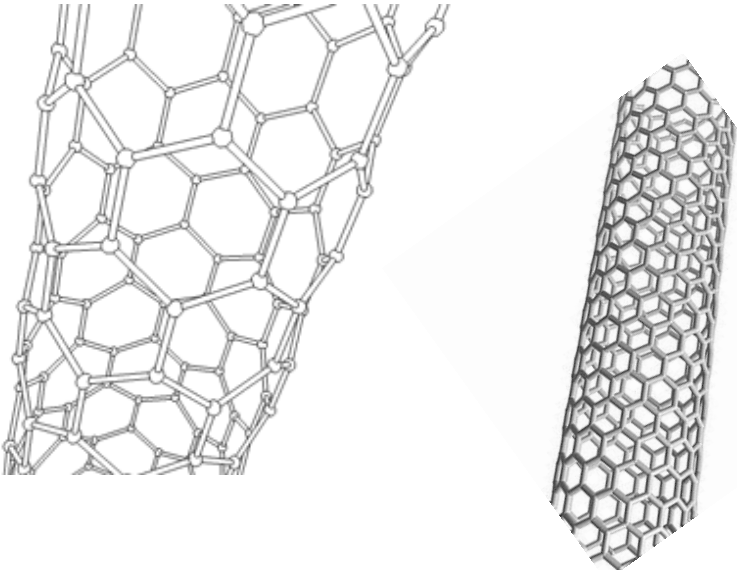


2 a Graphene sheet and b schematic diagram showing how graphene sheet might be rolled to form tube¹⁶

Table 1 Measured strength of carbon nanotube based ropes as function of length

Length	Strength, GPa	Reference
460 nm	150	25
1.8 μm	24	26
2.9 μm	28	26
6.0 μm	39	26
6.5 μm	20	26
6.7 μm	35	26
6.9 μm	63	26
11.0 μm	21	26
1–2 mm	3.6	27
2 mm	1.7	28

Carbon nanotubes



SUPERHYDROPHOBIC CNT SURFACES

Bouncing Water Droplet on a Superhydrophobic Carbon Nanotube Array

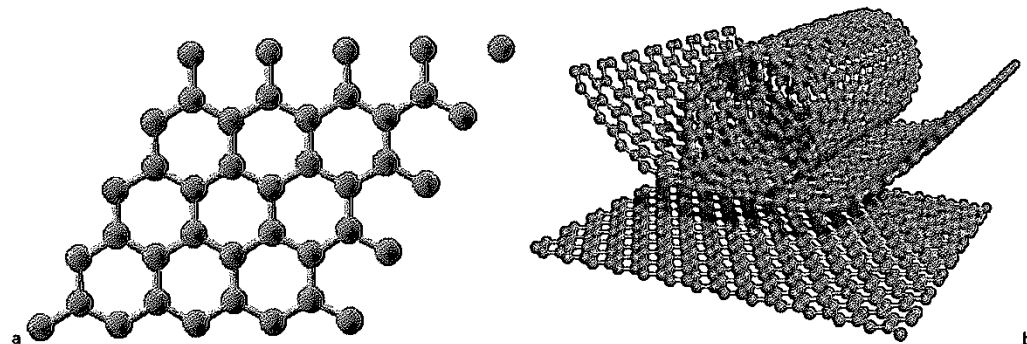
Adrianus I. Aria and Morteza Gharib

Graduate Aeronautical Laboratories,
California Institute of Technology, Pasadena, CA 91125, USA

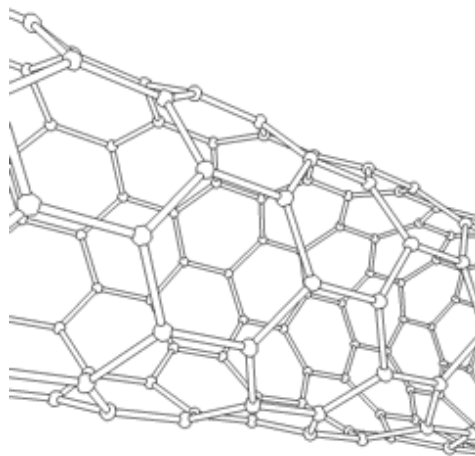
October 8, 2010

Abstract

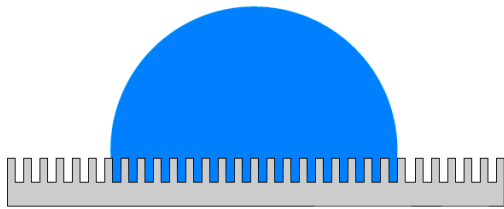
Over the past few decades, superhydrophobic materials have attracted a lot of interests, due to their numerous practical applications. Among various superhydrophobic materials, carbon nanotube arrays have gained enormous attentions simply because of their outstanding properties. The impact dynamics of water droplet on a superhydrophobic carbon nanotube array is shown in this fluid dynamics video.



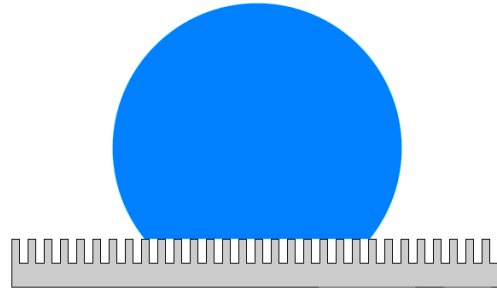
2 a Graphene sheet and b schematic diagram showing how graphene sheet might be rolled to form tube¹⁶



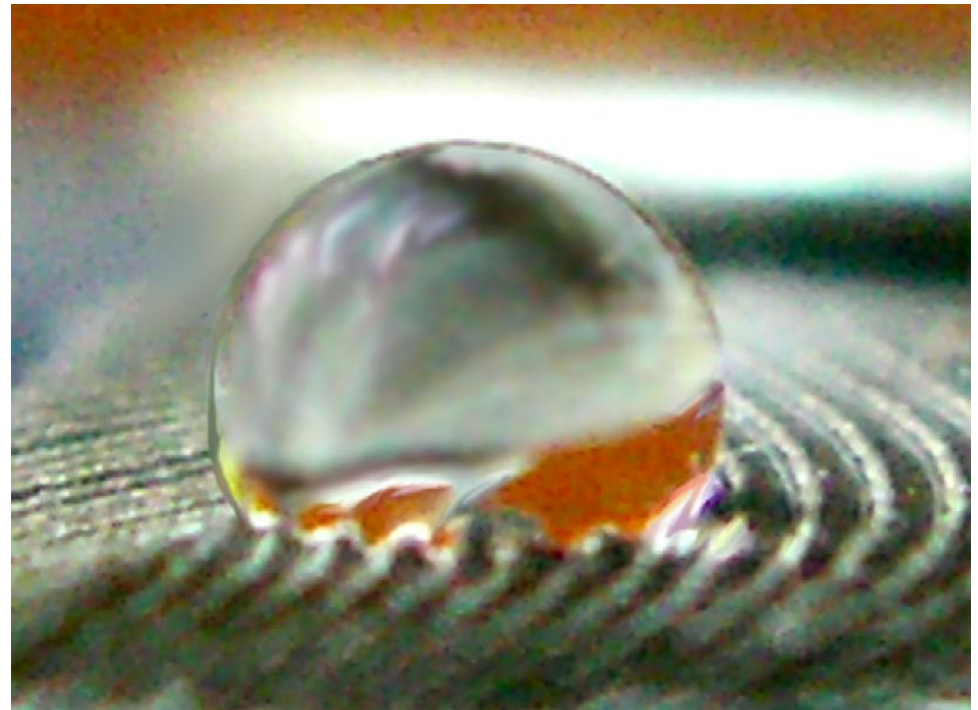
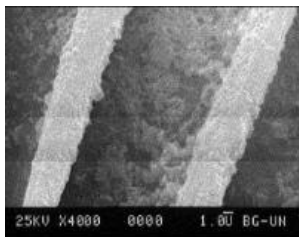
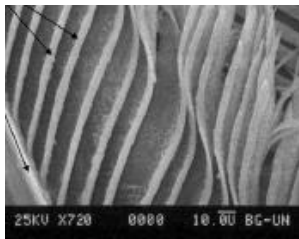
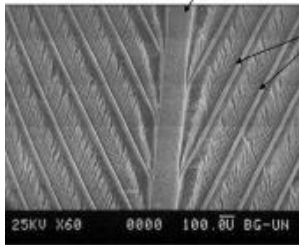
Wenzel



Cassie - Baxter



Pigeon feathers



Lotus leaf



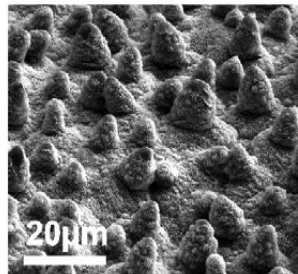
Macroscale

Non-wetting water droplet



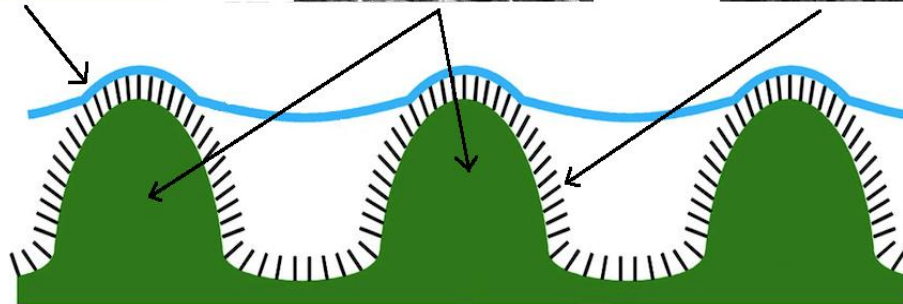
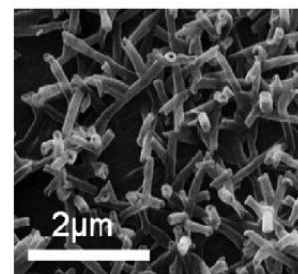
Microscale

Epidermal plant cells

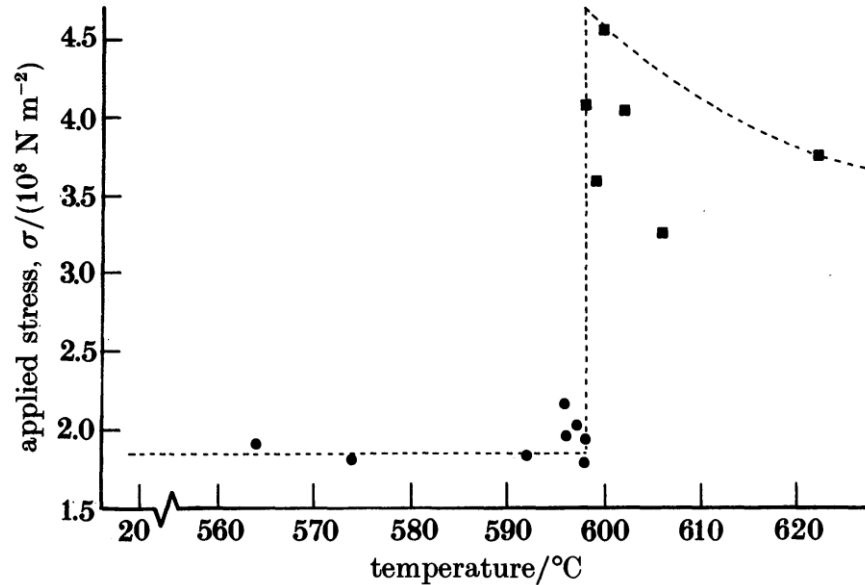


Nanoscale

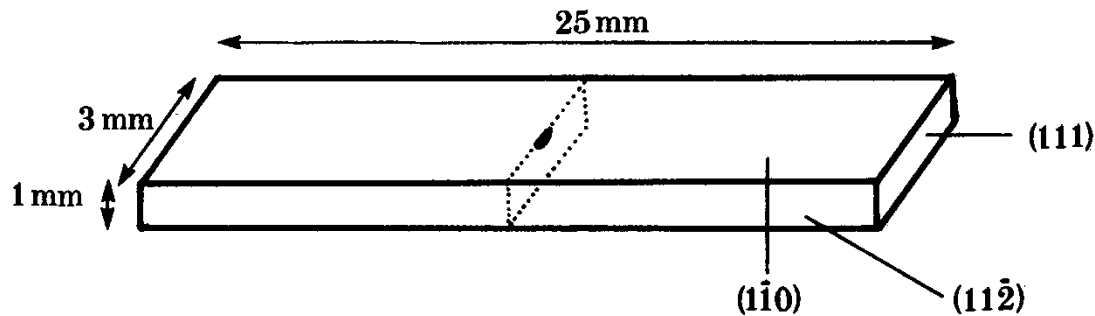
Hydrophobic wax crystals



Brittle to Ductile Transition (BDT) measurements on single crystals silicon



Sharp transition from brittle to ductile behavior



- **Pair potential:** all bonds depend only on pairs of atoms

$$\phi_i = \frac{1}{2} \sum_{j=1..N_{neigh}} \phi(r_{ij})$$

- **EAM potential:** in addition to pairs of atoms have contribution due to environment of atoms, expressed through electron density (which is a pair potential)

$$\phi_i = \sum_{j=1..N_{neigh}} \frac{1}{2} \phi(r_{ij}) + F(\rho_i(r_{ij}))$$

depends on all neighbors of i (multi-body)

- **MEAM potential:** electron density itself is also a multi-body potential (depends on bond angles)

$$\phi_i = \sum_{j=1..N_{neigh}} \frac{1}{2} \phi(r_{ij}) + F(\rho_i(r_{ij}, \theta_{ijk}))$$

Modeling of silicon: Interatomic Potential

Several empirical potentials fitted to experimental data:

*Stillinger-Weber*¹

*Tersoff*²

EDIP (Environment dependent Interatomic Potential)³

Problems:

1. Inaccurate description of silicon bonds close to fracture
2. Incorrect predictions of fracture modes (ductility and crack opening instead of brittle).

Coupling Tight-Binding or QM with empirical potentials

1. TB/EDIP and TB/Tersoff coupling^{4,5}
2. DFT/Stillinger-Weber coupling⁶

Can model brittle fracture well but too small reactive regions for dislocation emission and plasticity.

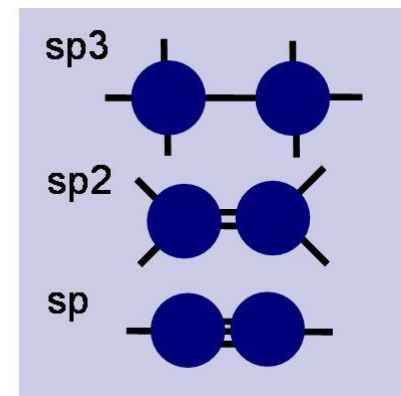
1. Stillinger and Weber, PRB **31**(8), 5262 (1985); 2. Tersoff, PRL **56**(6), 632 (1986); 3. Justo et al, PRB **58**(5), 2539 (1998); 4. Abraham et al, Europhys. Lett. **44**, 783 (1998); 5. Bernstein and Hess, PRL **91**(2), 025501 (2003); 6. Csanyi et al, PRL **93**(17), 175503 (2004).

Reactive force field (ReaxFF)¹

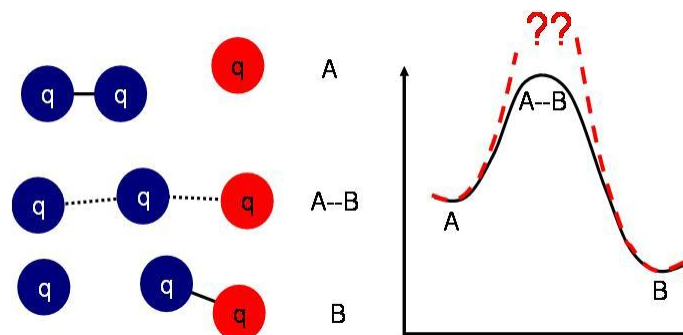
$$E_{system} = E_{bond} + E_{vdWaals} + E_{Coulomb} + E_{val} + E_{tors} + E_{over} + E_{under}$$

2-body
3-body 4-body

multi-body



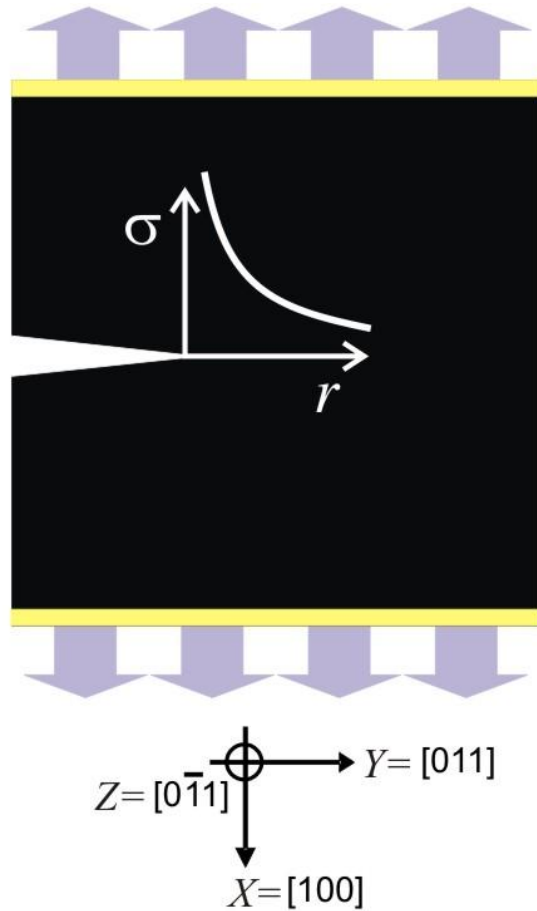
	Nonreactive FFs	Reactive FFs ReaxFF
Ground state energies (e.g. distinguish sp ³ -sp ² -sp...)	Yes (few states)	Yes
Excited / transition states (go from one to another ground state; see also Figure 4)	No	Yes
Breaking of bonds and continuous energies during reactions	No (sometimes: Morse functions for bond breaking but energetics are typically wrong)	Yes
Formation of bonds	No	Yes
Charge flow during reactions	No	Yes
Organic-Inorganic interfaces (or between other materials)	No (mostly)	Yes (bridging FFs)
Retyping necessary after reaction	Yes (have C2,C3 etc. for different hybridization)	No (atom types are element types)



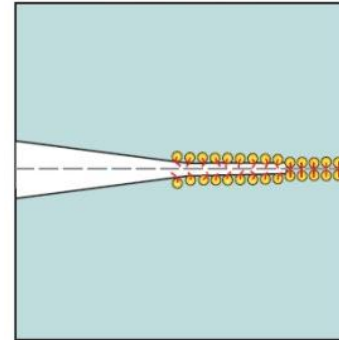
A bond length/bond order relationship is used to obtain smooth transition from non-bonded to single, double, and triple bonded systems.

1. A.C.T. van Duin et al, J Phys Chem A **105(41)**, pp. 9396 (2001).

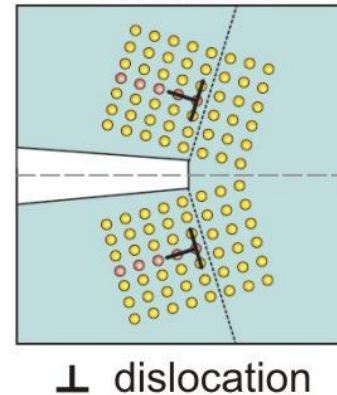
Fracture model



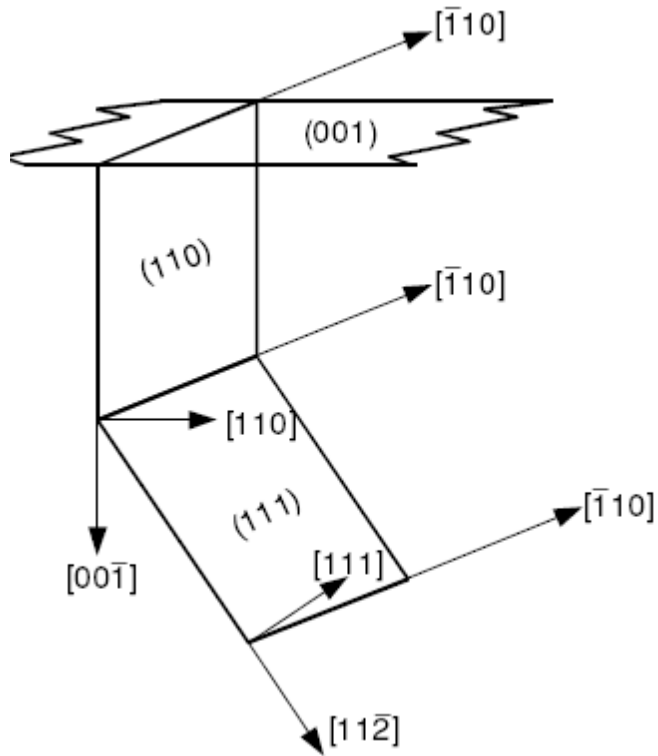
brittle



ductile



- Use of parallelized code with entire system (30.000-200.000 atoms) modeled by ReaxFF.
- Mode I loading of a crack in single crystal silicon. Notch in $[011]$ direction on a (100) plane. Periodic boundary conditions in x- and z direction



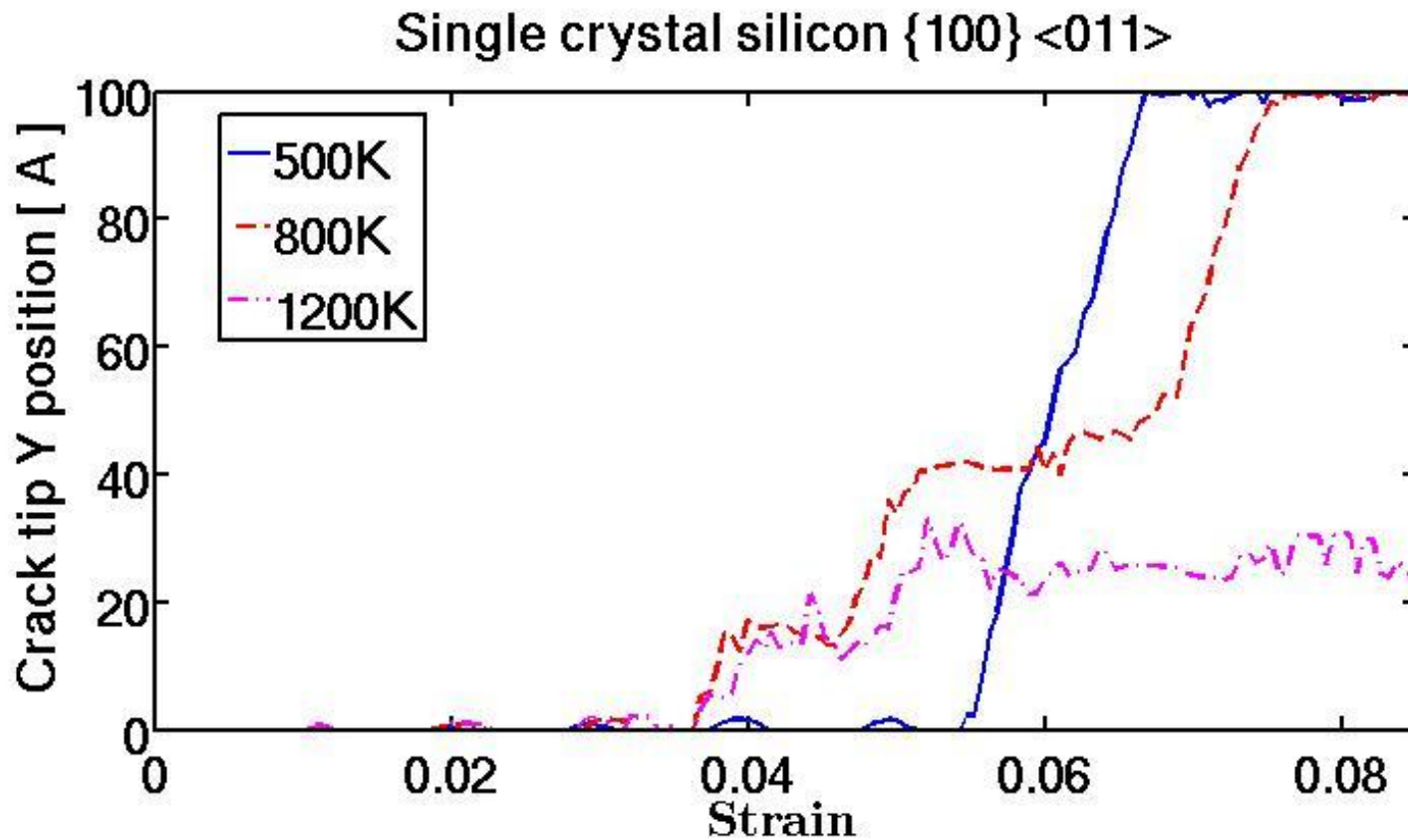
Case 1: {110} cleavage fracture plane
 in the $\langle 100 \rangle$ and $\langle 110 \rangle$ directions.
 Semiconductors, MEMS devices

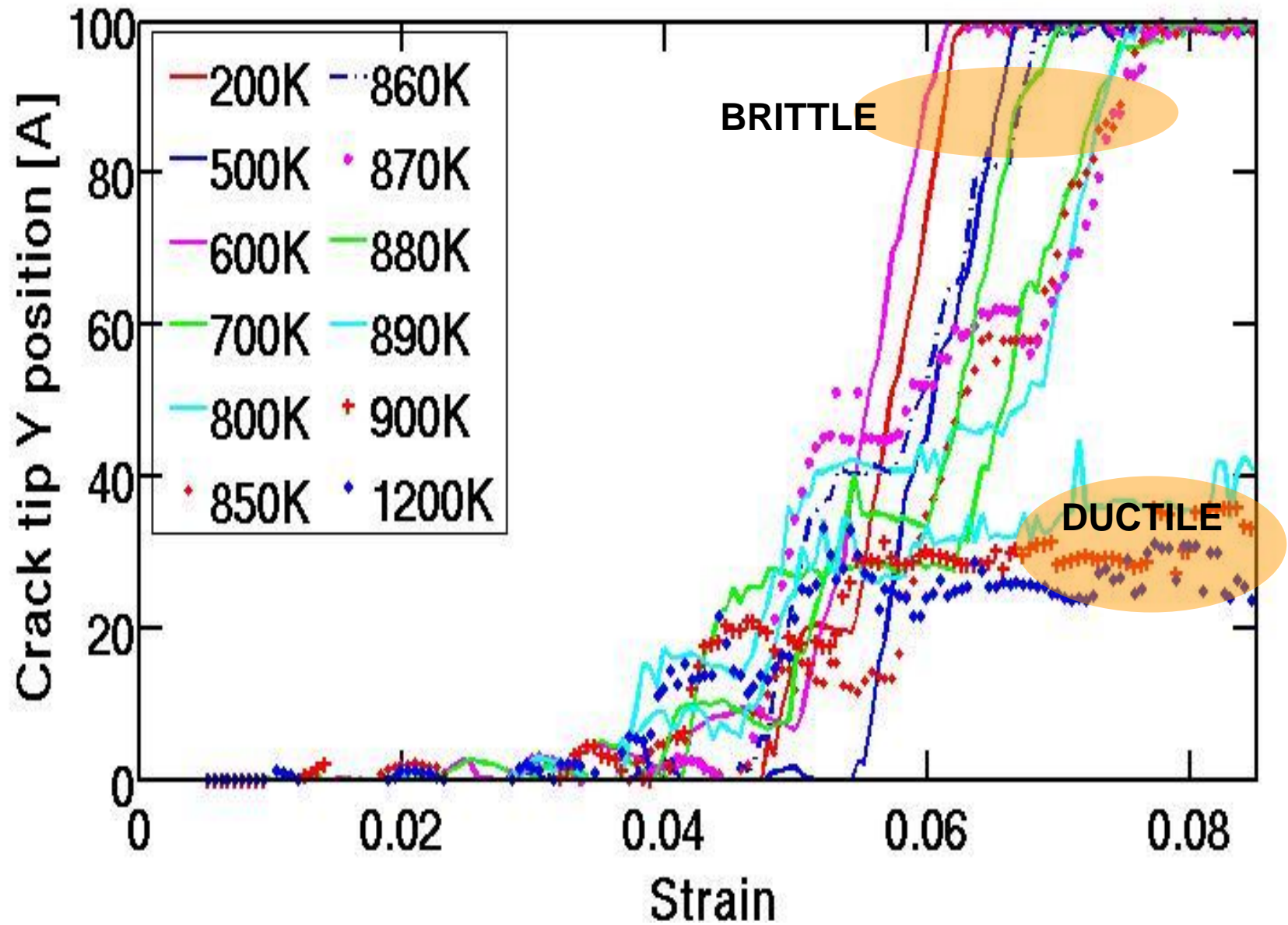
Case 2: {111} cleavage fracture plane
 in the $\langle 110 \rangle$ and $\langle 112 \rangle$ directions.
 Fundamental studies

Case 3: {100} cleavage fracture plane
 In the $\langle 011 \rangle$ direction.
 Not observed in practice

Small Model:

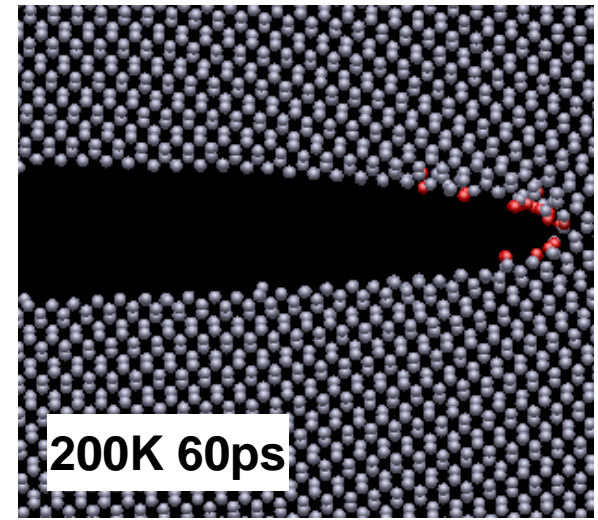
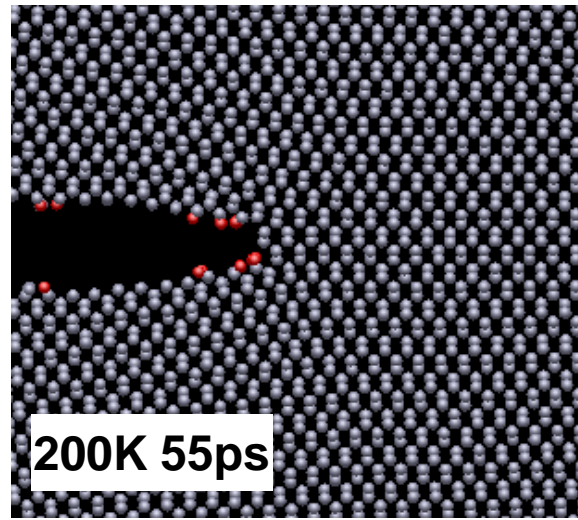
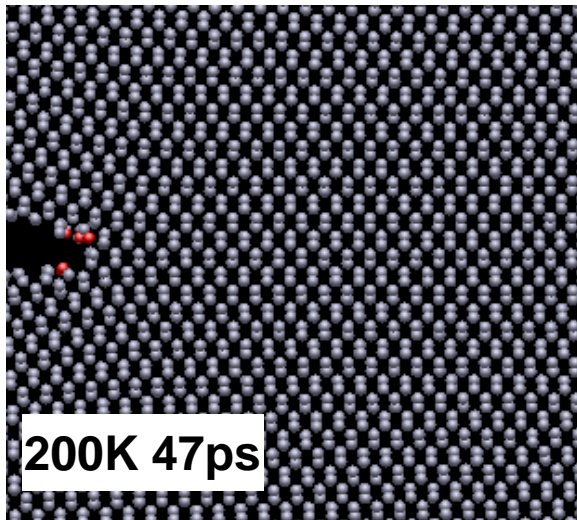
27.000 atoms, 200Å long and wide, thickness 15Å



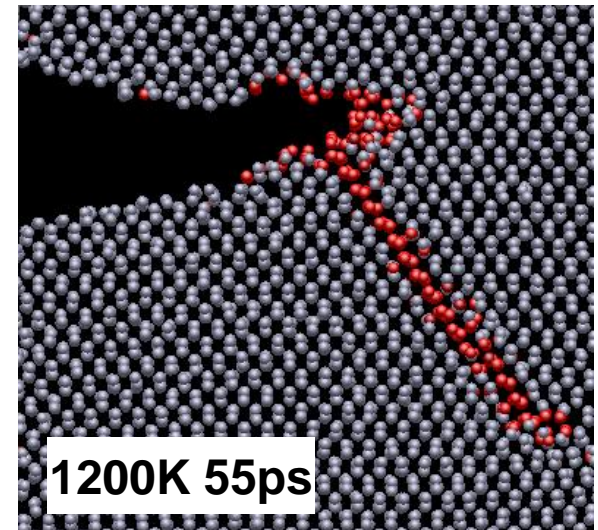
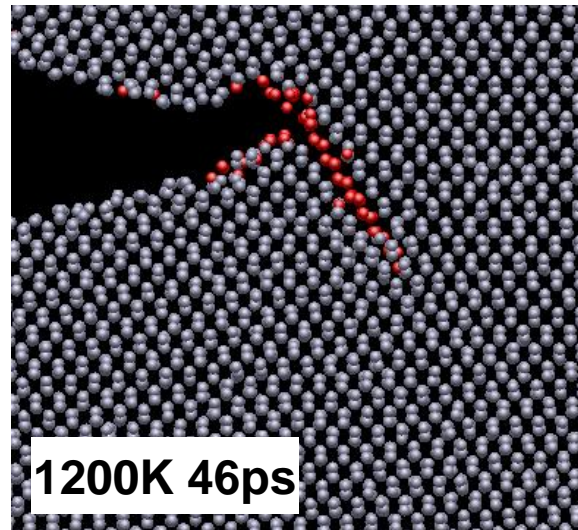
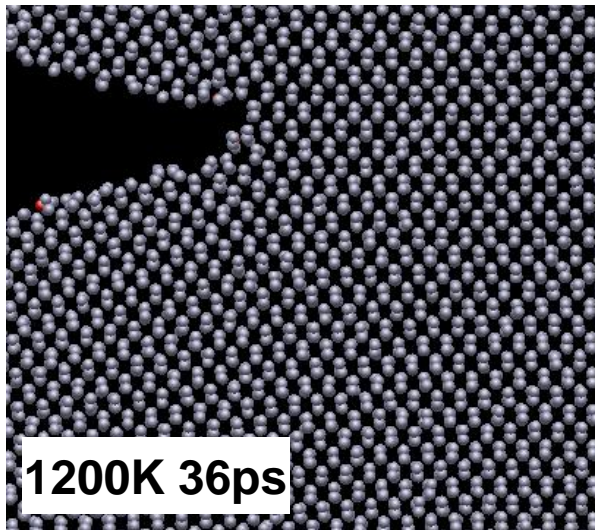


Atomistic Study of Crack-Tip Cleavage to Dislocation Emission Transition in Silicon Single Crystal
 Dipanjan Sen, Christian Thaulow Stella V. Schieffer Alan Cohen and Markus J. Buehler
 PRL 104, 235502 (2010)

Crack motion at different temperatures



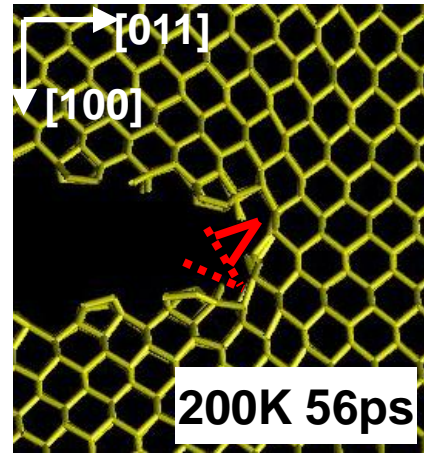
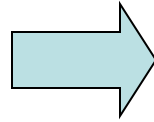
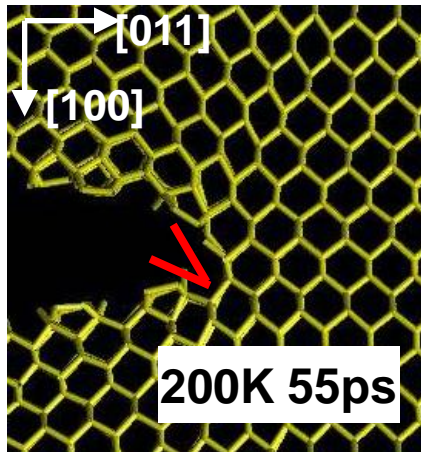
Crack propagation snapshots at low Temp- brittle fracture



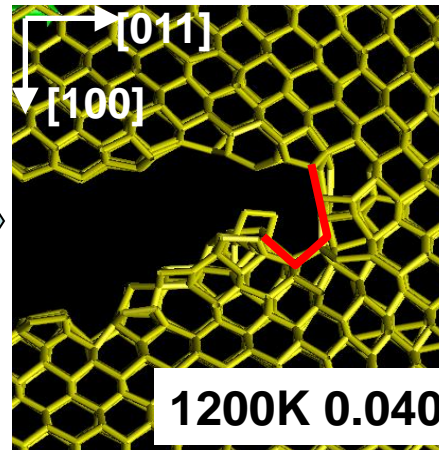
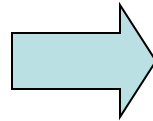
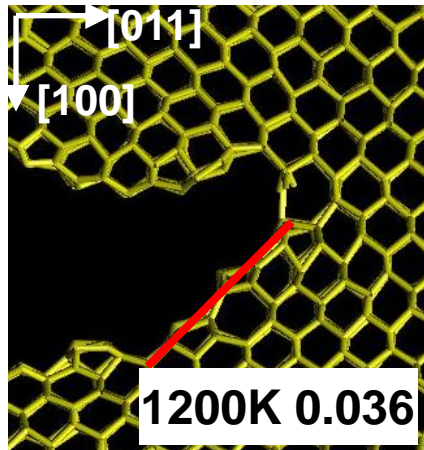
Crack propagation snapshots at high Temp- ductile fracture (slip vector analysis)¹

1. Zimmermann et al, PRL **87**, 165507 (2001).

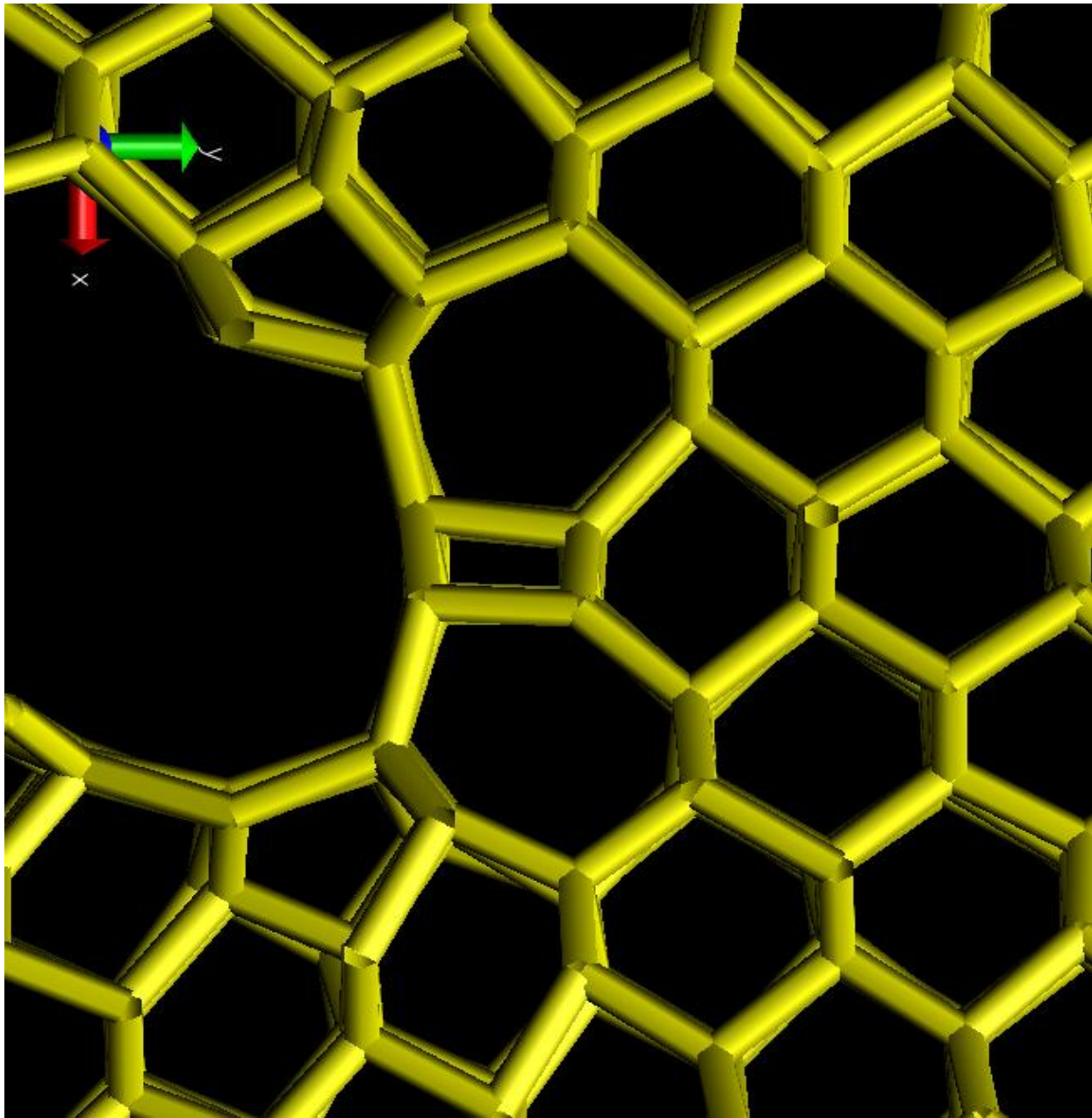
Details of crack tip motion at low and high temperature



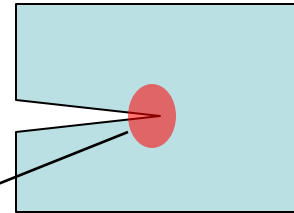
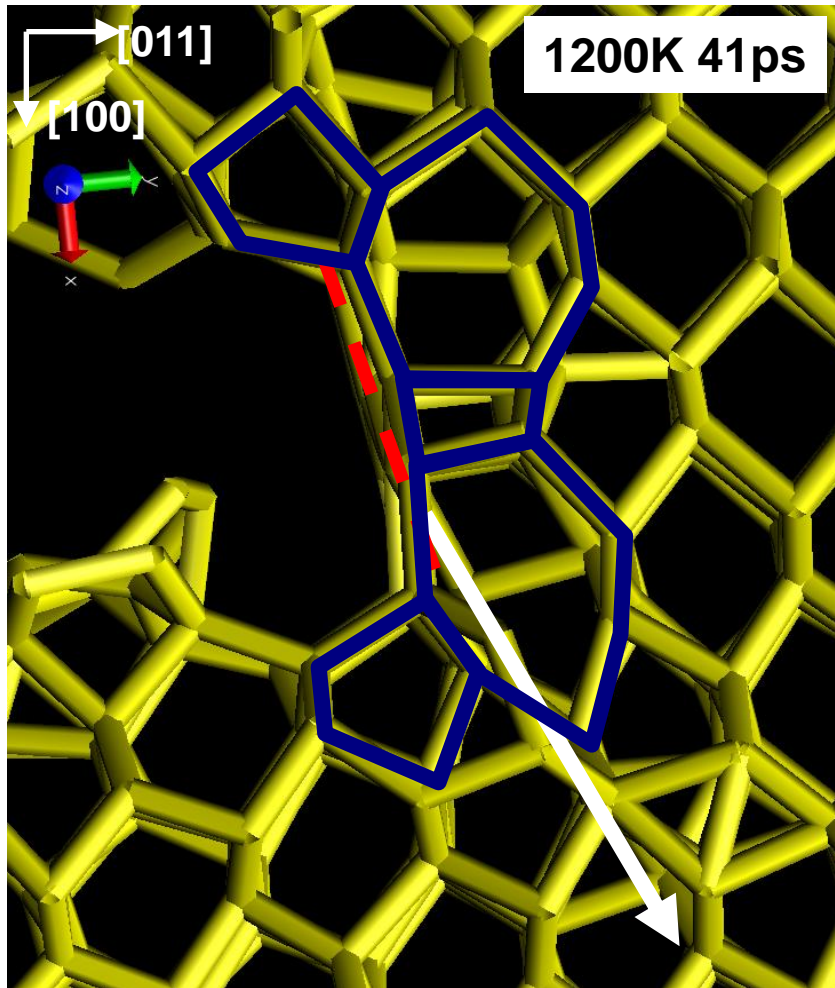
200 K: Crack proceeds in a jagged manner by small steps along (111) planes



1200 K: Crack forms ledges and small amorphous zones consisting of 5-7 defects

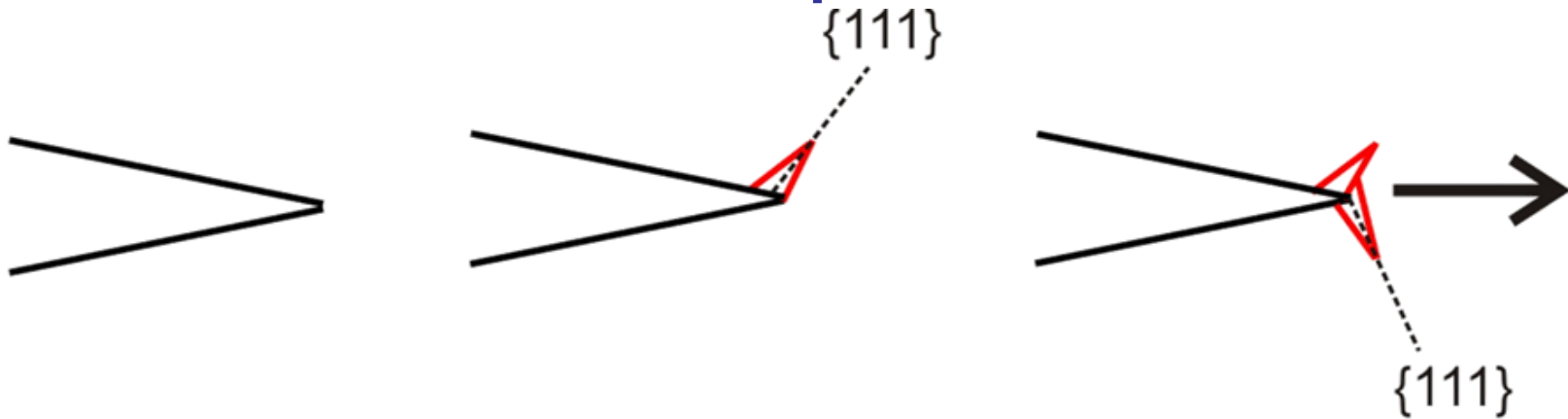


Atomistic mechanism at the crack tip at time of dislocation emission

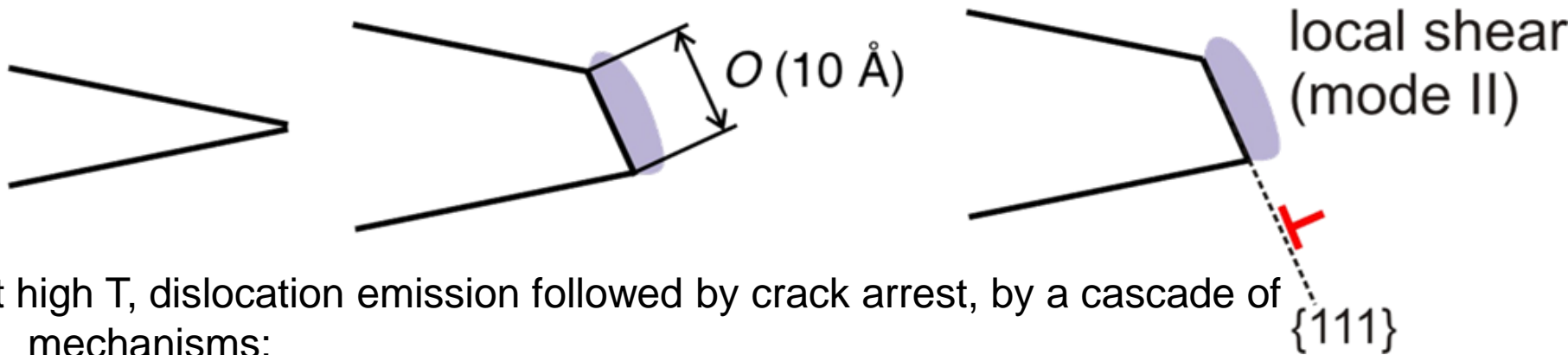


- Ledge formation
- 5-7 ring cluster formation around crack tip

Schematic of crack tip mechanisms observed



At low T, brittle fracture by small crack steps on (111) plane, expected as (111) surface energies are lower.

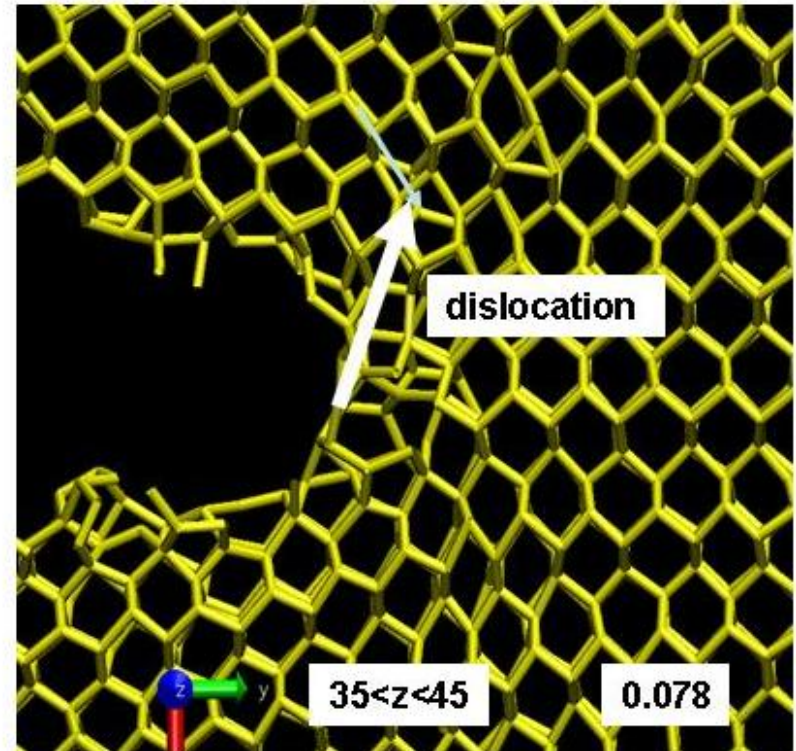
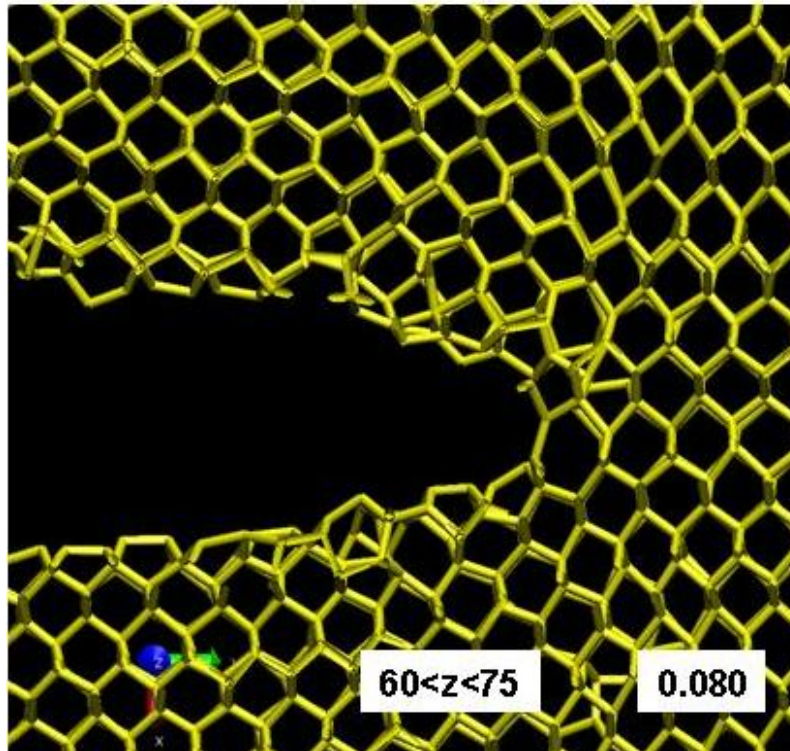


At high T, dislocation emission followed by crack arrest, by a cascade of mechanisms:

- small ($\approx 10 \text{ \AA}$) disordered zone formed consisting of 5-7 rings at crack tip reducing mode I stress intensity at the tip
- ledge formation on (111) planes
- dislocation emission at the ledge due to increased mode II loading

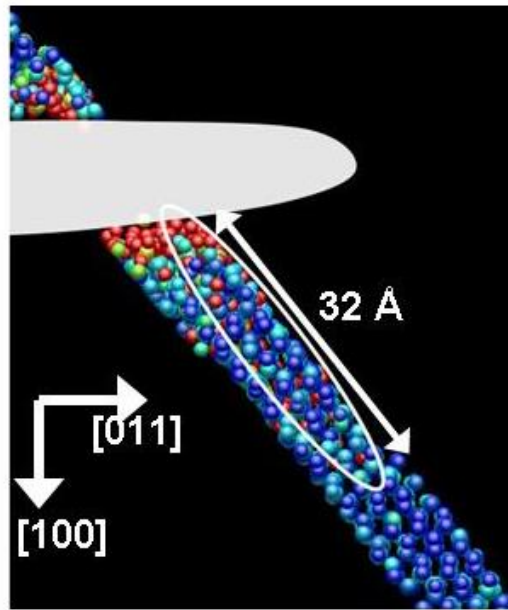
Large model

Increase the thickness of the model, 200.000 atoms,
100Å thickness

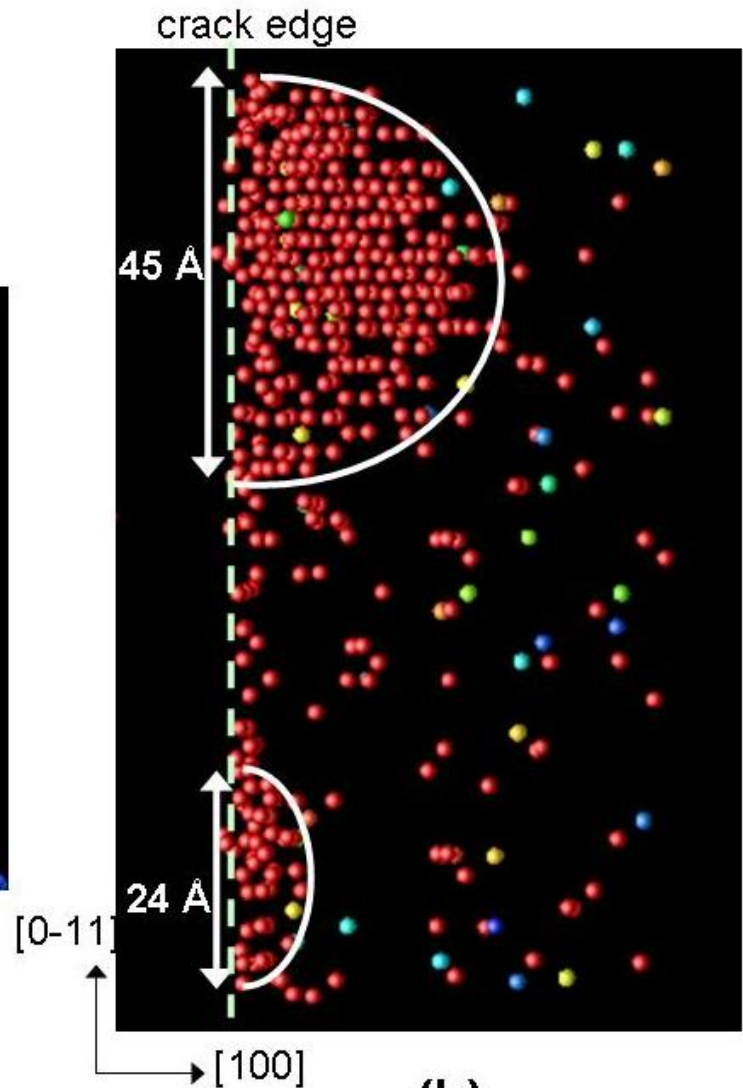


Example of crack front structure at two positions along the crack front.

Analysis of the partial dislocation loop emission at the crack tip on the lower crack surface

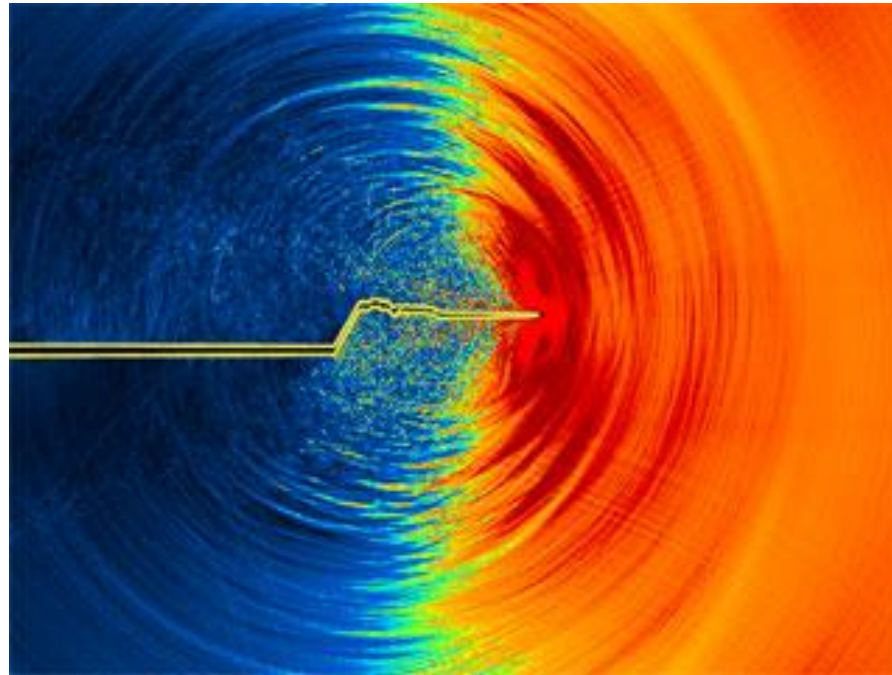


(a)



(b)

Must the ledges be formed as an integrated part of the dynamic crack front events?



Dynamic instability occurring on the crack tip. As the crack velocity increases, its forward motion becomes more and more unstable: the crack changes direction and leaves behind an increasingly irregular surface. M J Buehler



f02n02io.301605.0	forecast	6/4	19:51	R	50	forecast	f01n11
f05n02io.301592.0	forecast	6/4	19:51	R	50	forecast	f03n08
f02n02io.301606.0	forecast	6/4	19:51	R	50	forecast	f04n11
f05n02io.301593.0	forecast	6/4	19:51	R	50	forecast	f06n05
f02n02io.301607.0	forecast	6/4	19:51	R	50	forecast	f05n04
f05n02io.301594.0	forecast	6/4	19:51	R	50	forecast	f06n04
f02n02io.301608.0	forecast	6/4	19:51	R	50	forecast	f06n11
f05n02io.301595.0	forecast	6/4	19:51	R	50	forecast	f06n10
f02n02io.301609.0	forecast	6/4	19:51	R	50	forecast	f06n08
f05n02io.301596.0	forecast	6/4	19:51	R	50	forecast	f06n03
f02n02io.301610.0	forecast	6/4	19:51	R	50	forecast	f01n06
f05n02io.301597.0	forecast	6/4	19:51	R	50	forecast	f06n12
f02n02io.301611.0	forecast	6/4	19:51	R	50	forecast	f06n09
f05n02io.301598.0	forecast	6/4	19:52	R	50	forecast	f05n06
f02n02io.301612.0	forecast	6/4	19:52	R	50	forecast	f06n01
f05n02io.301599.0	forecast	6/4	19:52	R	50	forecast	f04n09
f02n02io.301613.0	forecast	6/4	19:52	R	50	forecast	f04n06
f05n02io.301600.0	forecast	6/4	19:52	R	50	forecast	f03n12
f02n02io.301614.0	forecast	6/4	19:52	R	50	forecast	f04n08
f05n02io.301601.0	forecast	6/4	19:52	R	50	forecast	f01n12
f02n02io.301615.0	forecast	6/4	19:52	R	50	forecast	f03n01
f05n02io.301602.0	forecast	6/4	19:52	R	50	forecast	f03n09
f02n02io.301616.0	forecast	6/4	19:52	R	50	forecast	f04n04
f05n02io.301603.0	forecast	6/4	19:52	R	50	forecast	f01n10
f02n02io.301617.0	forecast	6/4	19:52	R	50	forecast	f02n03
f05n02io.301604.0	forecast	6/4	19:52	R	50	forecast	f03n04
f02n02io.300916.0	christth	6/2	22:22	E	50	large	

Arctic Challenges



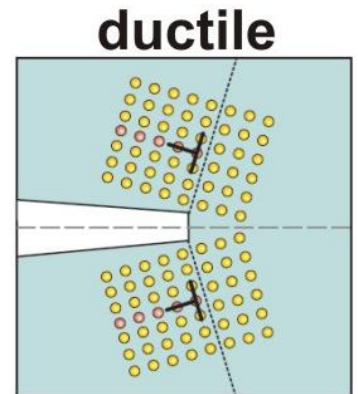
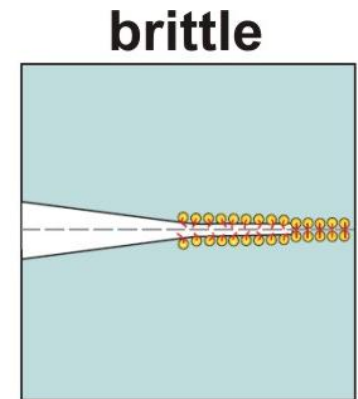
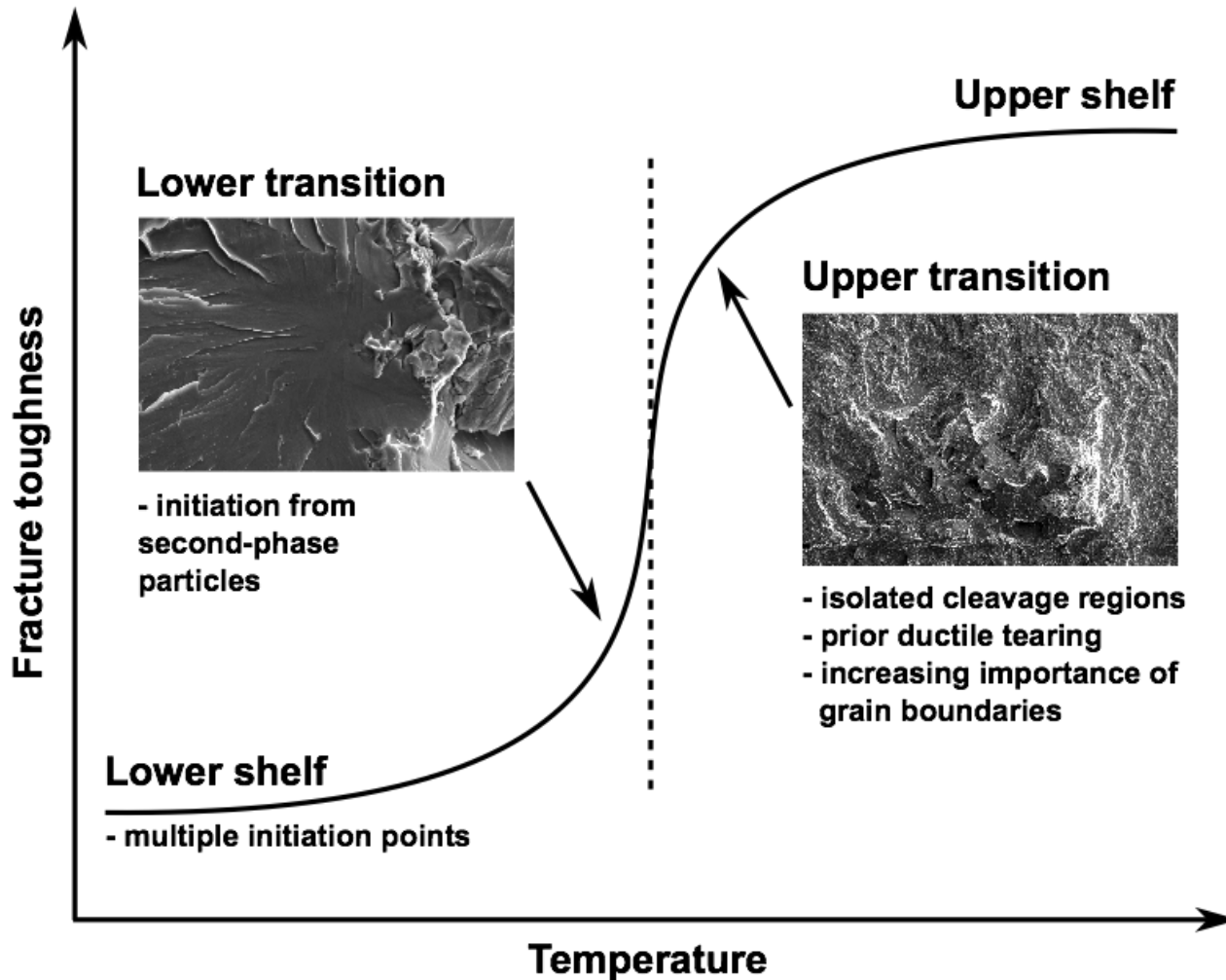
- Design temperature minus 60°C
- Icebergs
- Ice loads
- Thaw settlement
- Landslides

There is a strong motivation to understand the mechanisms of the BDT

Brittle to Ductile Transition (in Steel)

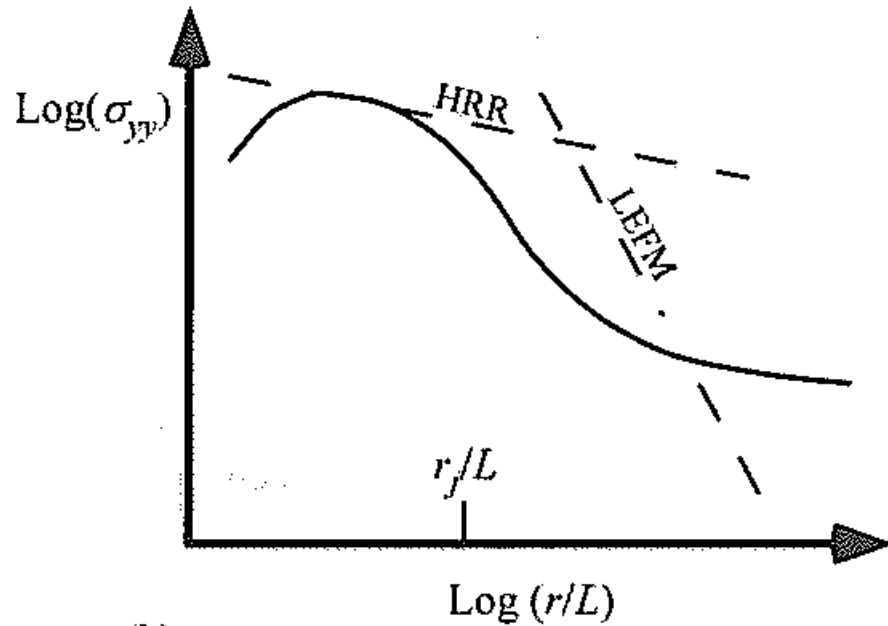
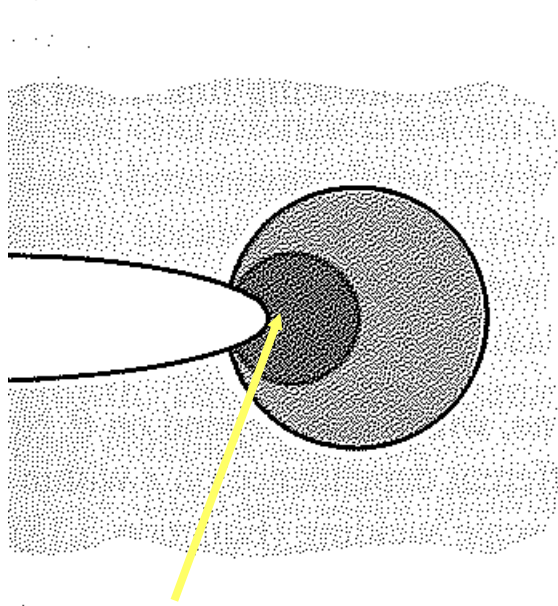


BRITTLE – DUCTILE TRANSITION



\perp dislocation

J and CTOD characterizes crack-tip conditions



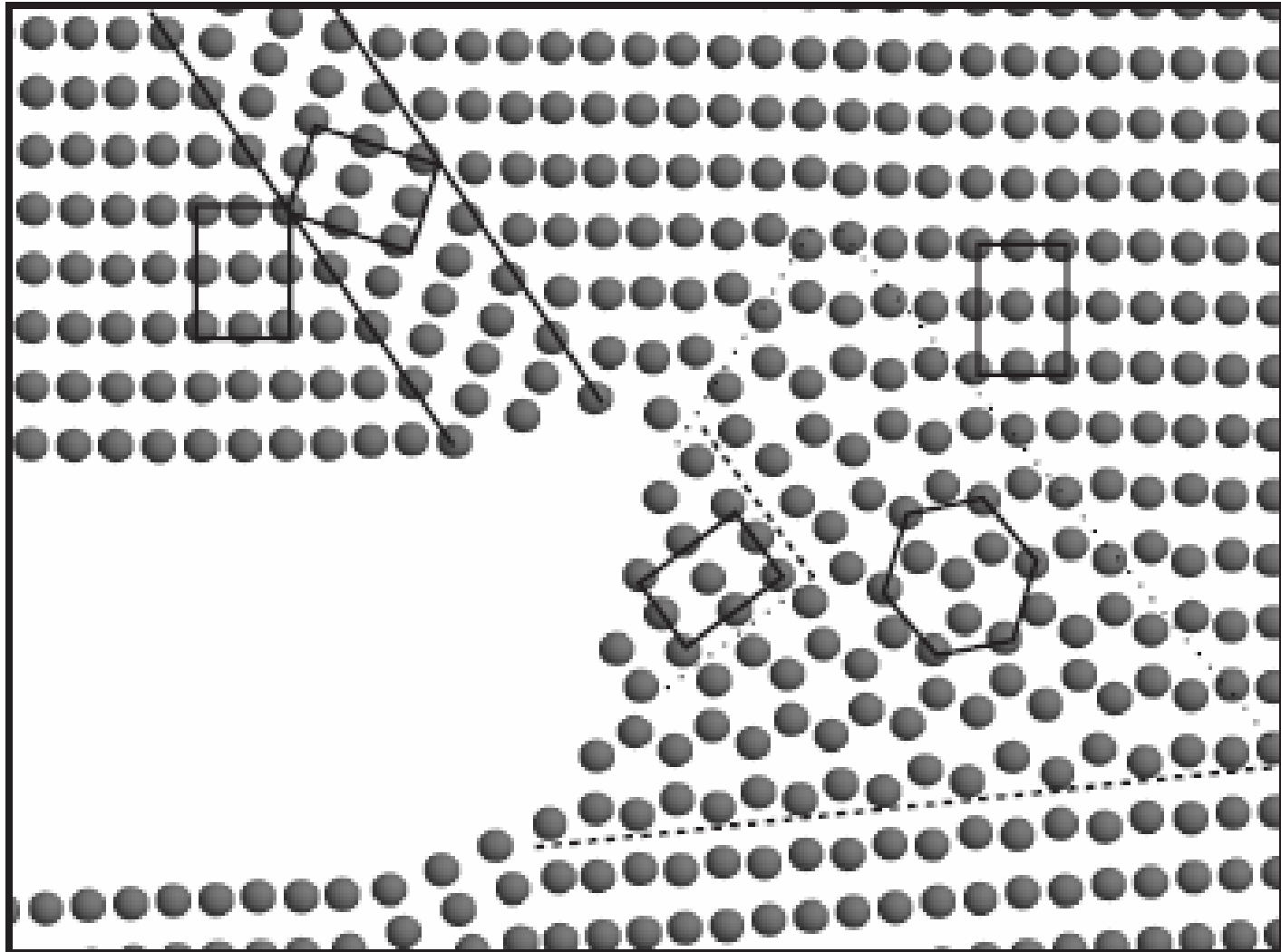
(b)

Crack Tip Process Zone

Legend:

-  Large Strain Region
-  J-Dominated Zone
-  K-Dominated Zone
-  No Single-Parameter Characterization

Crack tip mechanisms:

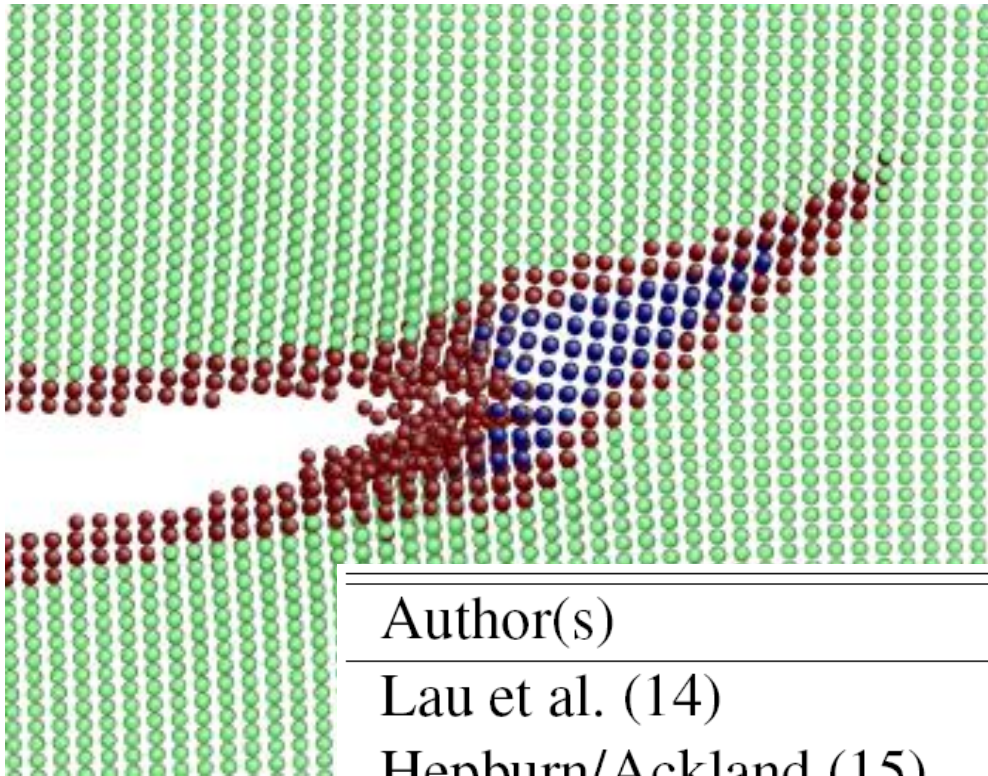


Christer H Erslund, PhD Arctic Materials

Atomistic modeling of bcc-Fe

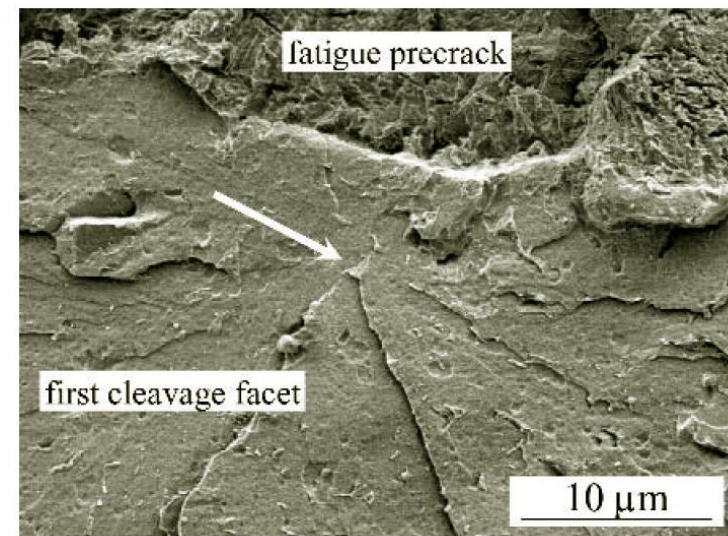
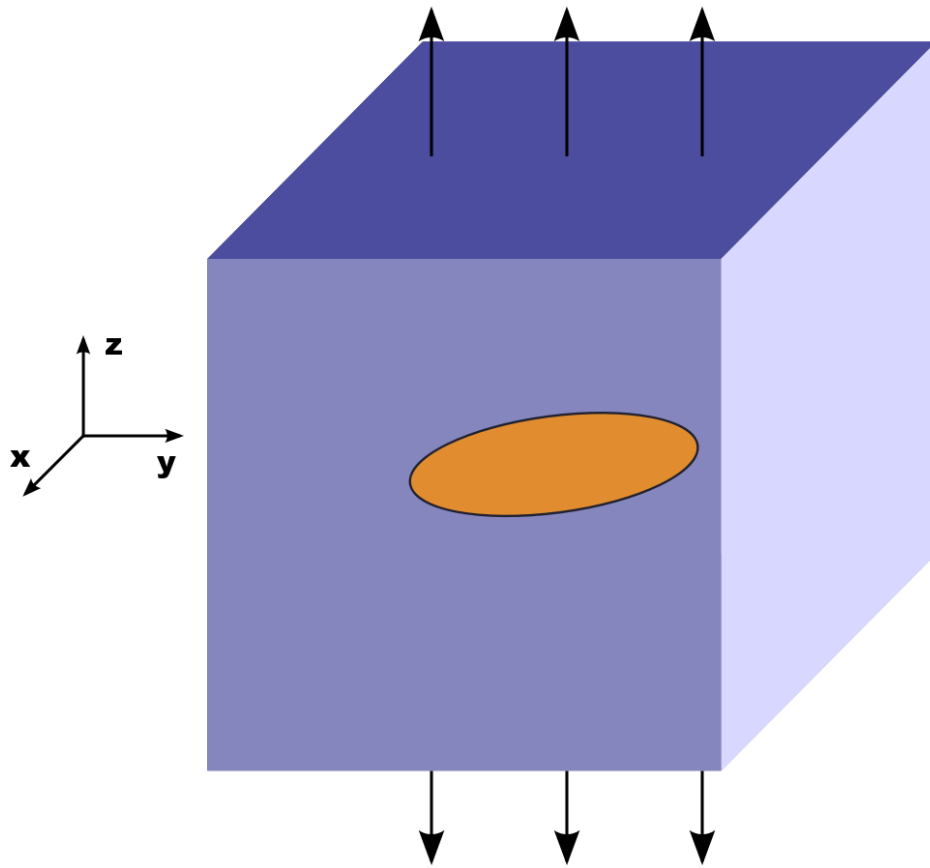


C H Erslund, C Thaulow, D Farkas and E Østby, “Atomistic studies and comparison of α -Fe potentials in mode I fracture” Presented at ECF18, Dresden, Germany, Sept 2010.

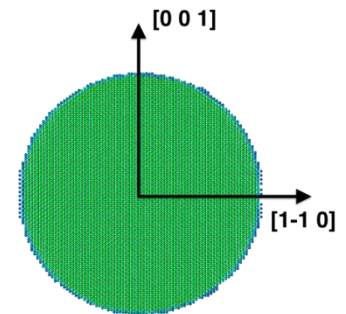


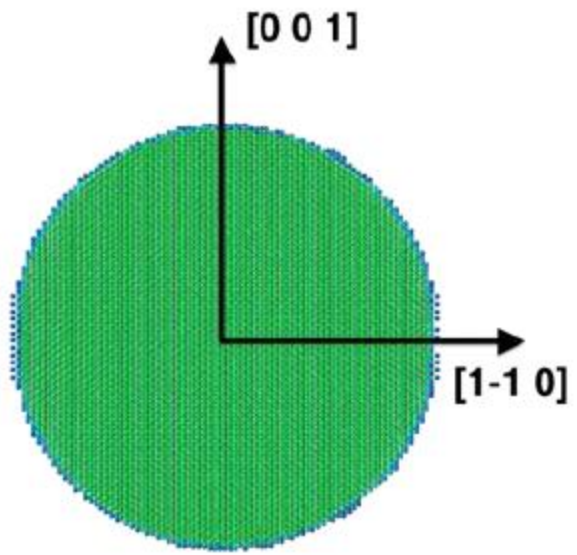
Author(s)	Year	Element(s)	Type
Lau et al. (14)	2007	Fe, C	EAM-FS
Hepburn/Ackland (15)	2008	Fe, C	EAM
Ruda et al. (16)	2009	Fe, C	EAM
Mendelev (17)	-	Fe	EAM
Müller et al. (19)	2007	Fe	ABOP

Penny shaped crack

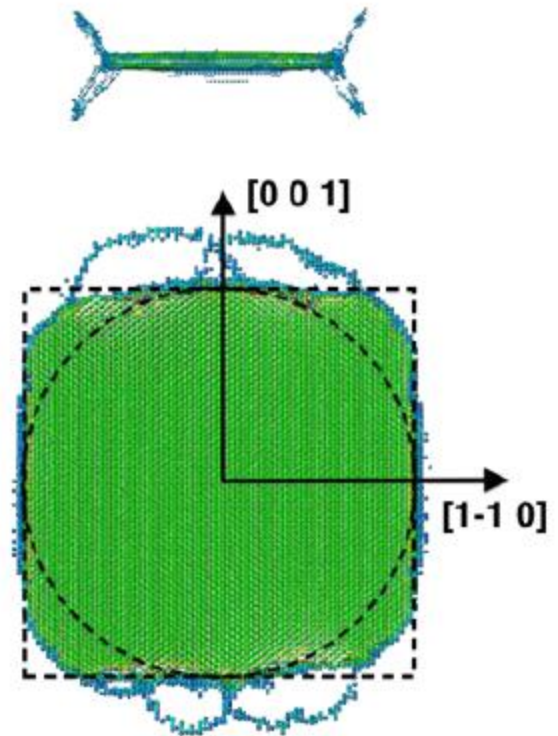


Example: Crack located on the $\{110\}$ plane

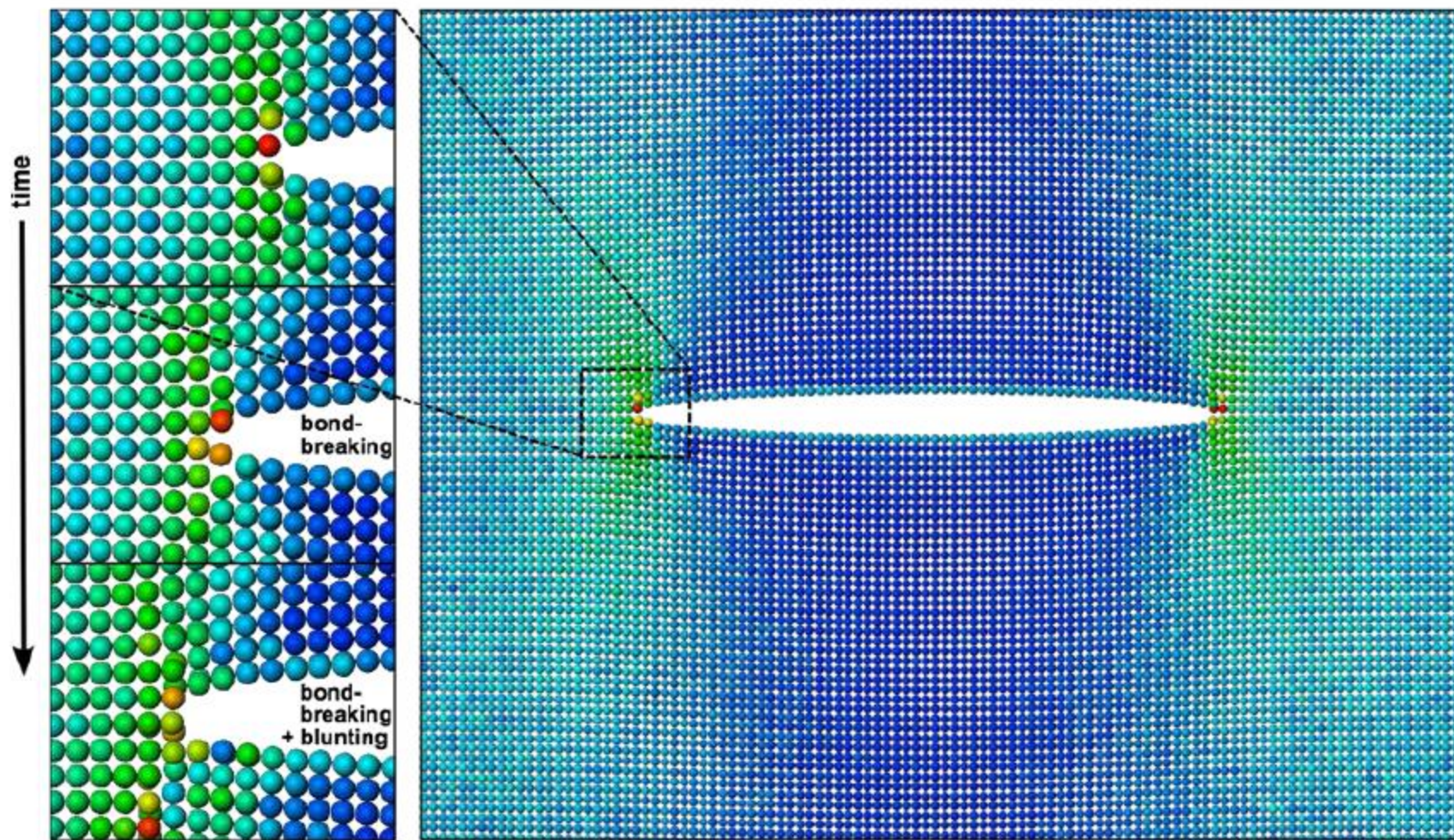


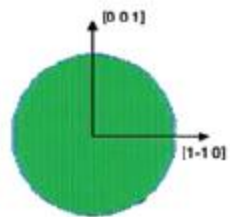


Step 1

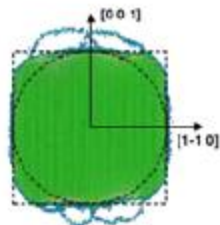


Step 2

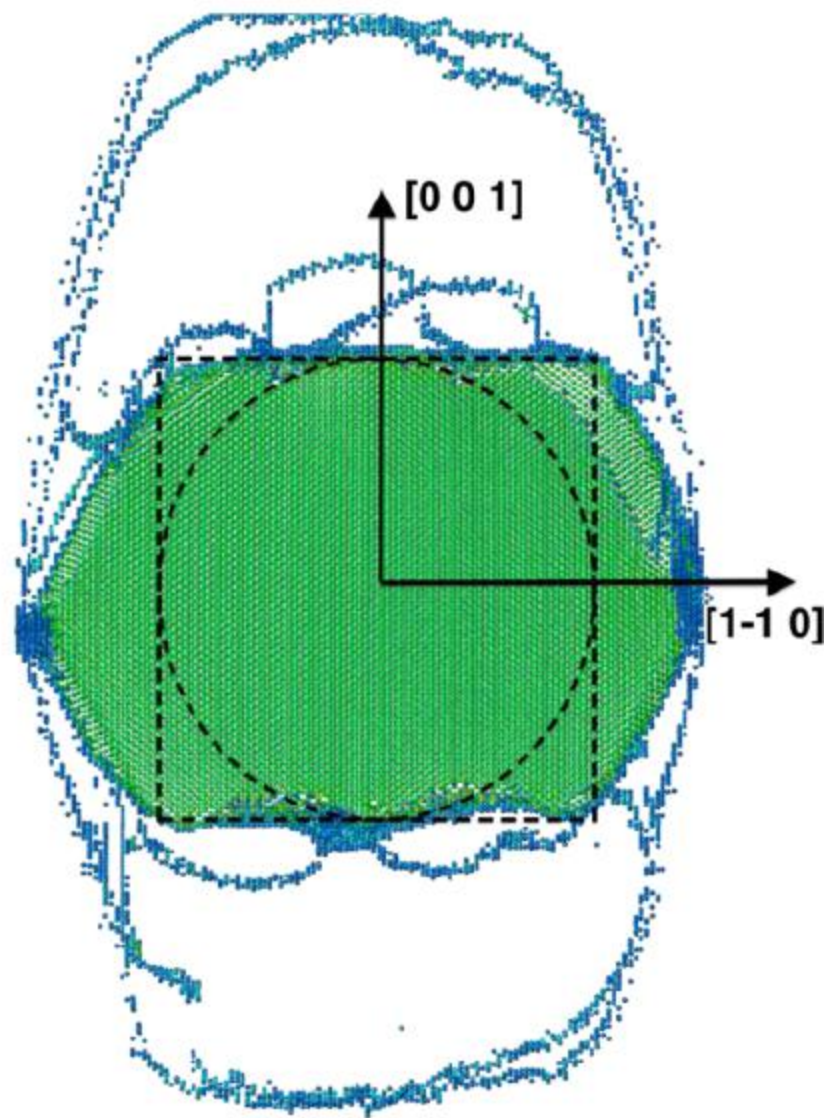
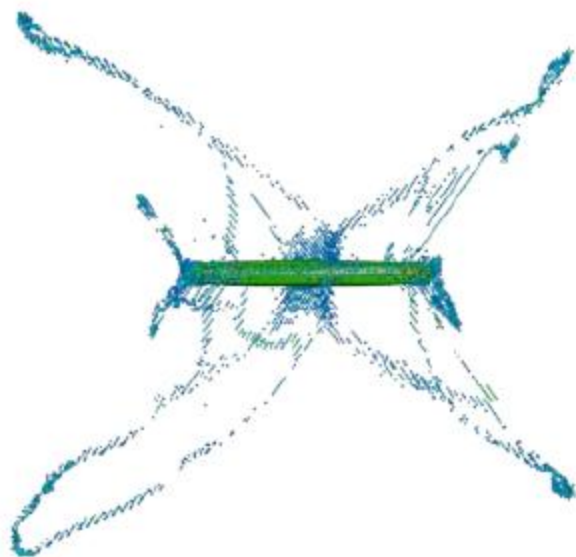




Step 1

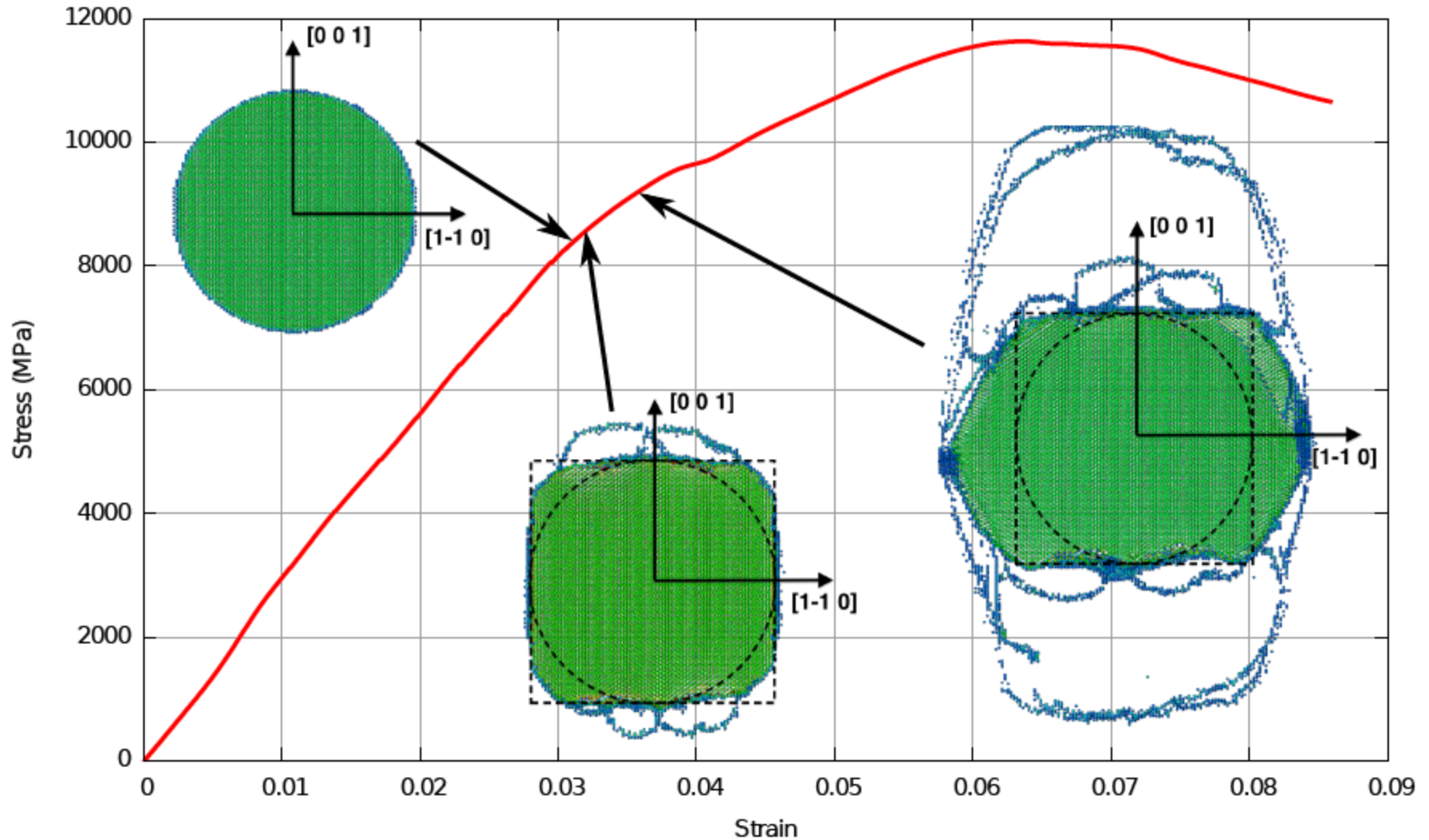


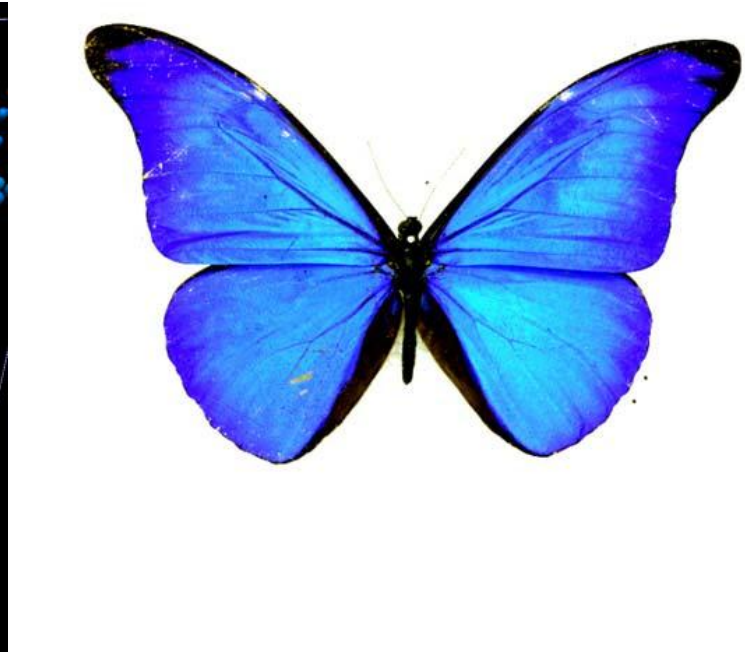
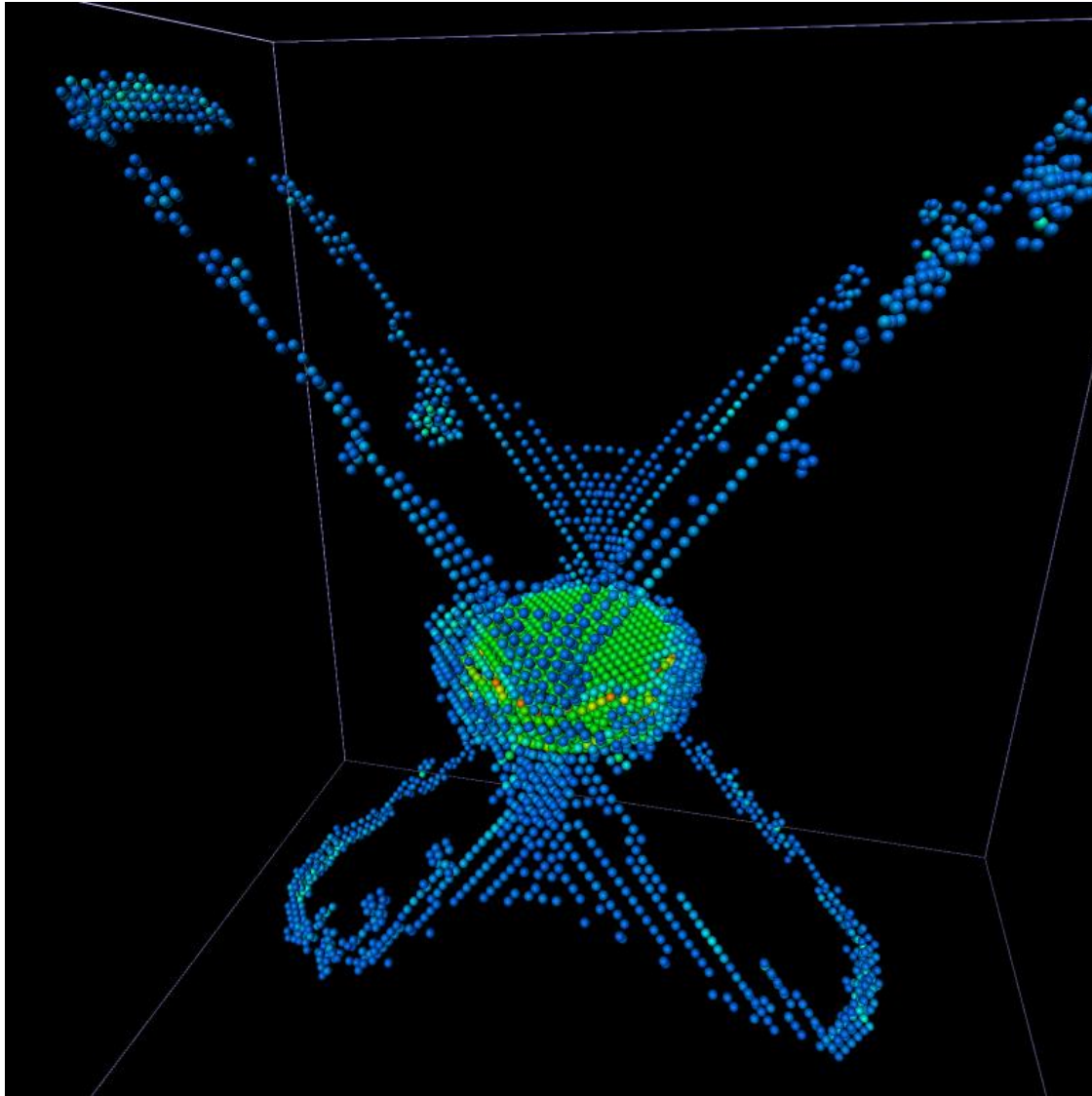
Step 2



Step 3

Evolution of a penny-shaped crack in the (110)-plane of a pure bcc iron crystal loaded in mode I

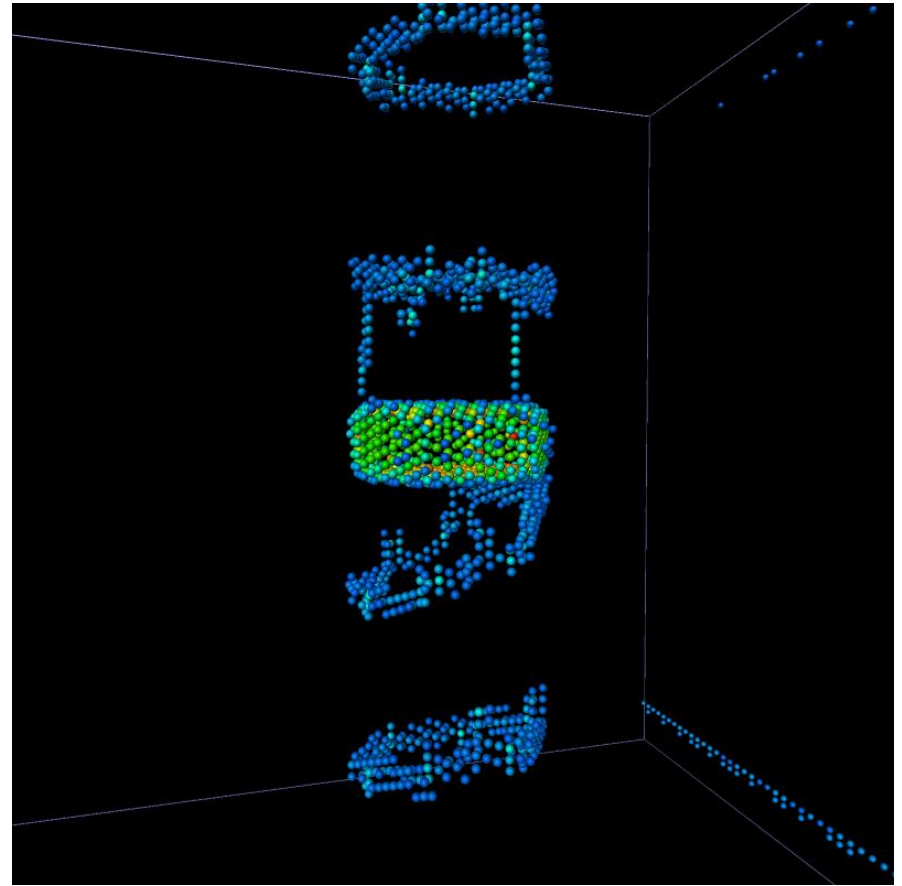




Smoke-rings



search ID: ena0181



Dual-beam FIB-SEM instrument



Helios NanoLab

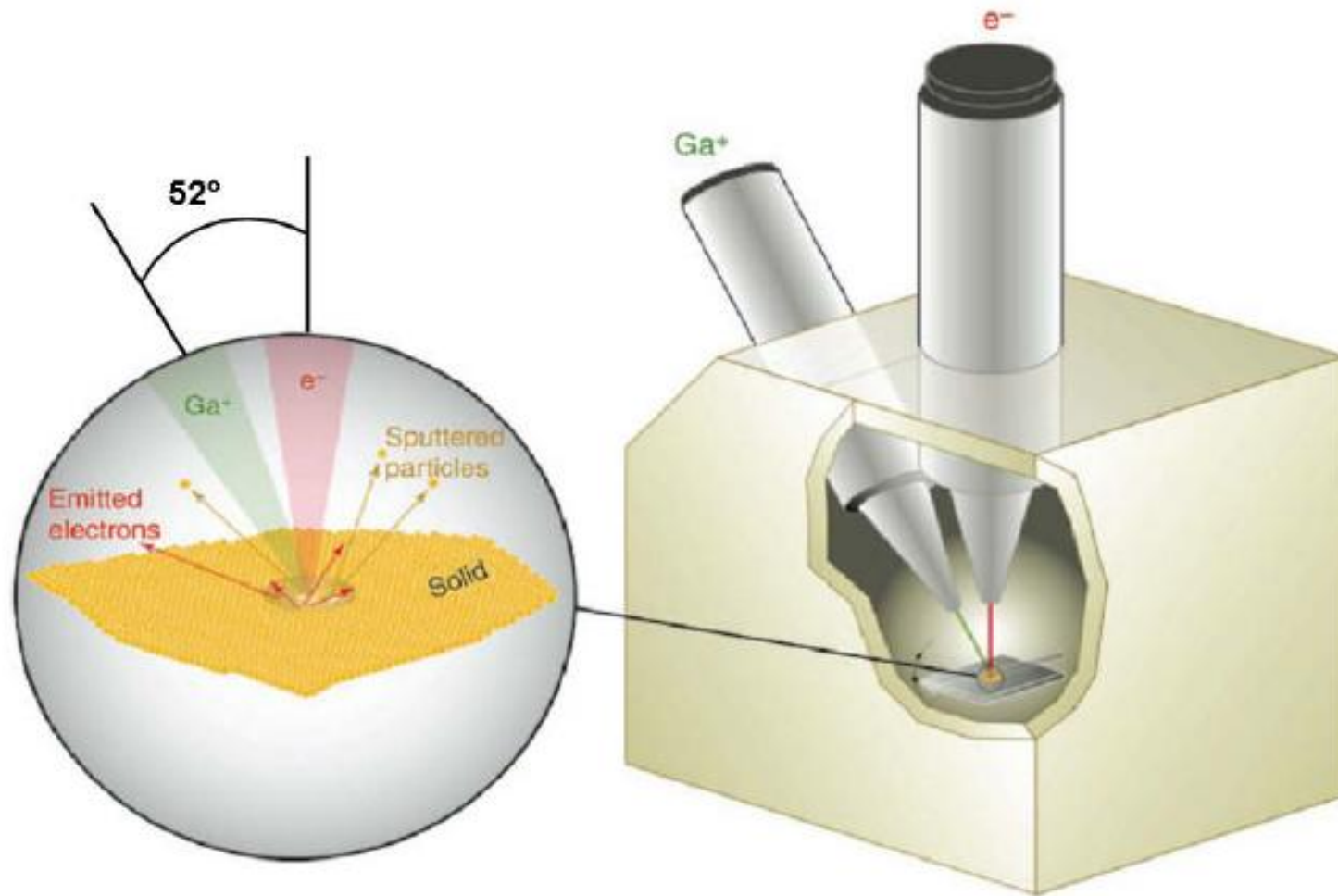
PhD student
Bjørn Rune Sørås Rogne
Nanomechanical testing



FIB:

Beam Current	Best Use
1.5 - 9.7 pA	High resolution
28 - 48 pA	Standard imaging
>93 pA	Milling

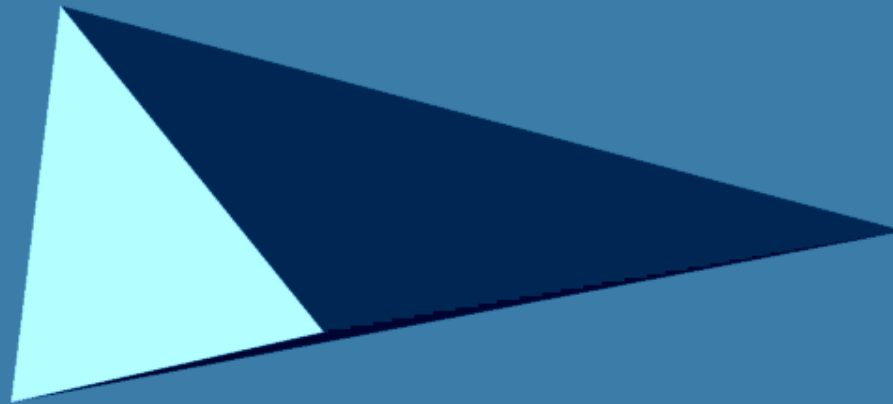
Dual-beam FIB-SEM instrument





Nanoindenter tip

Indentation
into the
surface

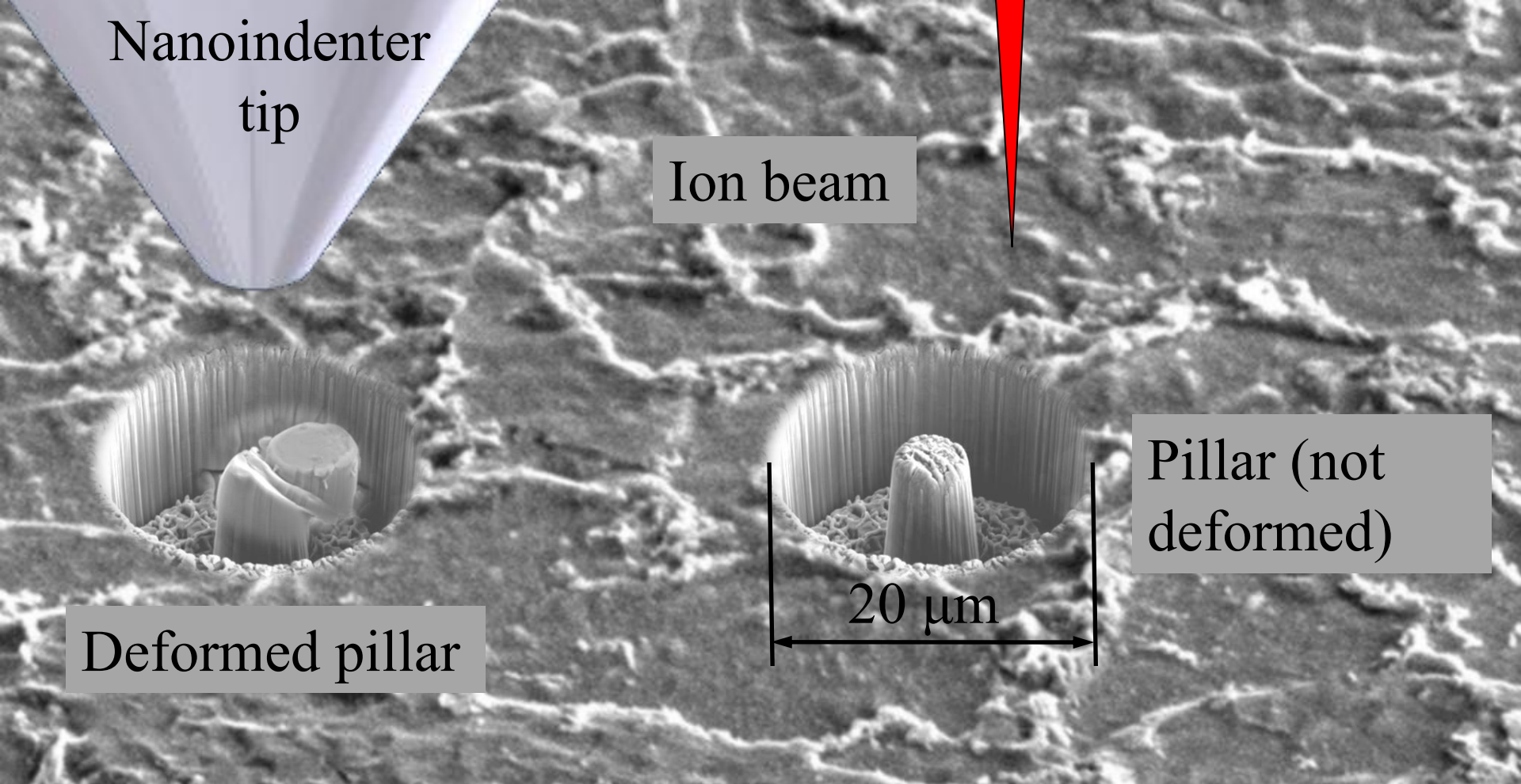


Nanoindentation test – Local hardness test

Material properties:

→ Hardness (H)

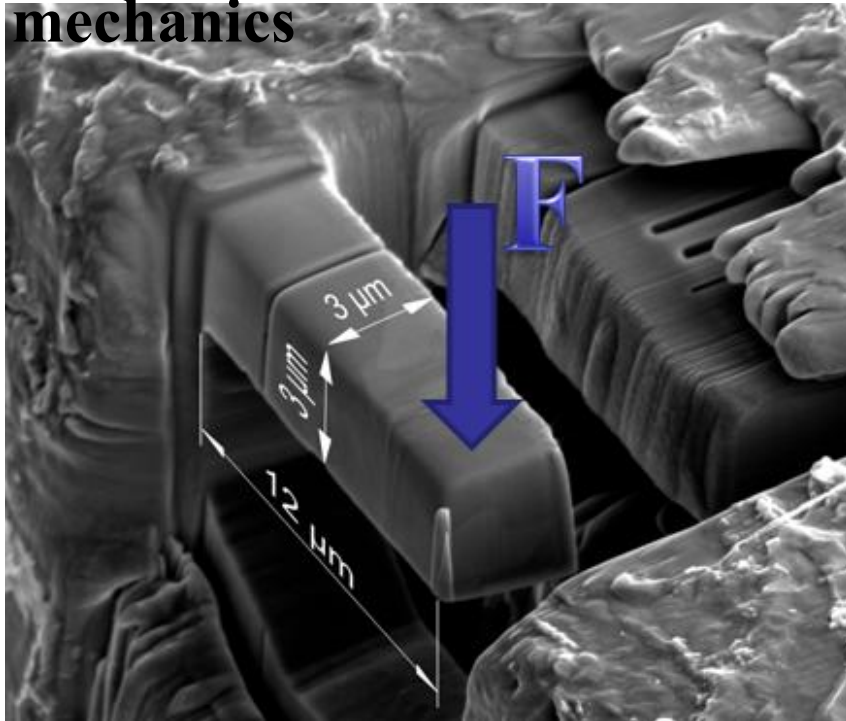
→ Young's modulus (E)



1. Machine out specimens by using a Focused Ion Beam (Ga^+) (NTNU NanoLab).
 2. Load the specimens with a flat ended nanoindentation tip (Nanomekanisk lab)
- Additional material properties can be calculated.

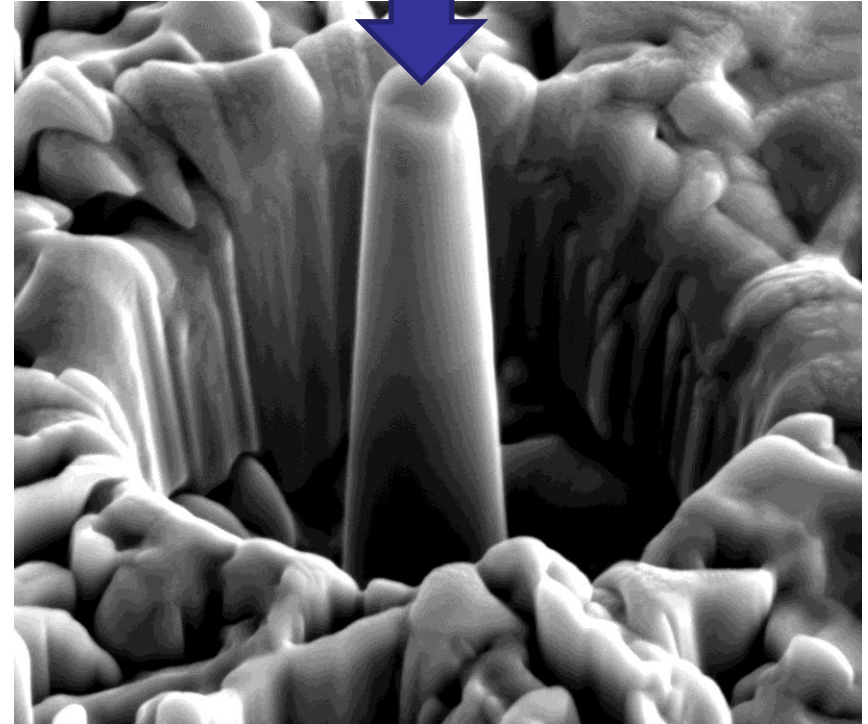
Test specimens

Fracture
mechanics

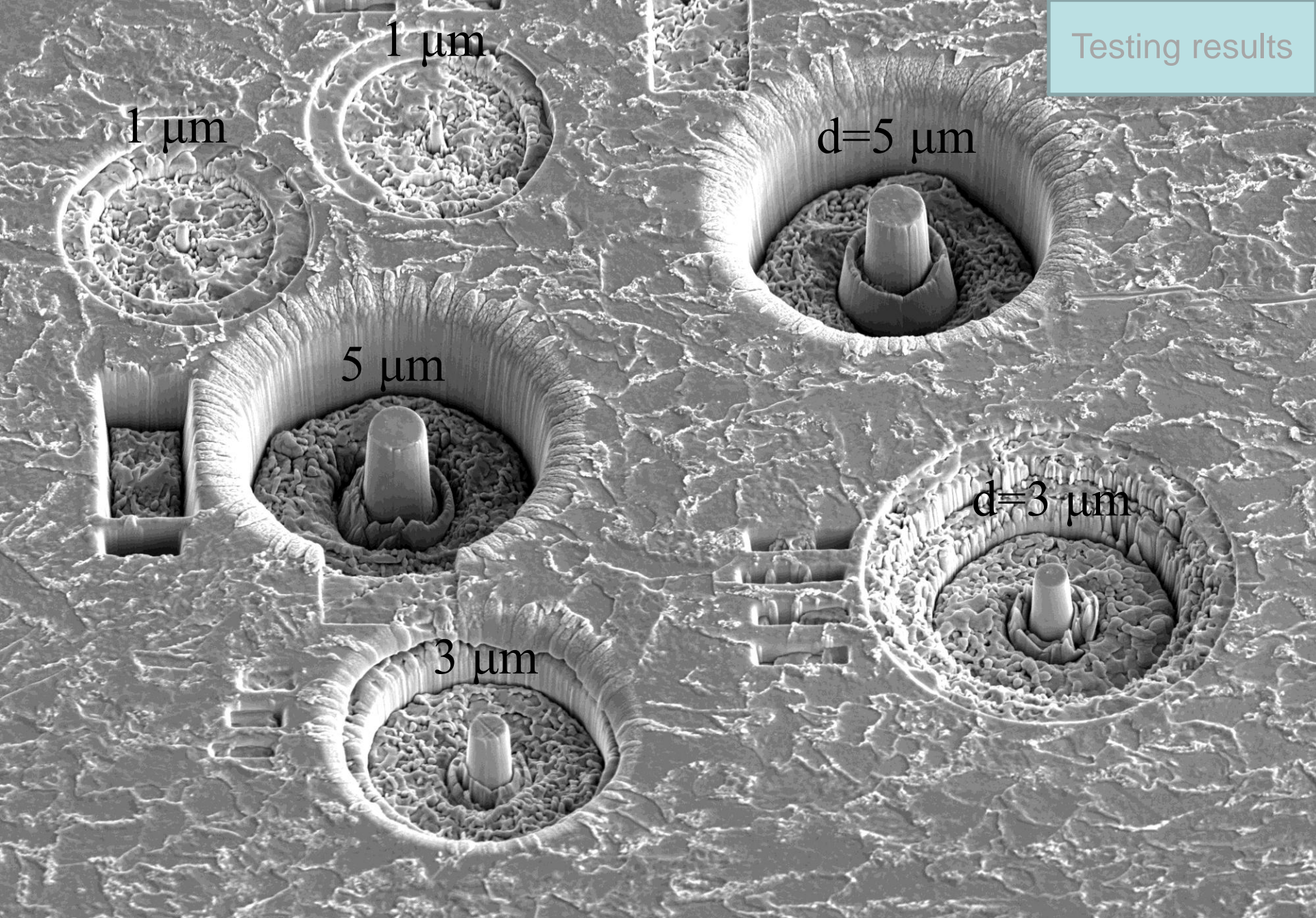


→ Fracture toughness (K_{Ic})

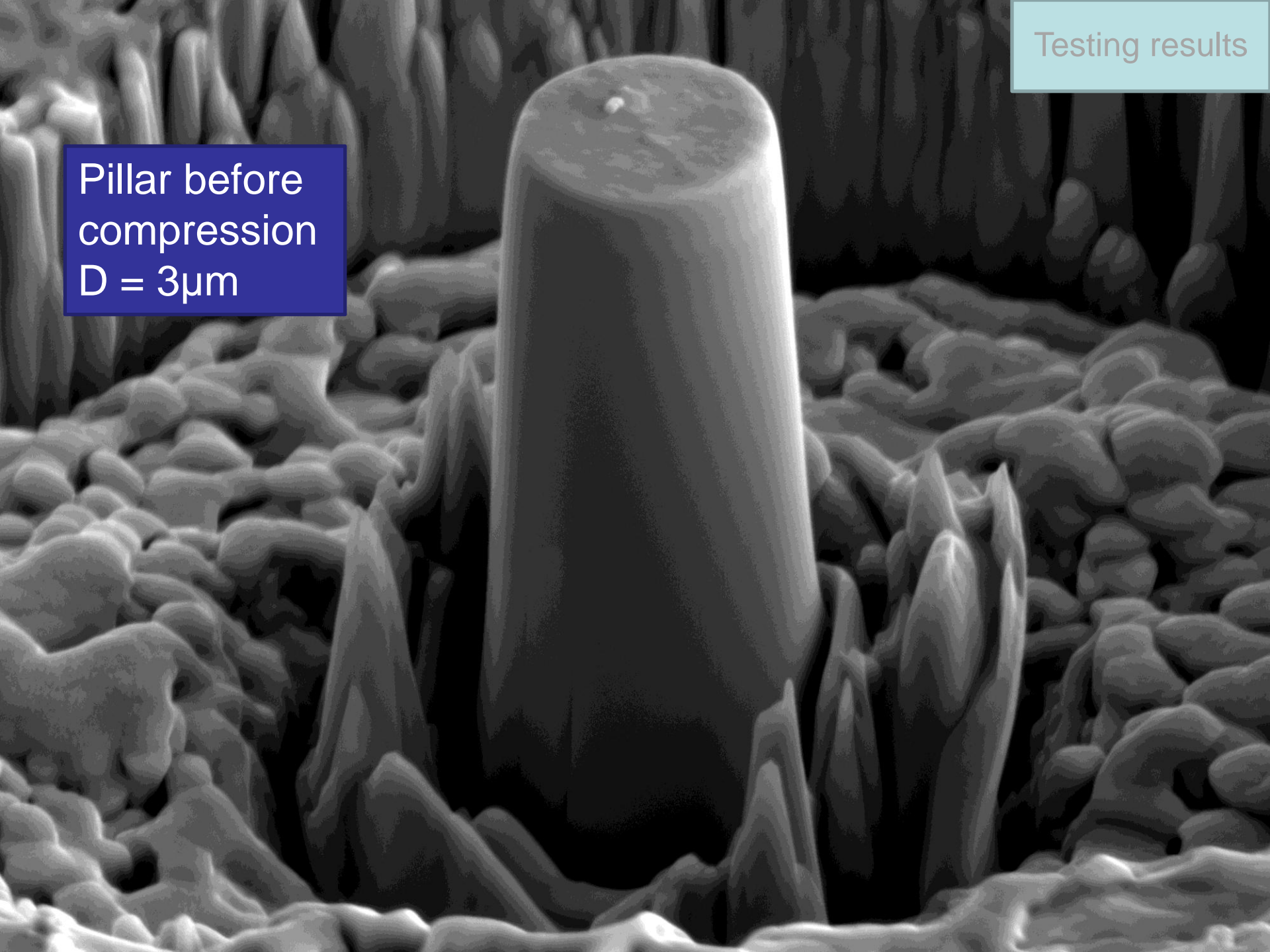
Compression **F**



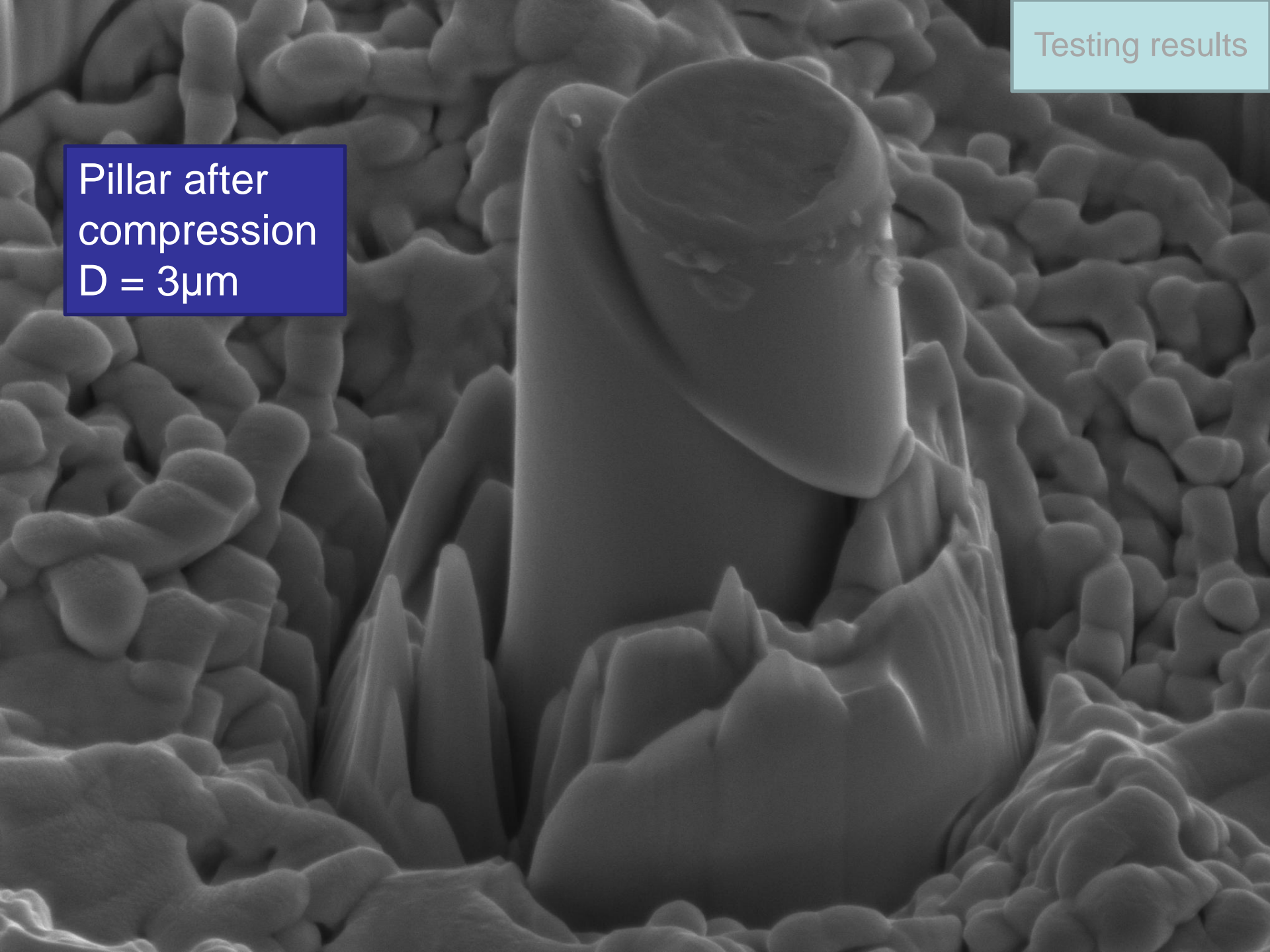
→ Yield stress (σ_y)



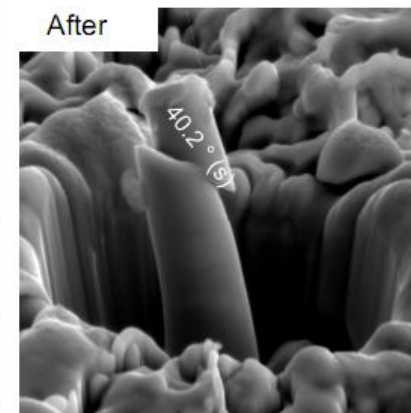
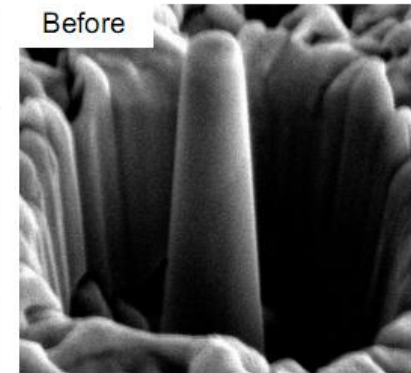
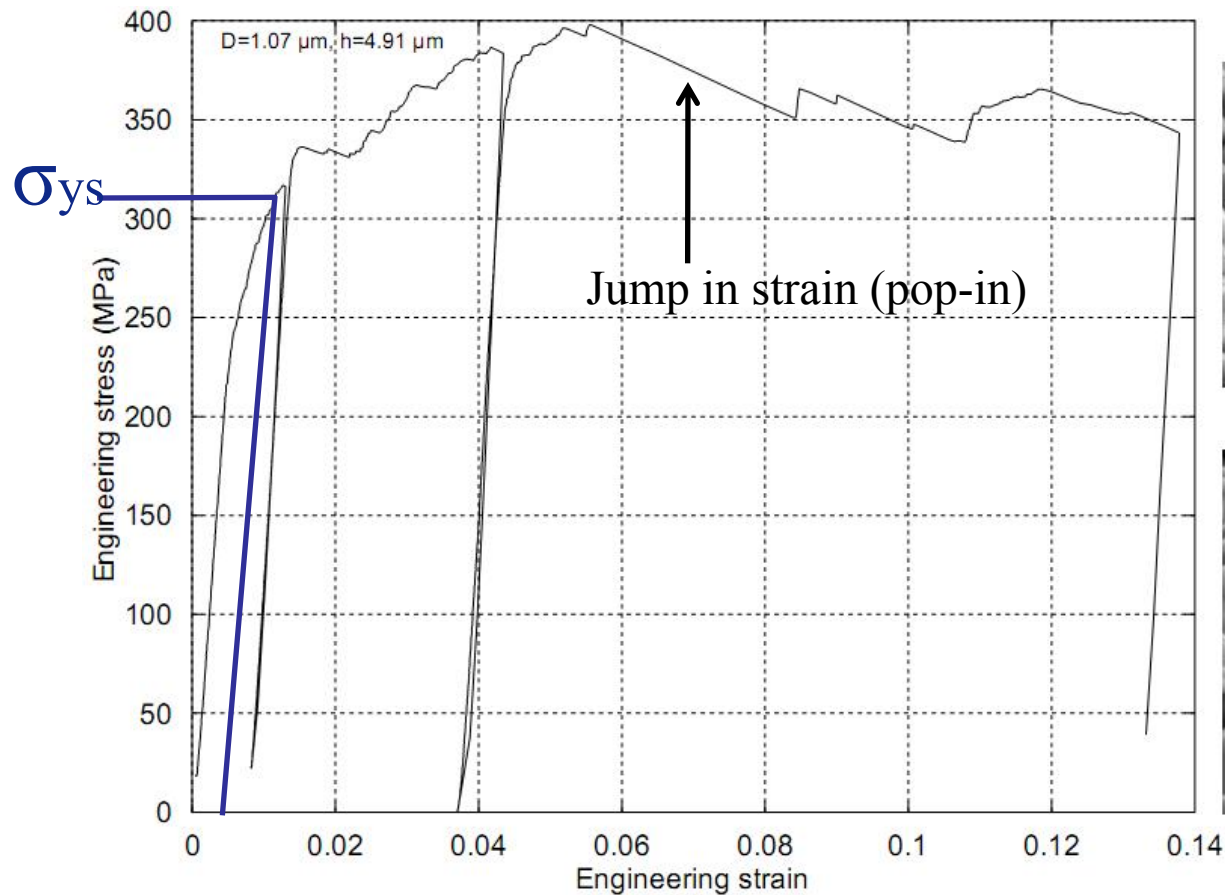
Pillar before
compression
 $D = 3\mu\text{m}$



Pillar after
compression
 $D = 3\mu\text{m}$

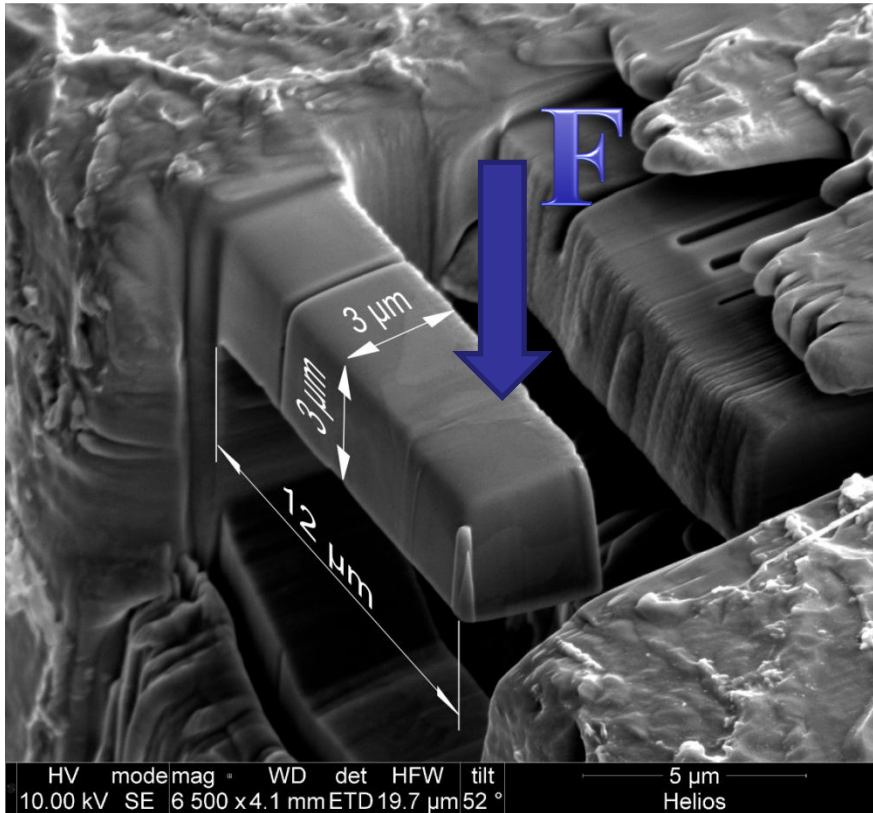


Stress-strain test result from compression testing of pillars

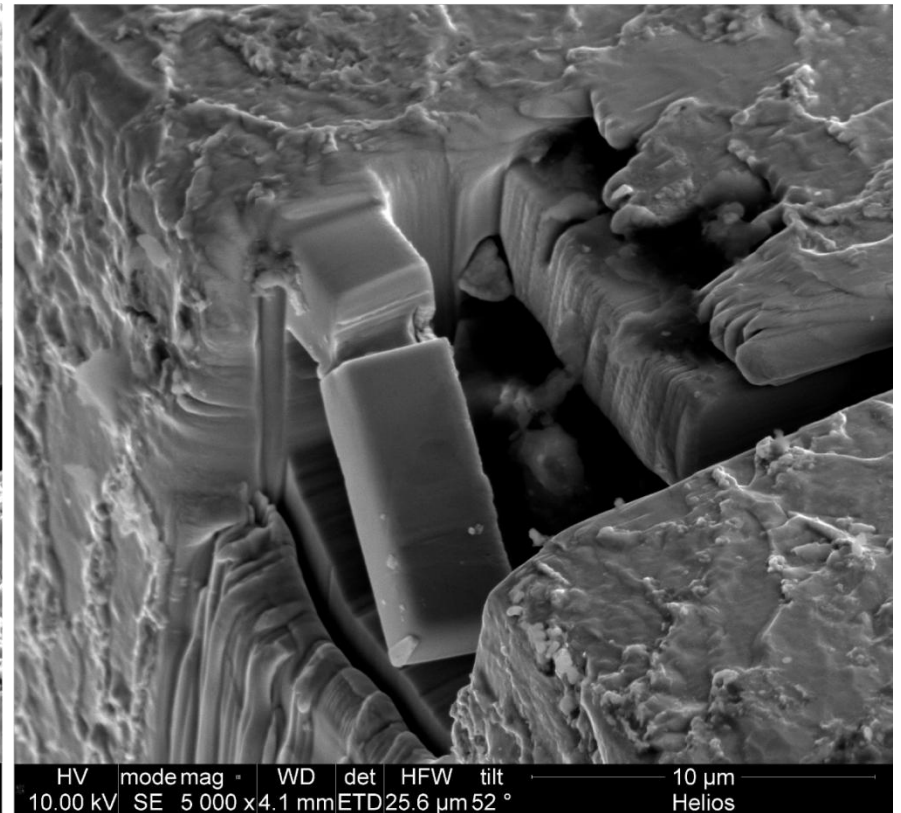


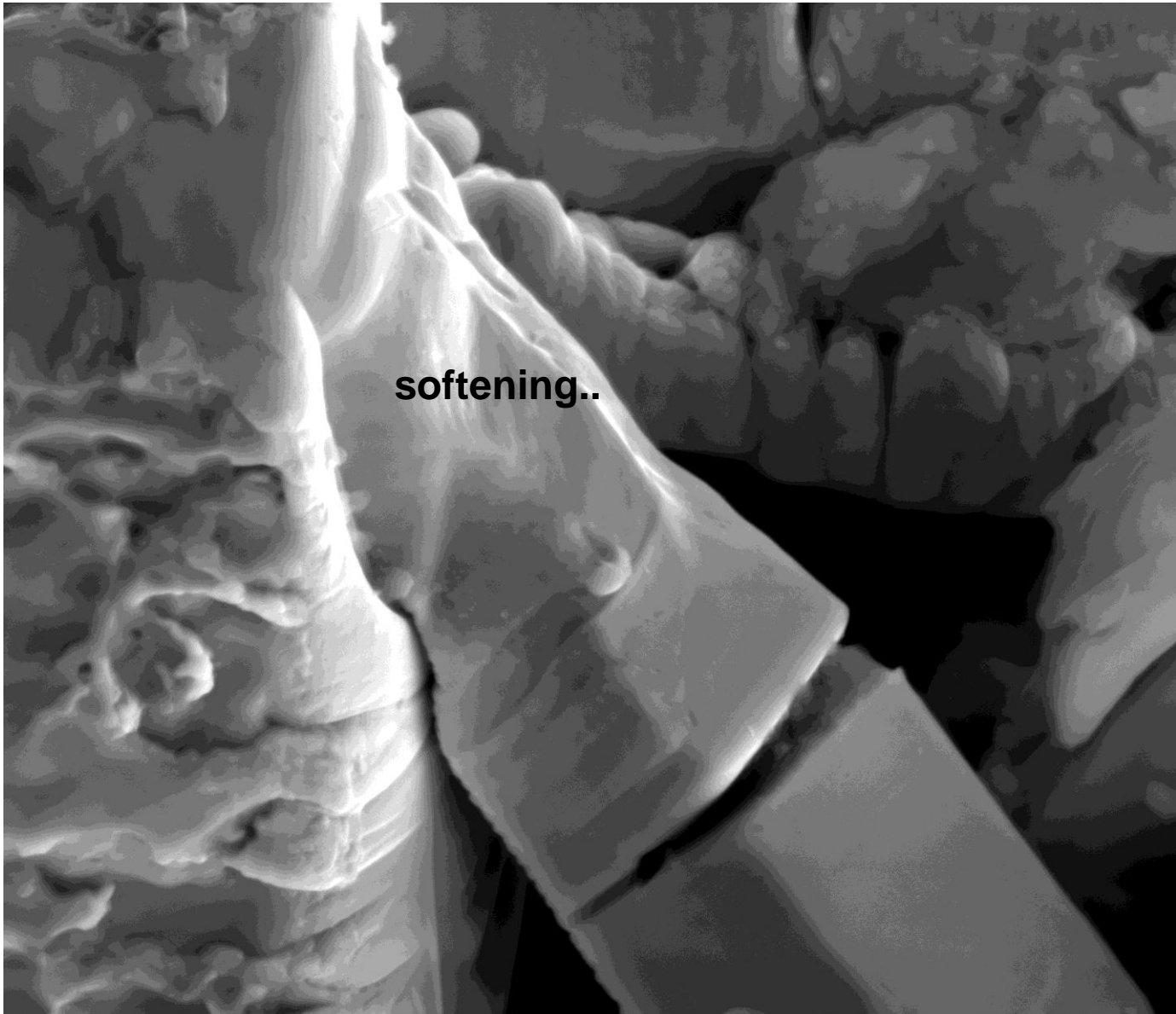
Fracture mechanics test: cantilever beam with notch

Before loading



After loading

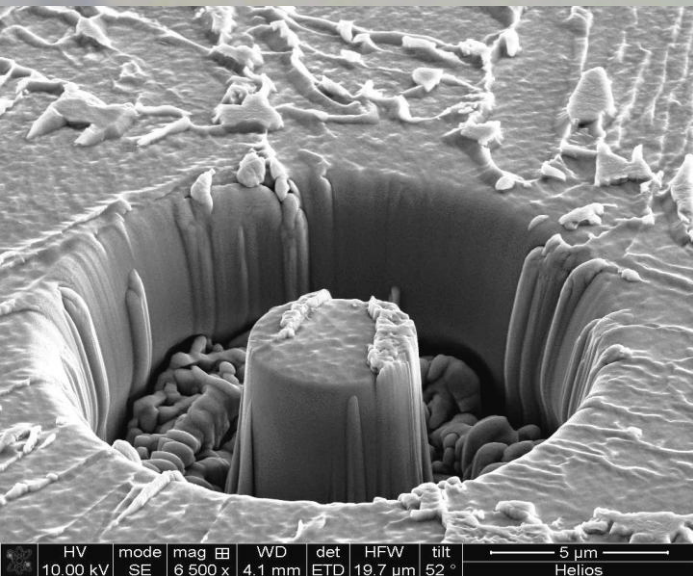




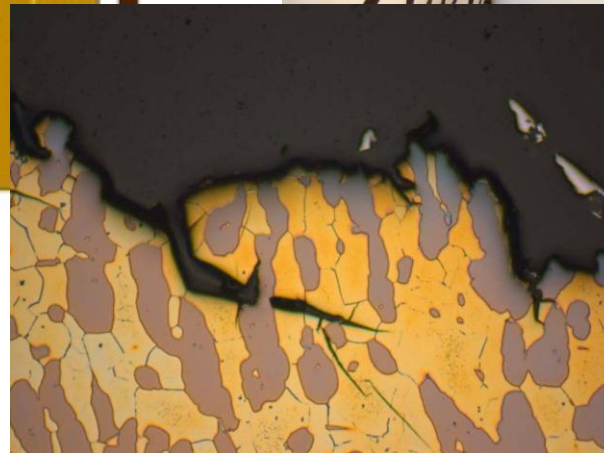
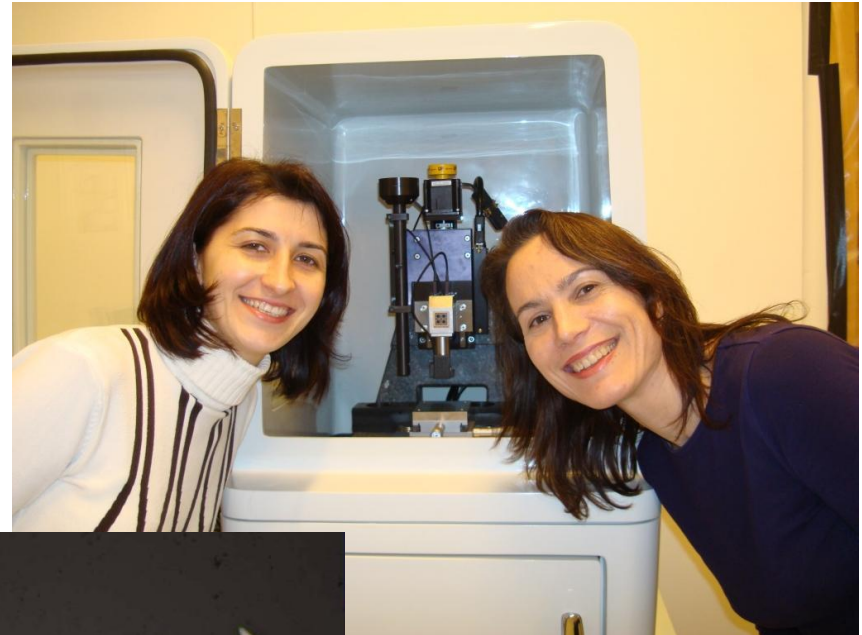
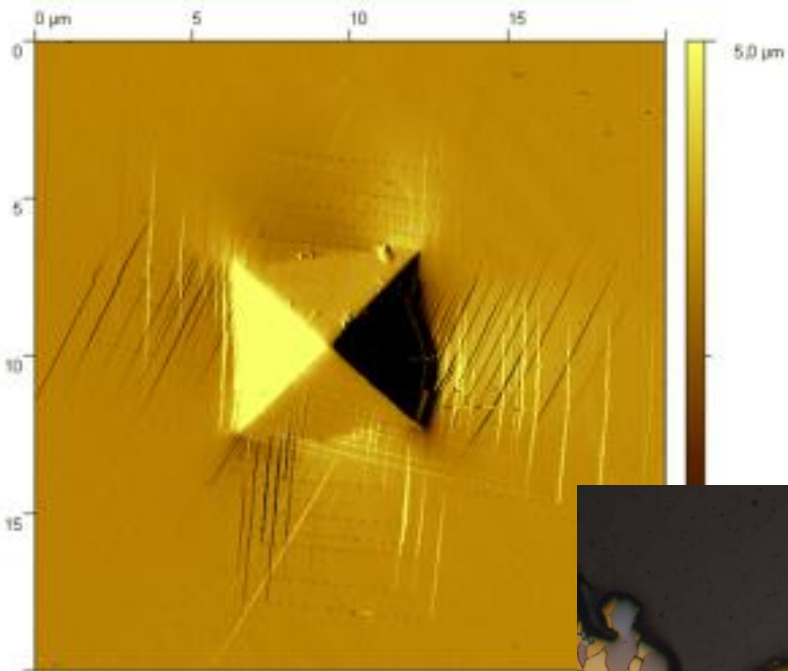
softening..

HV	mode	mag	WD	det	HFW	tilt	4 μm
10.00 kV	SE	12 000 x	4.1 mm	ETD	10.7 μm	52 °	Helios

My first pillar

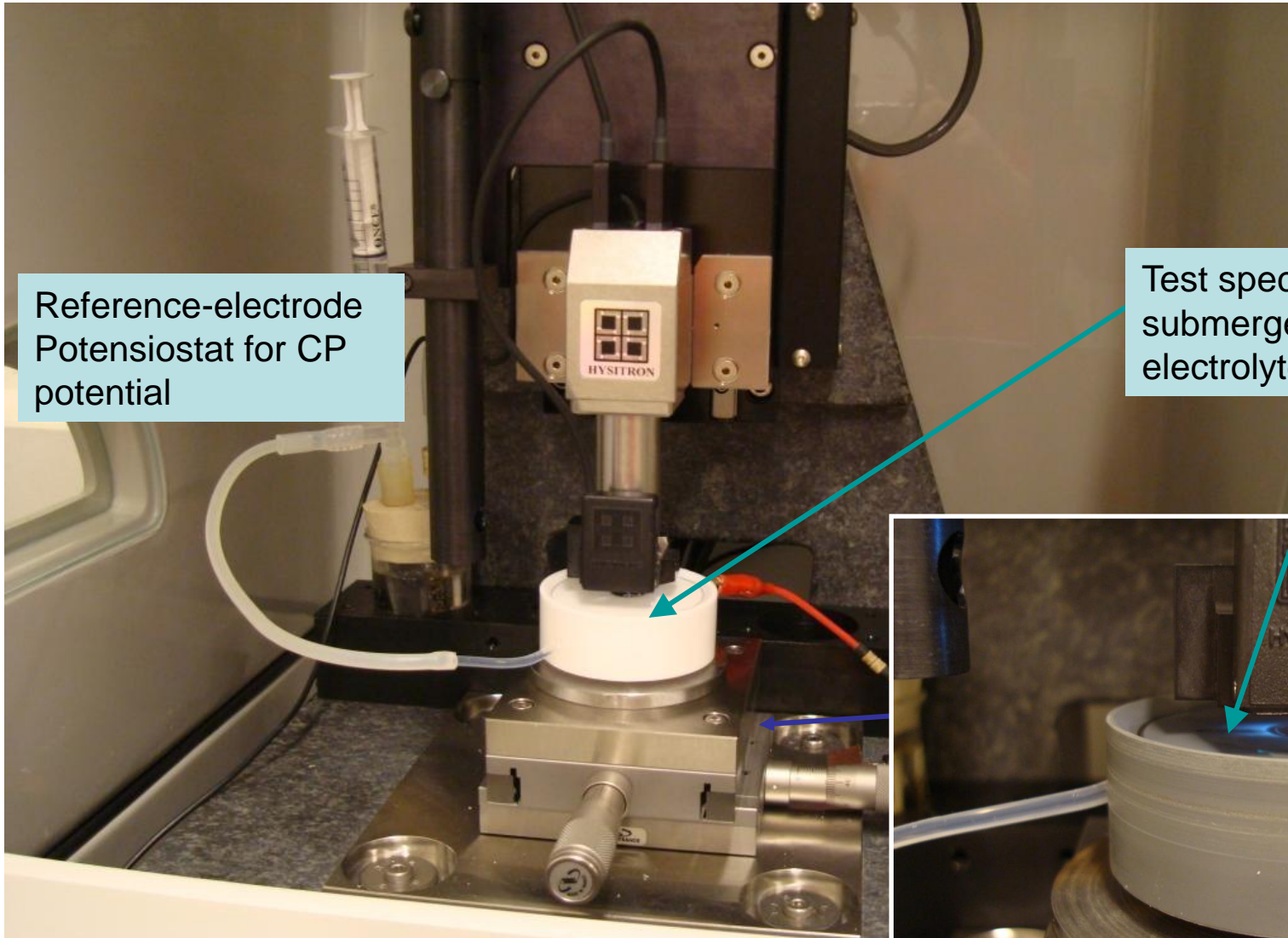


Adina Basa, PhD HISC project
Nanoindentation of stainless steels with in situ hydrogen charging



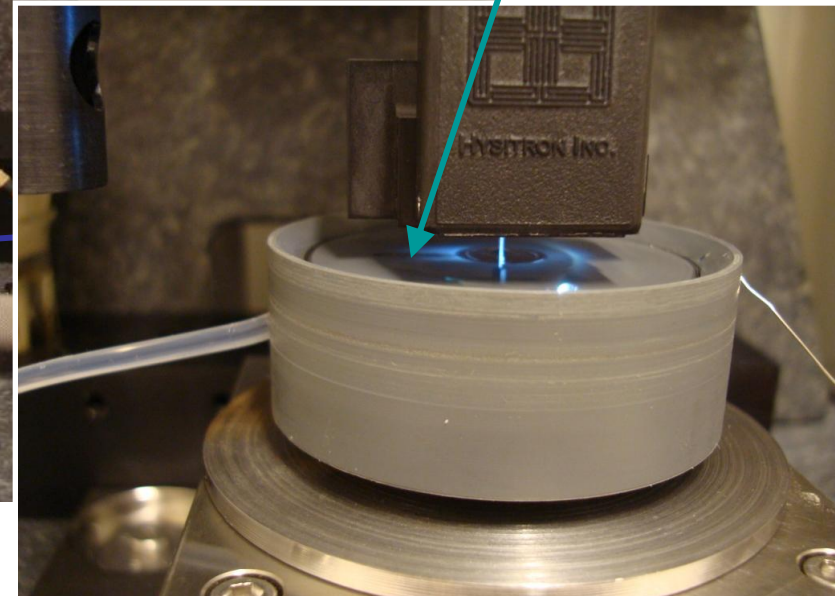
Superduplex stainless steel
26%Cr-7%Ni-4%Mo
austenite - ferrite

Nanoindentation with in situ hydrogen charging of stainless steel

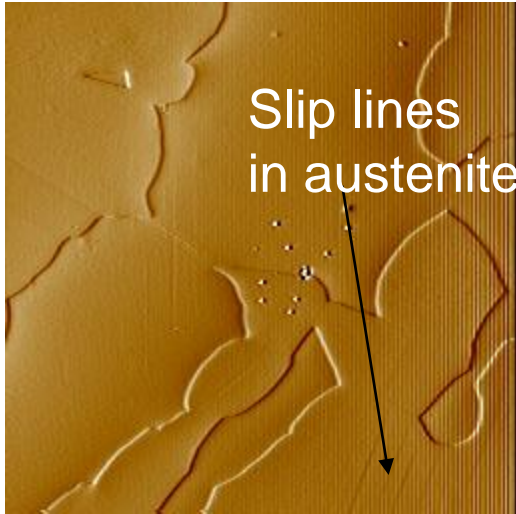
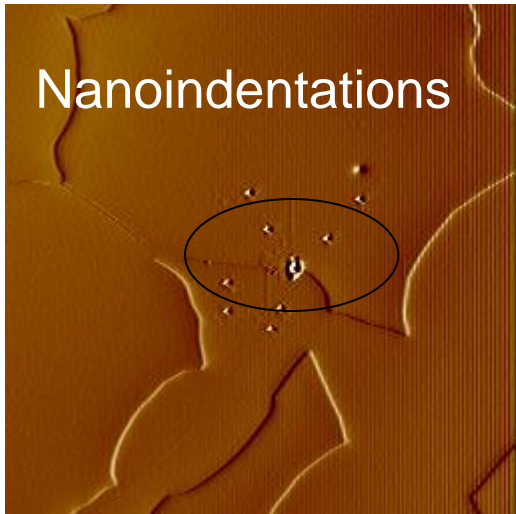
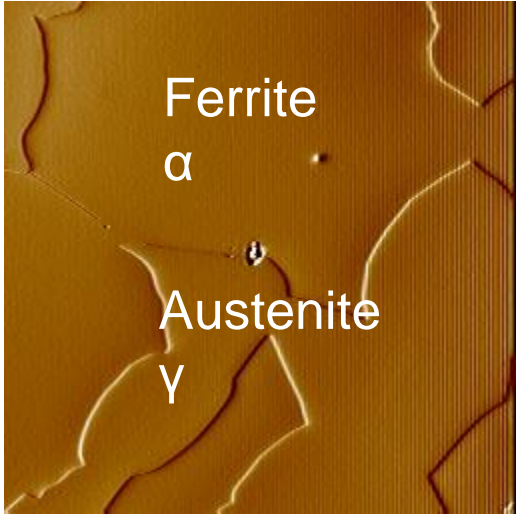


Reference-electrode
Potentiostat for CP
potential

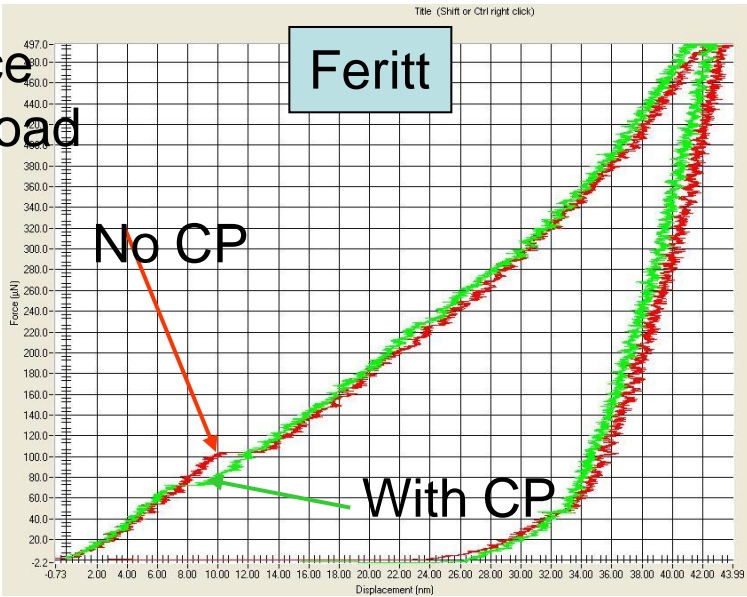
Test specimen
submerged in
electrolyte



CP for 1 hour at $-1050\text{mV}_{\text{sce}}$



CP reduce
"pop in"-load



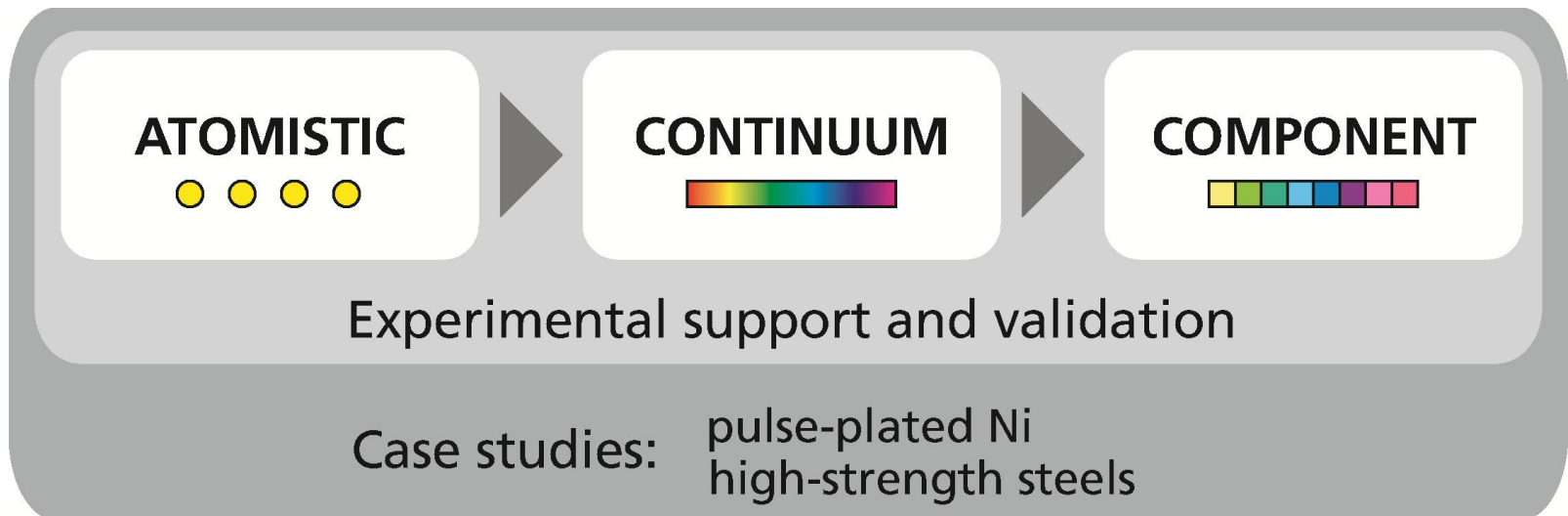
Multiscale modelling of hydrogen embrittlement in crystalline materials

MultiHy

Collaborative Project
(Small or medium-scale focused research project)



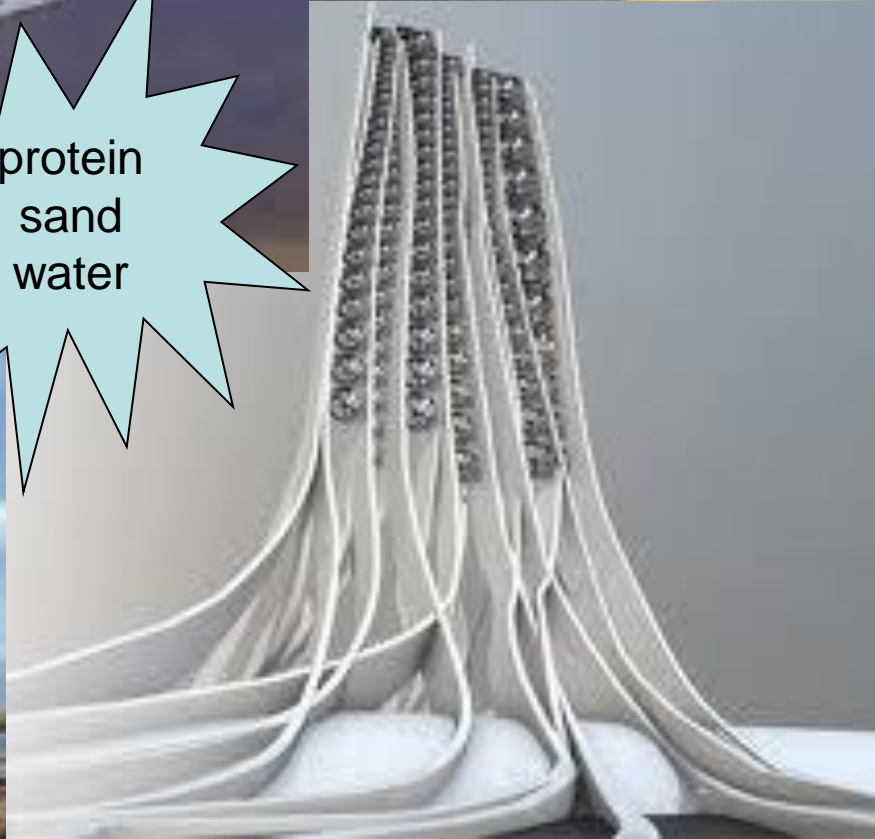
NMP Theme
Call Identifier: FP7-NMP-2010-SMALL-4



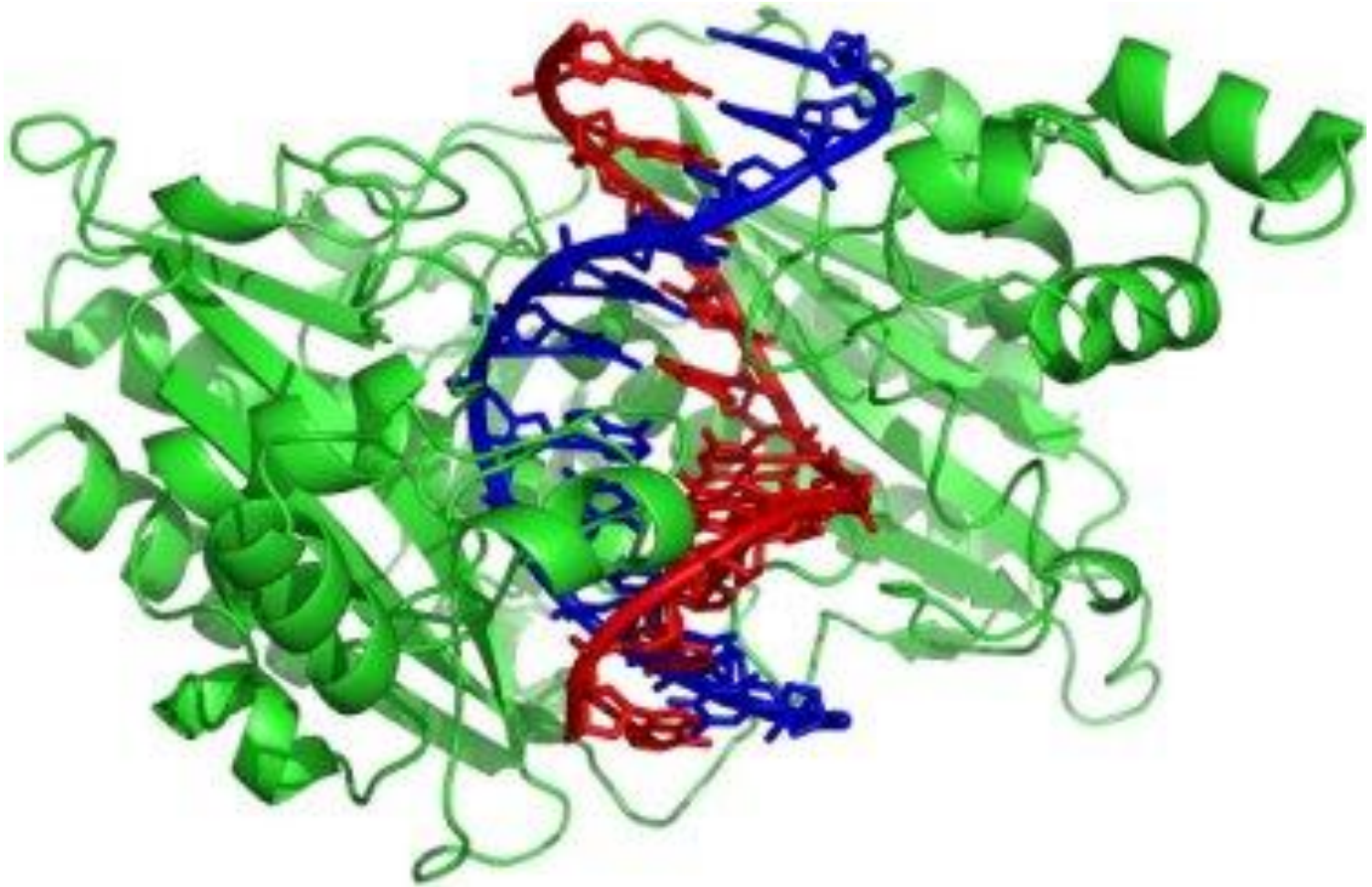
Nanomechanical properties and fracture toughness from local microstructural constituents charged with hydrogen



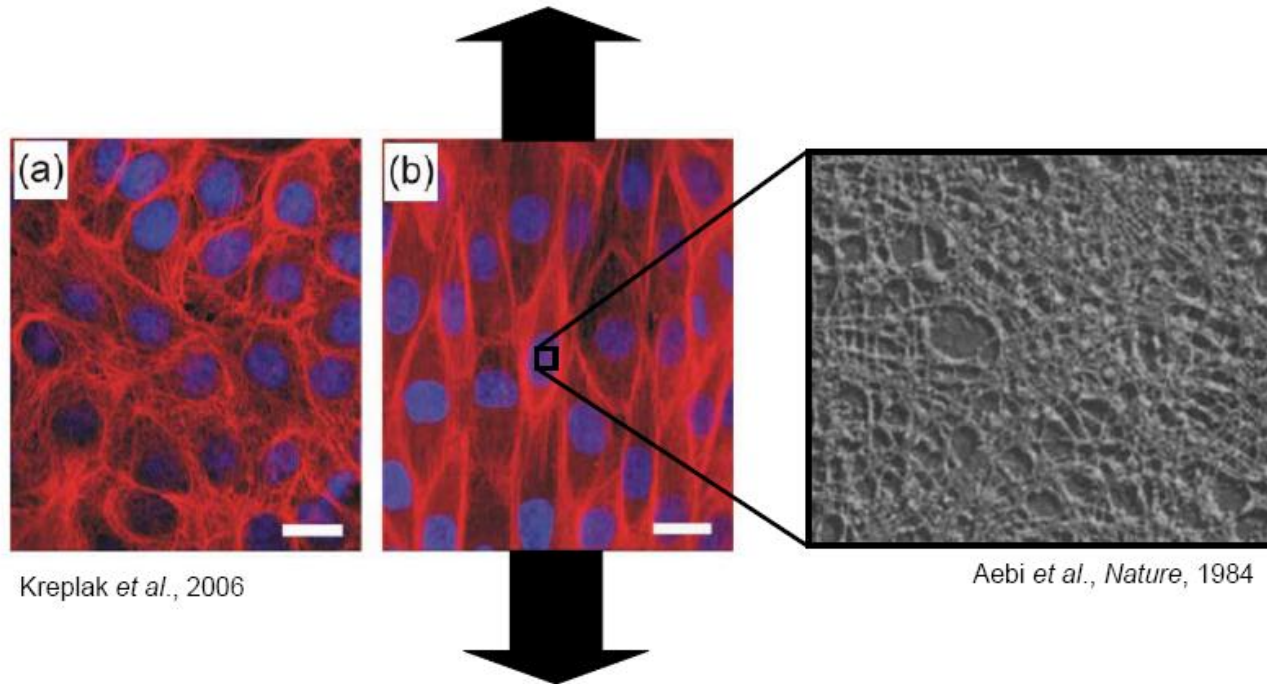
protein
sand
water



Proteins



Cell deformation



How does behavior of protein network at larger scale depend on the structure?

Alpha-Helical Protein Networks Are Self-Protective and Flaw-Tolerant

Theodor Ackbarow¹, Dipanjan Sen^{1,2}, Christian Thaulow¹, Markus J. Buehler^{1,3*}

1 Laboratory for Atomistic and Molecular Mechanics, Department of Civil and Environmental Engineering, Massachusetts Institute of Technology, Cambridge, Massachusetts, United States of America, **2** Department of Materials Science and Engineering, Massachusetts Institute of Technology, Cambridge, Massachusetts, United States of America, **3** Center for Computational Engineering, Massachusetts Institute of Technology, Cambridge, Massachusetts, United States of America

Abstract

Alpha-helix based protein networks as they appear in intermediate filaments in the cell's cytoskeleton and the nuclear membrane robustly withstand large deformation of up to several hundred percent strain, despite the presence of structural imperfections or flaws. This performance is not achieved by most synthetic materials, which typically fail at much smaller deformation and show a great sensitivity to the existence of structural flaws. Here we report a series of molecular dynamics simulations with a simple coarse-grained multi-scale model of alpha-helical protein domains, explaining the structural and mechanistic basis for this observed behavior. We find that the characteristic properties of alpha-helix based protein networks are due to the particular nanomechanical properties of their protein constituents, enabling the formation of large dissipative yield regions around structural flaws, effectively protecting the protein network against catastrophic failure. We show that the key for these self protecting properties is a geometric transformation of the crack shape that significantly reduces the stress concentration at corners. Specifically, our analysis demonstrates that the failure strain of alpha-helix based protein networks is insensitive to the presence of structural flaws in the protein network, only marginally affecting their overall strength. Our findings may help to explain the ability of cells to undergo large deformation without catastrophic failure while providing significant mechanical resistance.

Citation: Ackbarow T, Sen D, Thaulow C, Buehler MJ (2009) Alpha-Helical Protein Networks Are Self-Protective and Flaw-Tolerant. PLoS ONE 4(6): e6015. doi:10.1371/journal.pone.0006015

Editor: Laurent Kreplak, Dalhousie University, Canada

Received: February 15, 2009; **Accepted:** April 23, 2009; **Published:** June 23, 2009

Copyright: © 2009 Ackbarow et al. This is an open-access article distributed under the terms of the Creative Commons Attribution License, which permits unrestricted use, distribution, and reproduction in any medium, provided the original author and source are credited.

Funding: This research was supported by a grant from the Air Force Office of Scientific Research (AFOSR), grant number FA9550-08-1-0321, with additional support from the National Science Foundation, grant number CMMI-0642545 and the Army Research Office, grant number W911NF-06-1-0291. TA acknowledges support from the German National Academic Foundation (Studienstiftung des Deutschen Volkes) and the Hamburg Foundation for research studies abroad (Hamburger Stipendienprogramm). The funders had no role in study design, data collection and analysis, decision to publish, or preparation of the manuscript.

Competing Interests: The authors have declared that no competing interests exist.

* E-mail: mbuehler@mit.edu

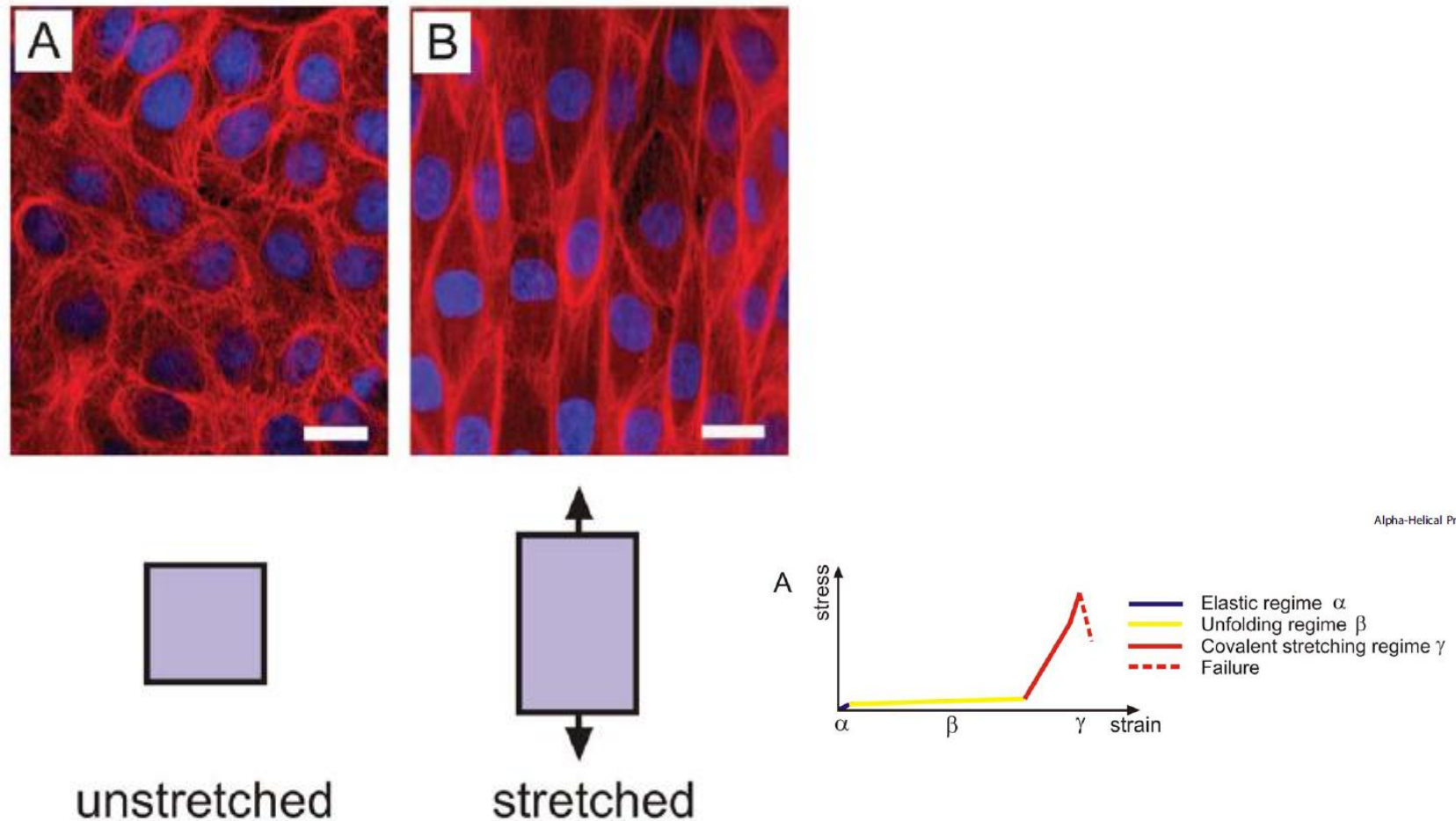
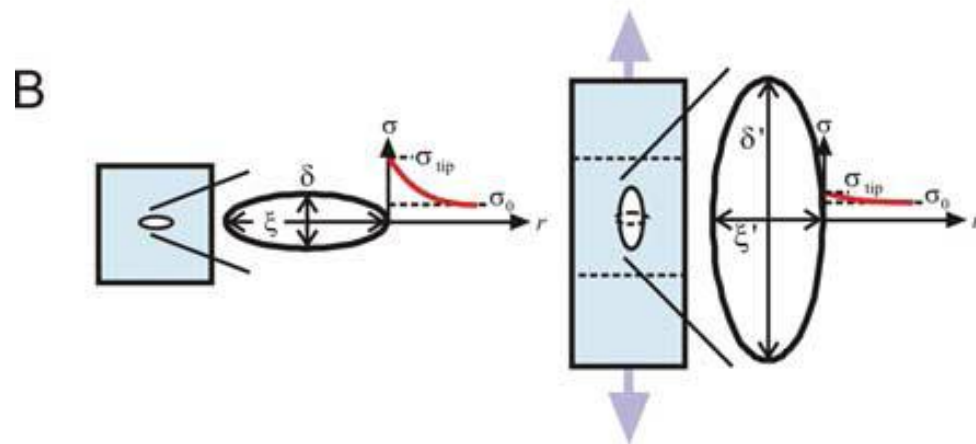
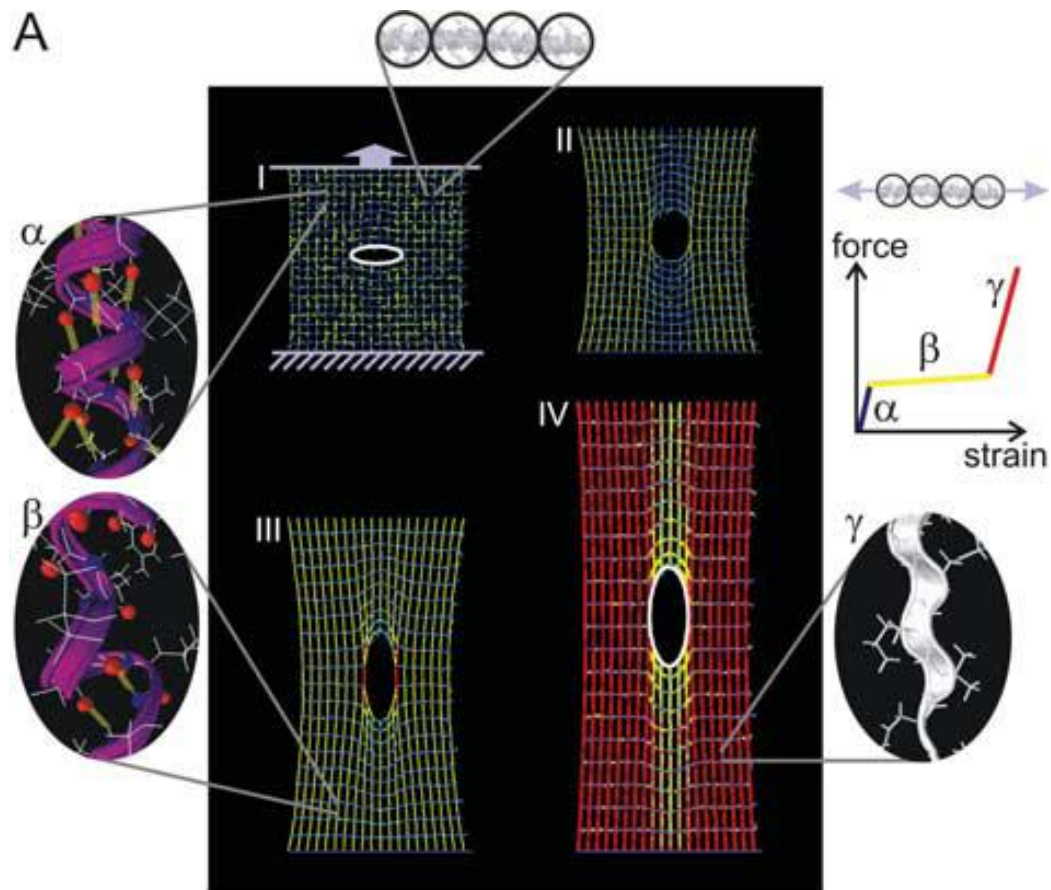


Figure 2. Effect of large uniaxial stretch on the intermediate filament network in MDCK cells, illustrating the ability of intermediate filament network to undergo very large deformation without catastrophic failure. The cells were grown on collagen-coated silastic membranes and stretched using a custom cell stretcher that was mounted on a confocal microscope. Cells were fixed and stained for immunofluorescence (red=keratin IFs, blue=DNA). Subplot A: Control cells were processed on a relaxed silastic membrane. Subplot B: Stretched cells were fixed, stained and imaged on membranes that were held in the stretched state. The approximate uniaxial strain in stretched cells is 75%. Scale bar is approximately 25 μm . Images reprinted with permission of John Wiley & Sons, Inc. from reference [46], *Biomechanical properties of intermediate filaments: from tissues to single filaments and back*, Vol. 29, No. 1, 2007, pp. 26–35, copyright © 2007 John Wiley & Sons, Inc. doi:10.1371/journal.pone.0006015.g002

Self-protecting and flaw-tolerant protein material networks



Ackbarow, T, Sen, D, Thaulow, C, and Buehler, MJ. "Alphahelical protein networks are self protective and flaw tolerant." *PLoS ONE* 4(6), (2009) e6015.